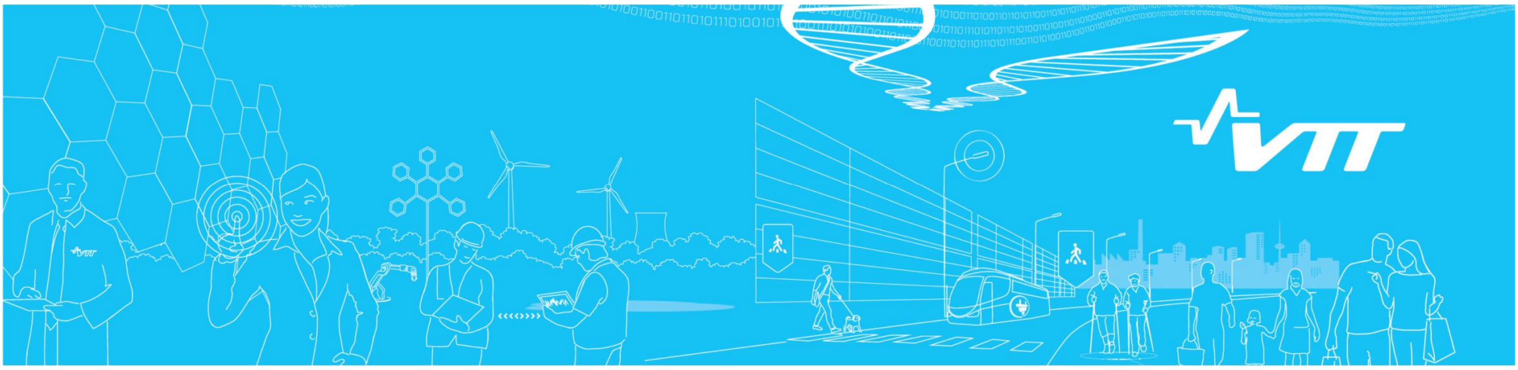

RESEARCH REPORT

VTT-R-05999-15

OffshoreDC: Electricity market and power flow impact of wind power and DC grids in the Baltic Sea

Authors: Niina Helistö, Vin Cent Tai

Confidentiality: Public

Report's title	
OffshoreDC: Electricity market and power flow impact of wind power and DC grids in the Baltic Sea	
Customer, contact person, address Nordic Energy Research	**Order reference** TFI PK-int 02
Project name OffshoreDC (Nordic Energy Research)	**Project number/Short name** 100393
Author(s) Niina Helistö (VTT), Vin Cent Tai (NTNU)	**Pages** 65/10
Keywords HVDC transmission, offshore wind power, offshore grid, power system planning	**Report identification code** VTT-R-05999-15

Summary

This report analyses offshore wind power development and offshore grid options in the Baltic Sea region. 27 GW of offshore wind power was assumed to be built in the Baltic Sea. The approach in this study links offshore wind power plant clustering, onshore connection point determination, offshore grid structure optimisation, unit commitment and economic dispatch simulation and power flow calculation together. The study compares the investment costs of different offshore grid topologies as well as the impacts of the offshore grids on the total operational costs of the power system, electricity production per fuel type, wind power curtailment and CO_2 emissions. Annual electricity transmissions between regions as well as power flows in selected one-hour snapshots are studied as well. The results show that additional interconnections between price regions are clearly beneficial in the Baltic Sea region. Multi-terminal offshore grids may beat offshore grids consisting of two-terminal links in profitability, provided that high voltage direct current (HVDC) circuit breakers are available and their price is low enough. Annual electricity transmissions were generally from north to south and from east to west in the modelled area, which consisted of Nordic and Baltic countries, Germany and Poland. In power flow calculation, loop flows, which were not captured with the unit commitment and economic dispatch model, were detected inside and between Norway and Sweden. The grid model did not allow loop flows in Central Europe to be investigated.

Confidentiality	Public

Espoo 14.12.2015

Written by	Reviewed by	Accepted by
Niina Helistö, Research Scientist	Sanna Uski, Research Scientist	Tuula Mäkinen, Head of Research Area

VTT's contact address

P.O. Box 1000, FI-02044 VTT, Finland, Tel. +358 20 722 111

Distribution (customer and VTT)

VTT, Nordic Energy Research

Preface

The works and developments required for the elaboration of this report have been carried out within OffshoreDC project (DC grids for integration of large scale wind power) which belongs to the Top-level Research Initiative funded by Nordic Energy Research under project no. TFI PK-int 02.

The objectives of the project were to drive the development of voltage source converter (VSC) based high voltage direct current (HVDC) grid technologies for large scale offshore grids, support a standardised and commercial development of the technology, improve the opportunities for the technology to support power system integration of large scale offshore wind power, and to help the Nordic stakeholders to benefit from the uniquely ambitious plans for offshore wind power development in the area.

This report presents the methods, scenarios and results in the collaboration of work packages 5 and 6 where both electricity market and power system impacts of offshore grids were studied. The focus in the study was on the possible offshore wind power and offshore grid development in the Baltic Sea in the time horizon up to 2030. It was assumed in the study that 27 GW of offshore wind power will be built in the Baltic Sea. The amount of onshore and offshore wind power in the study was approximately 22 % of the annual electricity demand in the modelled area, which consisted of Nordic countries, Baltic countries, Germany and Poland.

Section 2.2.2 (Net-Op) in this report is written by Vin Cent Tai from NTNU (Norway) and the rest of the report is written by Niina Helistö from VTT (Finland).

Espoo 14.12.2015

Authors

Contents

Abbreviations

ENTSO-E	European Network of Transmission System Operators for Electricity
HVAC	high voltage alternating current
HVDC	high voltage direct current
LCC	line commutated converter
MT	multi-terminal
NPV	net present value
PV	photovoltaics
TSO	transmission system operator
TYNDP	Ten Year Network Development Plan
VSC	voltage source converter
WILMAR JMM	WILMAR Joint Market Model

1. Introduction

1.1 Background

Offshore DC grids can improve the integration of overseas electricity markets and the exploitation of offshore wind power resources, which both require sufficient offshore transmission connections. An offshore DC grid could connect different generation and load areas to facilitate the integration of renewable energy sources and the balancing and transportation of electricity. An offshore DC grid could potentially strengthen the transmission system, relieve congestions, increase system stability and reliability and improve power flow control in the grid.

Technical and economic requirements for offshore grid include high power transfer capability, high transmission efficiency, high reliability, competitive price, compatibility with the current infrastructure and possibility for long distances and offshore connections. High voltage direct current (HVDC) transmission does not have reactive losses and fewer cables are needed compared to high voltage alternating current (HVAC) for equal transmission. Development of conversion technologies is important to minimize the costs of offshore wind power grid connection and multi-terminal grids.

There are two main technologies for HVDC systems: line commutated converters (LCC) and voltage source converters (VSC). The characteristics and capabilities of LCC and VSC technologies in multi-terminal grids are compared, e.g., in [1]. VSC is capable of setting voltage and frequency on an AC grid, it requires a smaller site area and its power reversal is achieved by reversing the direction of current. Thus, it is a better solution for connections to weak AC grids and offshore platforms and for multi-terminal HVDC grids compared to LCC.

The power control schemes of multi-terminal HVDC-VSC grids have been studied widely. In [2], the converter control strategies are classified into three groups: constant voltage control, constant current/power control and voltage droop control, whereas the grid control strategies are classified into two groups: centralized and distributed voltage control. In centralized voltage control, one converter controls a constant voltage at its bus and all other converters control their current or power to the set-point. In distributed voltage control, more than one converter operates in voltage droop mode and the rest in constant current/power mode. The power sharing of the droop controlled converters depends on their droop constants. In [3], a new hierarchical HVDC grid power control strategy similar to the control structure in AC transmissions systems is introduced. The strategy consists of primary, secondary and tertiary control. Primary control or DC voltage control can be implemented with voltage droop control. Secondary control or power control can be described as a system to change the DC voltage set-points or to achieve the desired power set-points. Finally, tertiary control can be based on optimal power flow algorithms in order to calculate the power set-points according to an optimal operation of the power system.

Different topologies of multi-terminal HVDC grids have been compared in literature. In [4], the topologies have been divided into the following six groups: point to point, general ring, star, star with a central switching ring, wind farms ring and substations ring. In [5], the topology groups are radial grid, ring-shaped grid, lightly meshed grid and densely meshed grid. The articles conclude that the optimal solution depends on the operation and reliability requirements as well as on the geography of the system and costs of the HVDC components.

The best configuration of offshore grid depends on, e.g., the distance of wind power plants to the shore and to each other and the trade constraints between the regions. A former study OffshoreGrid [6] states that clustering several wind power plants into one hub and connecting the hub to the onshore grid with one cable instead of connecting each wind power plant individually to onshore grid will reduce infrastructure costs and also mitigate the environmental and social impact of installing multiple cables in sensitive coastal areas. The same study predicts that connecting wind power plant clusters to interconnectors is more beneficial compared to direct interconnectors and connecting wind power plant clusters radially to onshore grid when the price differences between different regions are modest and the wind power plants are far from shore. Interconnection of several wind power plant clusters is beneficial when clusters are located close to each other. Connecting wind power plant clusters to interconnectors and to each other also improves the reliability of the wind power plant connection and can increase security of supply.

Another former study NorthSeaGrid [7], a follow-up to the OffshoreGrid project, analysed concrete offshore grid cases in the North Sea region from techno-economic perspective. The results showed that the construction of the selected cases in an integrated manner would generally lower the material requirement and costs compared to direct interconnectors and wind power plant cluster connections. The availability and utilization of the infrastructure was concluded to be greater in integrated implementations due to the availability of alternative paths in the case of an export cable failure. The technical risks were found to be largely similar for isolated and integrated developments. The study also proposed solutions to practical financial and regulatory barriers to offshore grid interconnectors, including suggestions to generator remuneration and monetary compensation mechanisms.

THINK was another European study identifying barriers to offshore grids and giving policy recommendations for European Union [8]. The study also included a literature review on the regulatory frames and economic features of offshore grid projects based on two-terminal and multi-terminal solutions. The study reminds that with multi-terminal solutions it is possible to reduce the number of converters required and thus achieve economic benefits but admits that the economic case for multi-terminal solutions is very uncertain due to the advanced HVDC hardware and software that is needed.

When planning a grid, both energy economics and reliable system operation need to be taken into account. In energy economics, the objective is to minimize investment and operational costs or to maximize social benefit. From system operation point of view, the objective is to ensure power system stability and security. However, combining investment optimization, unit commitment and economic dispatch simulation and grid studies is not a straightforward task. Unit commitment and economic dispatch models based on mixed integer linear programming do not cover the physics of power systems which leads to differences between market power flows and physical power flows. Different methods have been proposed to combine dispatch optimization and grid studies, ranging from zonal grid models and linearized power flow equations to nodal grid models and complete nonlinear power flow equations. Some methods have better accuracy whereas some win in computation time. Analysis of grid stability is even more difficult to automate and combine with investment and dispatch optimization.

1.2 Objectives

The aim of this study is to identify electricity market and power system impacts of offshore wind power and different offshore grid designs, ranging from single radial connections from each offshore wind power plant to a fully meshed offshore transmission grid. The purpose is to analyse the offshore grids themselves with wind power, but also the impact of offshore grids on the main power grids onshore, and define the operating frames the onshore power systems set for offshore grid options. The overall objective of the feasibility studies is to build more cost-efficient offshore wind power plants and interconnectors.

While many offshore grid studies in Northern Europe focus on the North Sea region, this study concentrates on the possible wind power and offshore grid development in the Baltic Sea region in the time horizon up to 2030. The offshore wind power scenario including wind power plant locations and capacities is based on TWENTIES project. In this study, over 27 GW of offshore wind power is assumed to be installed in the Baltic Sea. The countries taken into account in the analysis are Denmark, Norway, Sweden, Finland, Estonia, Latvia, Lithuania, Poland and Germany. Several cases with different HVDC component cost and grid topology assumptions are studied. The offshore grids in the case studies are assumed to be implemented using VSC-based HVDC technology.

The study is carried out based on identification of different offshore grid structures using a generation planning model Balmorel, power balance computation as determined by a unit commitment and economic dispatch model WILMAR Join Market Model (WILMAR JMM) and network analysis performed with PSS®E. It was also planned to define offshore grid structures using a grid optimization tool Net-Op but this part was left out due to time reasons.

First, a set of offshore DC grid structures is defined with Balmorel. Next, WILMAR JMM is run to get insight into electricity market impacts of the DC grid options and to determine hourly generation and load snapshots. A network model of the power systems in the Baltic Sea region is implemented in order to study the power flows in more detail than a pure unit commitment and economic dispatch model allows. Finally, power flows are analysed with the network model and PSS®E to check in technical sense the feasibility of some of the power system situation snapshots determined by WILMAR JMM.

Chapter 2 describes the methods, models and tools used in the analysis. Chapter 3 describes the scenarios about future electricity demand, generation capacities, fuel costs and HVDC component costs. Different grid topology type scenarios are defined in that chapter as well. Results from Balmorel, WILMAR JMM and PSS®E calculations are presented in Chapter 4. Chapter 5 discusses possible flaws in the method as well as technical risks in the different offshore grid topologies. Chapter 6 draws conclusions from the results. Finally, Chapter 7 summarizes the whole report.

Initial methods planned for the study and its preliminary results have been described in [9] and [10]; however, this report presents the final results from the study and the methodology that was used to obtain those.

2. Models and methodology

2.1 Overview of the methodology

This study includes several models and tools for the purpose of combined investment optimization, unit commitment and economic dispatch simulation and power flow analysis. These models and tools are described in Sections 2.2, 2.3 and 2.4. Section 2.5 describes the case study procedure as a whole. The basis for the grid planning consisted of the power systems onshore and the offshore wind power plant plans in the Baltic Sea. The data for these as well as other scenario data are described in Chapter 3.

2.2 Grid investment optimization

2.2.1 Grid investment optimization in general

Before the actual grid investment optimization, offshore wind power plants were combined suitably to form wind clusters, which operate as nodes in the offshore DC grid. The clustering was carried out using k-means method with the criterion that each country should benefit from the wind power plants belonging to the country. The intention was that in the offshore grid structure optimization, the wind power plant should become connected to the country it belongs to through the offshore grid. For example, if a wind power plant belonging to Sweden is clustered together with a group of Finnish wind power plants, the centre of the cluster will be very close to Finland and this will make the cluster likely to be connected only to Finland in the grid structure optimization phase. The number of clusters can be affected by specifying a maximum distance between a wind power plant and the cluster node and a maximum power rating within a cluster. The number of wind power plant clusters in this study was 22.

Suitable onshore connection points for the offshore grid were assumed to be existing and planned stations near offshore wind clusters. One onshore connection point was also selected from the southern part of Germany because the connection capacity in the coastal area of Germany may be insufficient. Rough estimates for potential connection capacities were made based on the number of existing and planned lines connected to the station and typical thermal limits of the lines. The number of onshore connection points was 17.

Figure 1 shows the location of offshore wind power plants and offshore wind clusters in the case studies as well as the location of onshore connection points for the offshore grid.

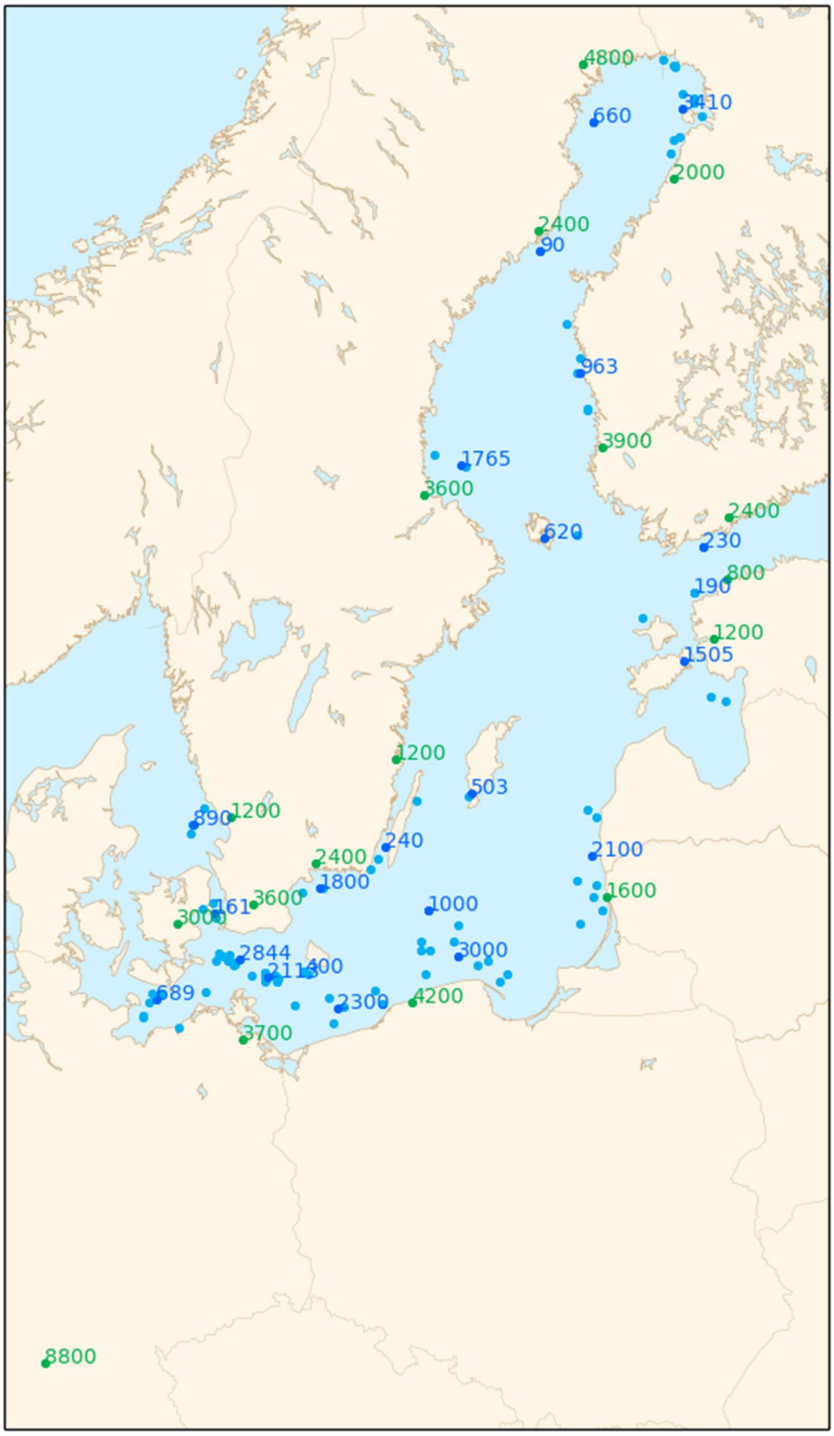

Figure 1 Wind power plants (light blue) and clusters (blue) as well as onshore connection points (green). The numbers show the wind cluster capacities and onshore connection point capacities in megawatts. Notice that for Germany, one onshore connection point was selected deeper from the continent because the connection capacity in the coastal area of Germany may be insufficient.

After the pre-clustering of the wind power plants and the determination of connection points and their potential connection capacities, follows the actual offshore grid investment optimization. Offshore grid topology types taken into consideration in this study include the following (see Figure 2):

1. Radial connection between each offshore wind power plant cluster and the onshore grid
2. Radial connection between each offshore wind power plant cluster and the onshore grid with separate two-terminal interconnections between regions
3. Multi-terminal offshore grid connecting wind power plant clusters and regions together, separate two-terminal interconnections between regions not allowed
4. Multi-terminal offshore grid connecting wind power plant clusters and regions together, separate two-terminal interconnections between regions allowed.

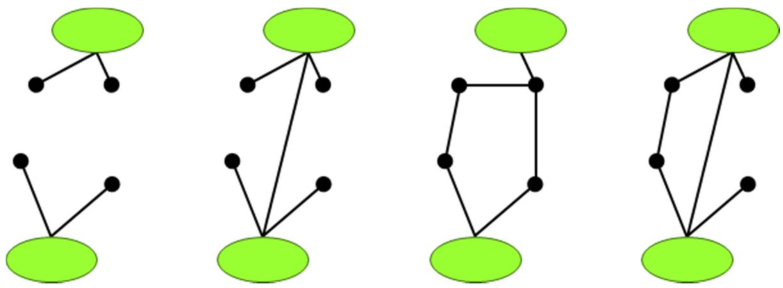

Figure 2 Offshore grid design types.

2.2.2 Net-Op

Net-Op (Network Optimisation tool) was originally planned to be used in this study to create different offshore grid designs, but it was left out due to time reasons and difficulties in getting the model to see the impact of wind power on the power prices. Net-Op is developed at SINTEF – NTNU for high level strategic planning of wind farm clustering and grid connection [11],[12]. It is capable of finding an optimal grid structure by taking into account the wind power variations, stochastic power prices, and load and generation scenarios (onshore and offshore). The power flow in the grid is modelled with transportation model. The results of the optimization are which cables to be built alongside with the type and capacity of the cables.

Following the work presented in [11] and [12], the network optimization is formulated as follows:

$min(C^T X)$, subject to $AX \leq b$

where C is cost coefficient vector and $X = \left[x_c, x_p, x_g, y_b, y_n\right]^T$ is the state variable vector which composed of the following continuous (x) and integer (y) variables :

x_c	=	Branch capacity
x_p	=	Branch power flow
x_q	=	Generator output
y_b	=	Number of cables or converters per branch
y_n	=	Number of substations per node

The matrix A and vector b are the constraints for the optimization problem, as follows:

i. the sum of the power flow at each node is zero (power balance)

ii. the sum of the power flow out of (or into) each node does not exceed the node capacity

iii. the output of each generator must be less than or equal to its available capacity

iv. the power flow of each branch does not exceed its branch capacity

v. each branch capacity is determined by the number of cables it contains

vi. each branch must have a substation at both ends

Compared with the constraint formulation in [11] and [12], constraint (ii) has been added to include the capacity of each node.

The following linear cost functions have been used to model the costs of branches, nodes and generation:

$$C_{Tot}^{bran} = \left(B + B_d \cdot D + B_{dp} \cdot D \cdot P\right) + \sum\left(C^L + C_p^L \cdot P\right) + \sum\left(C^S + C_p^S \cdot P\right)$$

$$C_{Tot}^{node} = \sum N^S + \sum N^L$$

$$C_{Tot}^{geno} = NPV\left\{P_g(t) \cdot mg_g(t)\right\}$$

where C_{Tot}^{bran}, C_{Tot}^{node}, and C_{Tot}^{geno} are the total branch cost, total node (platform) cost, and total cost of generation, respectively. Parameter B denotes the branch cost parameter with subscripts d and p represent the parameter is proportional to distance and power rating, respectively. Parameter C models the costs of the branch endpoint connections, with superscripts L and S denoting the endpoint is located onshore or offshore, respectively. The parameter D is the distance of the branch, N is the node costs, and P is the power rating of the branch. The term $NPV\{\cdot\}$ refers to the net present value function, $mg_g(t)$ and $P_g(t)$ denote the marginal cost of the generator and power generation at time t, respectively. The discount rates involved in the NPV calculation are 2% of operation and maintenance cost rate and 8% discount rate, for a total period of 20 years.

Offshore nodes, onshore connection points with their potential connection capacities, and cost parameters are given as input for the grid optimization tool Net-Op. Cost parameters for DC lines and VSC converters are obtained from [12]. The number of possible grid structures is typically extremely large, but the problem can be downscaled by specifying a set of allowable connections explicitly. Wind power variations, stochastic power prices, load and generation scenarios as well as grid constraints need to be taken into account when finding the optimal grid design. Therefore, the optimization of the grid structure with Net-Op was combined with a power market and network model in an iterative manner.

2.2.3 Balmorel

Balmorel was the model used to create different offshore grid designs in this study. Wind power plant clustering as well as connection point capacity determination was done before running Balmorel.

Balmorel is a regional generation planning model that minimizes total investment and operation costs taking into account the balance of supply and demand of electricity and heat [13],[14]. Figure 3 shows the division of price regions in this study. The transmission between the regions is limited by net transfer capacities. Balmorel includes deterministic time series for load, wind power and photovoltaics (PV). Power plant capacity restrictions and efficiencies as well as storage capacity limits are taken into account in Balmorel. The model also requires a proportion of the generation capacity to be set aside for reserve power demand. In this study, three weeks were selected to represent the whole annual variation in times series. Balmorel is capable of optimizing the investments to both new generation and transmission capacity. In this study however, the possibility to invest in new generation capacity was disabled and Balmorel was allowed to invest only in new transmission capacity.

In this study, Balmorel was run in linear programming mode which required that HVDC component costs needed to be linearized. Linearized costs result easily in very small transmission line capacities (e.g., a few megawatts) between some regions. To avoid such unrealistic investments, Balmorel was modified so that after the first optimization, all new lines smaller than 50 MW were removed and the capacity of the rest of the new lines was optimized again. After the second, third, fourth and fifth round, the same procedure was repeated for all lines smaller than 100 MW, 200 MW, 300 MW and 400 MW, respectively. However, a connection from each wind cluster to one onshore connection point was always allowed, even if the capacity had been smaller than the aforementioned limits.

To downscale the optimization problem, a set of allowable connections was selected from the total set of possible connections. To study different grid topologies, several cases were created and the set of allowable connections was altered between the cases.

2.3 Unit commitment and economic dispatch simulation

A unit commitment and economic dispatch model WILMAR Joint Market Model (WILMAR JMM) was used in this study for optimizing the operation of generation units taking into account several operational constraints. The model also gives power prices as a result.

WILMAR JMM simulates a zonal market design with liquid spot, intra-day, and balancing markets [15]. It minimizes the operational costs of the interconnected power system assuming transmission constraints based on net transfer capacities. The model procures reserves dynamically based on the forecast stochastics in addition to more conventional reserve requirements. It includes unit start-ups, part-load efficiencies, forecast errors for wind power and demand, CHP (combined heat and power) plants serving heat demand in district heating, as well as a separate model for calculating the water value for the reservoir hydro power.

In this study, WILMAR JMM was run in linear programming mode. One year of market operation with hourly dispatch resolution was simulated with WILMAR JMM for each offshore grid option. Day-ahead wind power and load forecasts were held until the hour of operation. The first three hours of the 36-hour model horizon contained realized wind power and electricity demand and these were the final results from the model. The division of price regions was the same as in Balmorel.

2.4 Power flow calculation

A sufficiently detailed power flow model was needed for studying the impacts of offshore DC grid options and new large offshore wind power plants on the power system. Results can only be as good as the models used, and there is no reason in using sophisticated calculation methods if the model input data itself contains significant errors.

Power injections at bus *s* can be expressed as [16]

$$P_s = \sum_{r=1}^{N} |V_s||Y_{sr}||V_r| \cos(\theta_{sr} + \delta_r - \delta_s)$$

$$Q_s = -\sum_{r=1}^{N} |V_s||Y_{sr}||V_r| \sin(\theta_{sr} + \delta_r - \delta_s)$$

where θ_{sr} is the angle of self or mutual admittance Y_{sr}, δ_s is the angle of voltage V_s and δ_r is the angle of voltage V_r. *N* is number of buses in the system. Self and mutual admittances are defined as

$$Y_{ss} = \sum_{r=0, r \neq s}^{N} y_{sr}$$

$$Y_{sr, r \neq s} = -y_{sr}$$

where y_{sr} is the admittance between buses *s* and *r*. Bus $r = 0$ refers to ground. In complete nonlinear power flow solution methods, bus voltages and voltage angles are first solved using iterative solution methods. After that, power flows on transmission lines can be calculated.

With complete nonlinear power flow ('AC power flow') studies, it is possible to achieve accurate steady state security results. The method also gives insight to undervoltages and overvoltages. However, the method requires accurate power system models in the aspect of electrical parameters and voltage control strategies. HVDC link models also need to be accurate. AC power flow method requires iterative solution methods and without good start values the convergence of the calculation becomes a real challenge. Modifying the voltage control strategies in the model in order to get a converging solution may give as unrealistic results as linearized power flow ('DC power flow') method, which does not cover voltage control and reactive power at all.

In DC power flow, resistances and capacitances in the π-representation of a line are neglected, therefore $y_{sr,r \neq 0}$ becomes purely reactive and $y_{s0} = 0$. In addition, the voltage profile is assumed to be flat ($|V_s| \approx |V_r| \approx 1$ per unit) and voltage angle differences are assumed to be small ($\sin(\delta_s - \delta_r) \approx \delta_s - \delta_r$ and $\cos(\delta_s - \delta_r) \approx 1$).

The combined grid model, used in this study for the first time, includes the existing power system model of the Baltic Sea region. The model depicts the power system with a very detailed representation at some parts and with a more generalized at other parts. The model is intended for linearized power flow analysis with PSS®E software. Figure 3 shows the lines and stations in the grid model.

Norwegian and Swedish power systems were represented with 23 generator model developed at SINTEF [17]. The model was originally intended for studying slow dynamic phenomena as control of frequency and active power. A reduced wind power grid model developed at Energinet.dk was used to represent the power system of eastern Denmark [18]. Previously, the model has been used in research to investigate the impact of grid faults on wind turbines and on the power system itself and in education to illustrate different problems regarding stability. Western Denmark, Germany and Poland were represented with a model developed at the University of Edinburgh [19]. The original model includes the whole synchronous power system of Continental Europe, and it is suitable for DC power flow studies. Only the representations of western Denmark, Germany and Poland were included in this study. The power systems of Baltic countries were represented with a power flow model that is based on the model constructed by Belonogova [20]. The model includes several dozen nodes and lines. The power system of Finland was represented with a detailed power flow model of the Finnish transmission grid [21]. The model has been developed at VTT Technical Research Centre of Finland (VTT) and it includes over 400 nodes and transmission lines. The model has been constructed based on publically available data. Appendix A describes the main data of the components in the model.

The grid models described above were combined together with interconnectors. The combined grid model was updated with additional data and new lines where necessary. Each offshore grid structure to be studied was implemented to the combined grid model separately. Multi-terminal offshore grids were modelled using voltage controlling generators in PSS®E.

Most of the submodels in the combined grid model are intended for complete nonlinear power flow analysis. However, since this is not the case with all of the submodels, the analysis in this study was performed using linearized power flow equations in PSS®E, i.e., DC power flow. The power flow on a branch between buses *s* and *r* in this method is defined as

$$P_{sr} = \frac{\delta_s - \delta_r}{x_{sr}}$$

where δ_s and δ_r are the angles of the voltages at buses *s* and *r,* respectively, and x_{sr} is the reactance between the buses *s* and *r*. Power injection at bus *s* is simply

$$P_s = \sum_{r=1}^{N} P_{sr} = \sum_{r=1}^{N} \frac{\delta_s - \delta_r}{x_{sr}}.$$

Contrary to a standard DC power flow method, transmission line losses are approximated by adding them as loads to the sending ends of branches [22].

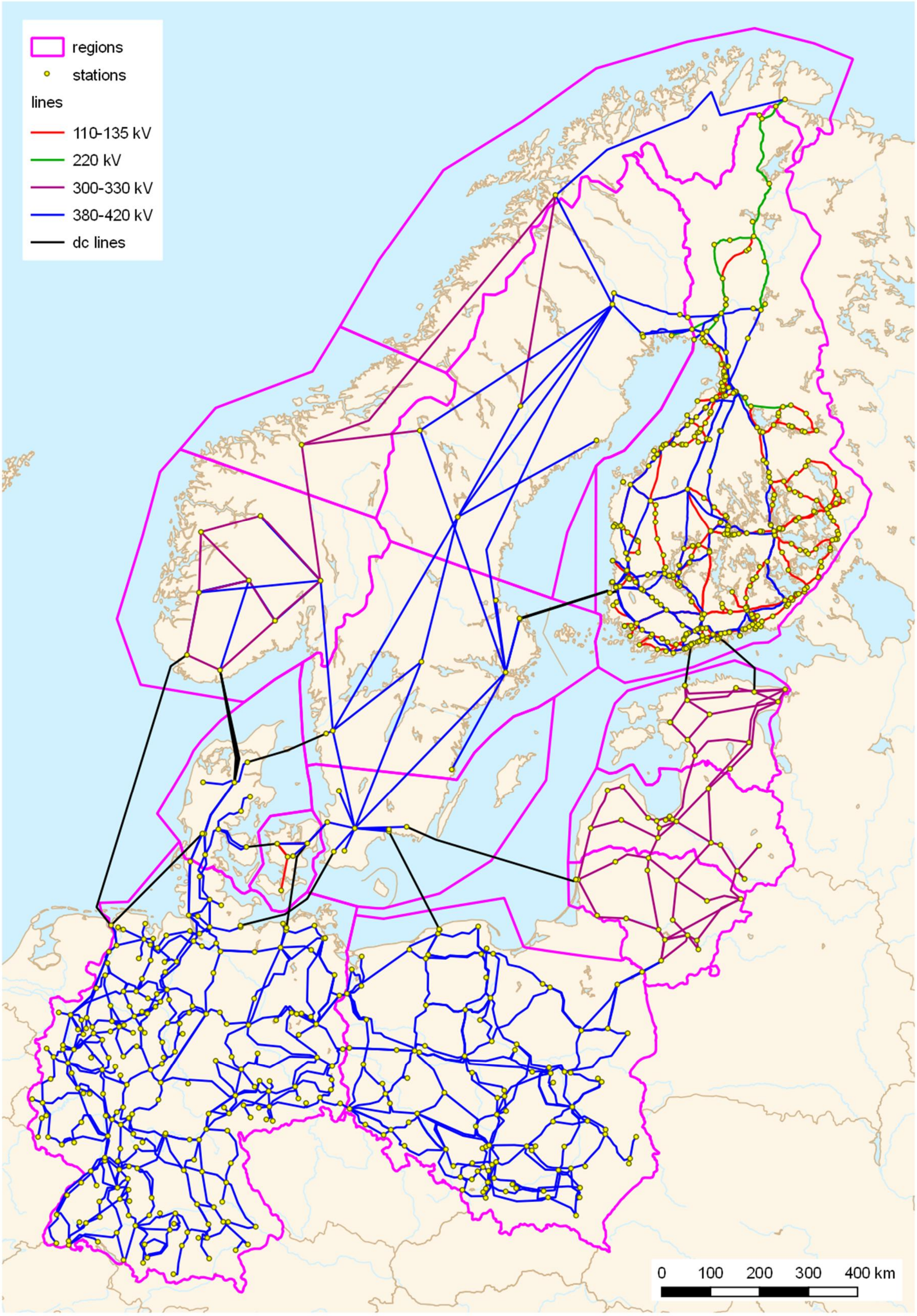

Figure 3 Price areas in the unit commitment and economic dispatch model as well as lines and stations in the combined grid model.

2.5 Case study procedure

The case study procedure consisted of offshore wind power plant clustering, onshore connection point determination, offshore grid structure optimization, unit commitment and economic dispatch simulation and power flow calculation. In the selected methodology, Balmorel was used for offshore grid structure optimization. Figure 4 shows the linkage of the three major models in the selected methodology in simplified form as well as how Net-Op was planned to be linked with the other models.

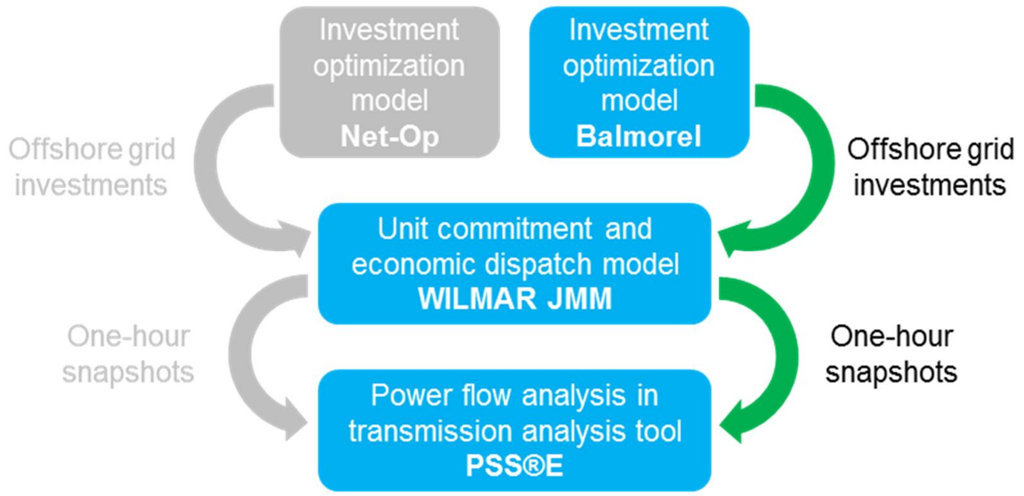

Figure 4 Simplified representation of the selected methodology with Balmorel shown with colours and the abandoned methodology with Net-Op greyed out.

The planned iterative case study procedure with Net-Op is presented in Figure 5. As the case study procedure with Net-Op did not function as expected, it was decided to utilize the existing link between WILMAR JMM and Balmorel. The case study procedure with Balmorel is shown in Figure 6. Both figures also show inputs and outputs of the models and possible iteration processes.

Modelling framework Sceleton [23] developed at VTT was utilized for linking the different optimization and calculation models together and for automating data transfer between them. A data transfer system based on FTP (File Transfer Protocol) was also implemented in Sceleton to handle data transfer between Net-Op run at NTNU and the models run at VTT and to start running models automatically when new input is available.

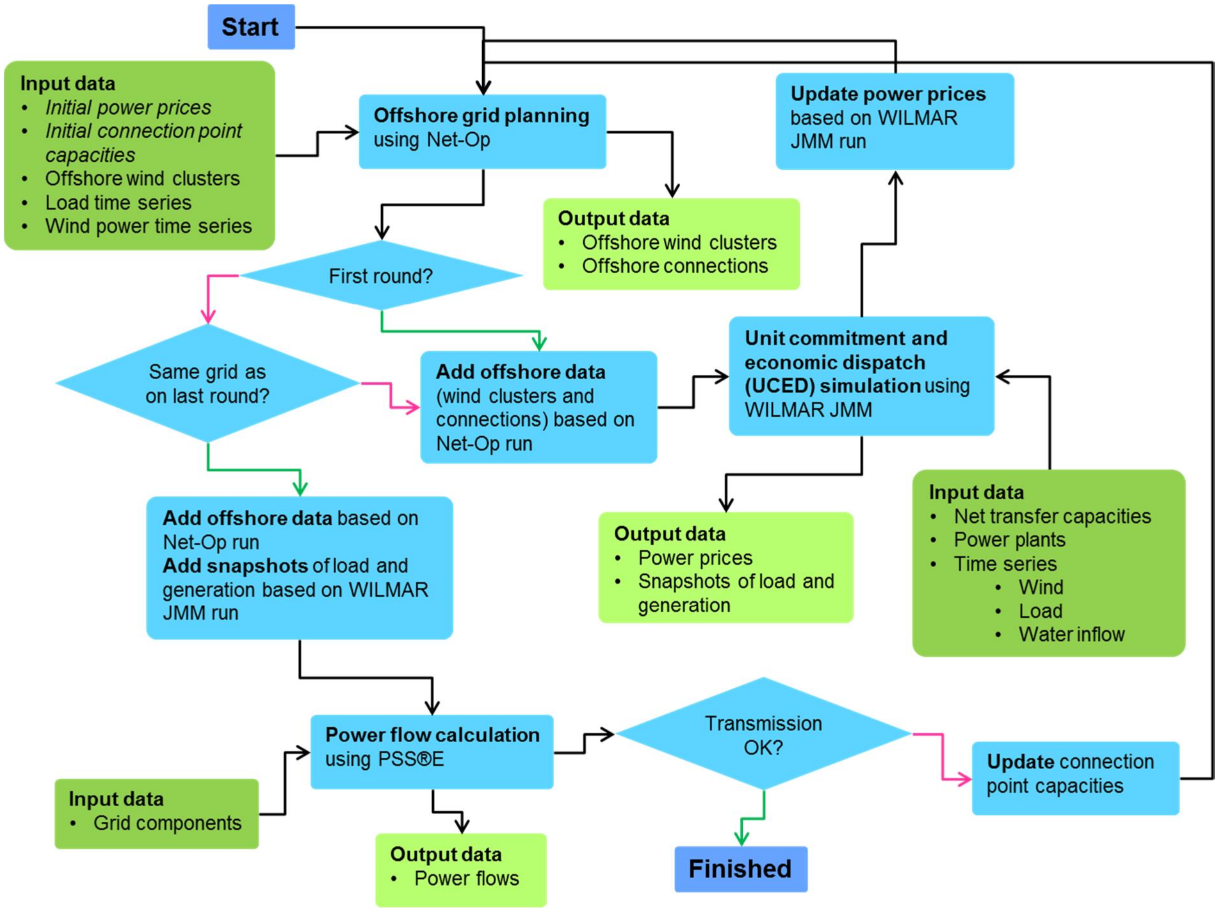

Figure 5 The planned case study procedure with Net-Op. Red arrows denote answer 'no' and green arrows denote answer 'yes'.

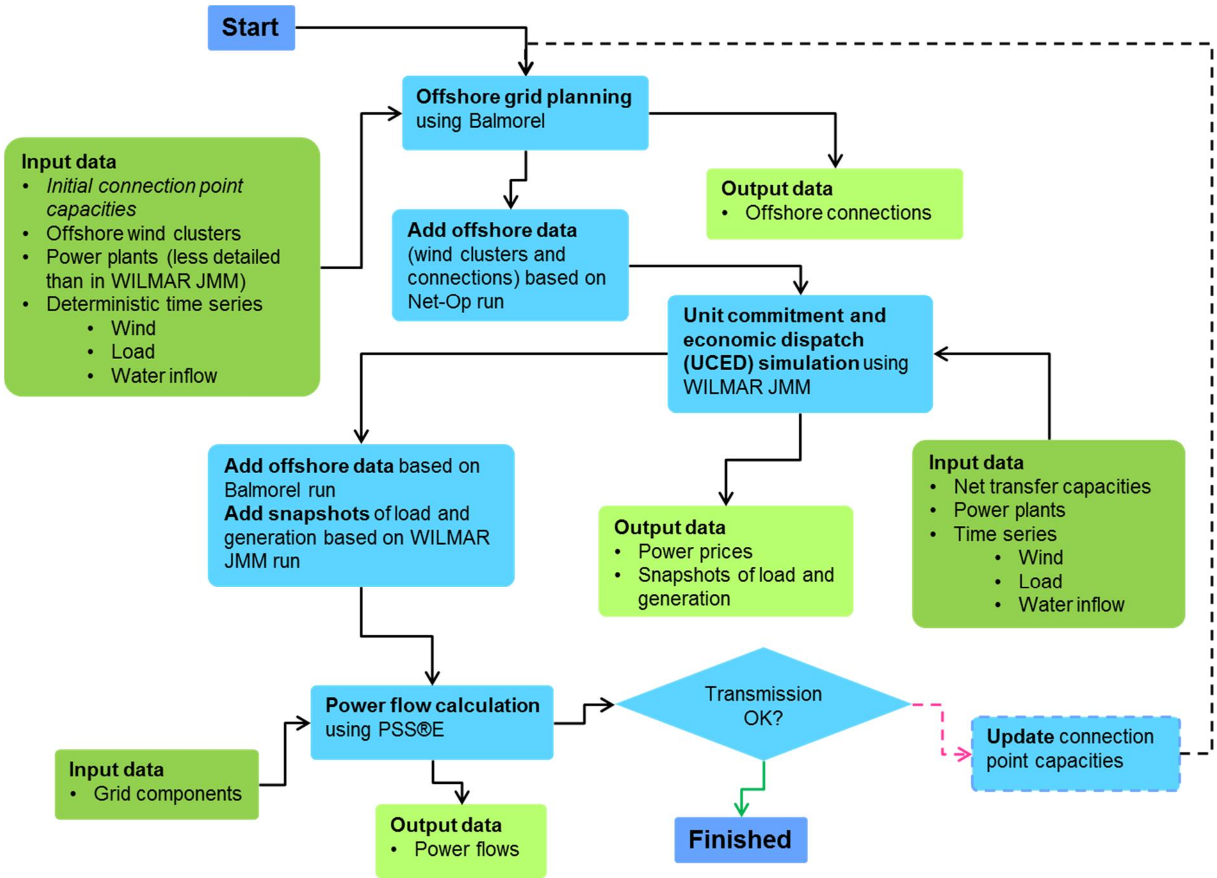

Figure 6 The case study procedure with Balmorel. Red arrows denote answer 'no' and green arrows denote answer 'yes'. Dashed lines denote processes that were planned but were found difficult to implement due to insufficient data about the onshore grids.

First, wind power plants in the Baltic Sea were clustered suitably and onshore connection points together with their estimated connection capacities were selected. Second, offshore DC grid structures were optimized with Balmorel and the investment costs in different cases were compared.

After this, WILMAR JMM was run to calculate, e.g., the operation costs, electricity production per fuel and CO_2 emissions in different offshore grid cases as well as to determine the hourly generation and load snapshots. Possibly difficult power flow situations were selected based on load and wind levels for further power flow studies.

Linearized power flow calculation was carried out in PSS®E for checking in technical sense the feasibility of power system situation snapshots. The power flow studies focused on power transfers on the lines and not on voltage levels, since the linearized power flow method does not give insight into them. Typical thermal ratings found from the literature and net transfer capacities published by transmission system operators (TSO) were taken into account in the studies. However, it is important to note that there may be significant constraints that occur only when examining N−1 faults and the dynamics of the power system.

3. Scenarios

3.1 Geographical extent and time horizon

The geographical extent in the study was the Baltic Sea region. The power systems of Norway, Sweden, Finland, Estonia, Latvia, Lithuania, Poland, Germany and Denmark were included in the modelling. Scenarios for wind power, other generation, load and onshore grid reinforcements were defined in the frame of 2020–2030.

3.2 Generation

The creation of wind power scenarios consisted of finding out the locations and capacities of planned wind power plants, clustering the offshore wind power plants suitably and creating realistic wind power time series for the offshore clusters and onshore areas.

The scenario for both offshore wind power plant and aggregated onshore wind power plant locations and capacities was mainly based on TWENTIES project. The capacities in the case studies corresponded to the high wind scenario in TWENTIES with some modifications [24]. Table 1 and Figure 7 present the installed capacities in the case studies. The installed wind power capacity on large islands Gotland and Åland, which were counted as possible offshore grid nodes in this study, was increased with 500 MW on each compared to TWENTIES scenarios.

Table 1 The scenario for installed offshore and onshore wind power capacities

	Offshore wind (MW)[1]	Onshore wind (MW)
Denmark	1824	5000
Estonia	1695	700
Finland	5223	2500
Germany	3853	55100
Latvia	1100	300
Lithuania	1000	1300
Norway	-	4300
Poland	5300	13400
Sweden	7498	8100
Total	27473	93300

[1] In the Baltic Sea
-, not applicable

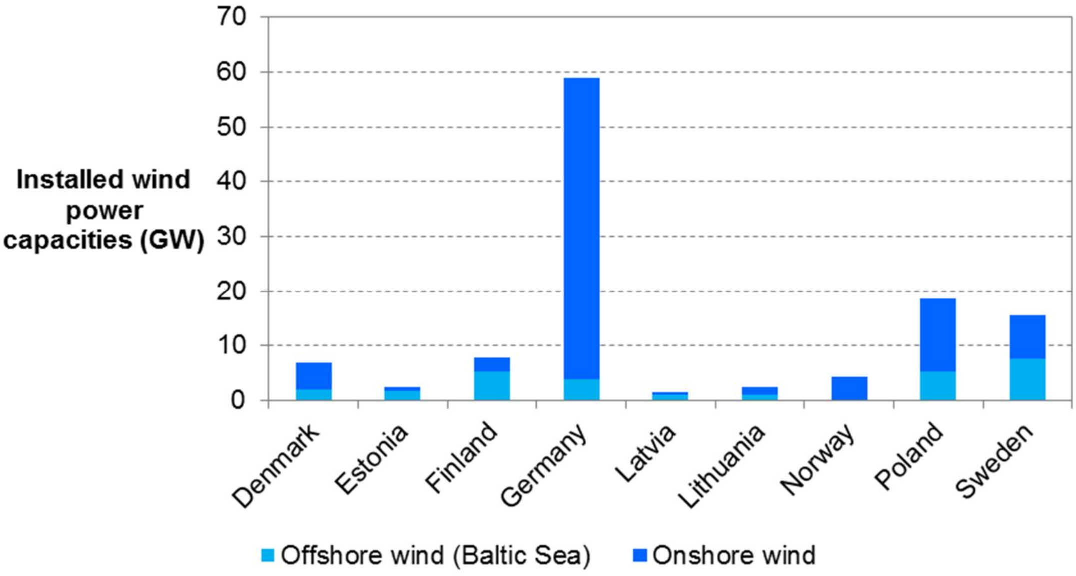

Figure 7 The scenario for installed offshore and onshore wind power capacities.

Wind power time series for each offshore wind cluster were simulated with CorWind power time series simulation model, developed at Risø DTU [25],[26]. When possible, historical wind power time series and day-ahead forecasts from Nord Pool Spot and TSO websites were utilized. Figure 1 on page 10 shows the location of offshore wind power plants and offshore wind clusters in the case studies.

The assumption for other generation capacity than wind power in each country was mainly based on the present and near-future data as provided by Platts in World Electric Power Plants Database and by national energy authorities. Table 2, Figure 8 and Figure 9 present the installed generation capacities in the case studies with offshore wind power lumped into an imaginary country 'Baltic Sea'.

Table 2 The scenario for installed generation capacities per country and fuel (MW). Offshore wind power summed to an imaginary country 'Baltic Sea'.

	Natural gas	Other fossil	Nuclear	Bio	Hydro	Solar	Wind	Pumped hydro
Denmark	2148	5421	0	904	0	0	5000	0
Estonia	369	1068	0	72	0	0	700	0
Finland	1293	3542	4352	1856	3141	0	2500	0
Germany	23562	40637	0	2766	9873	40000	55100	2798
Latvia	698	448	0	33	1512	0	300	0
Lithuania	1244	75	0	31	101	0	1300	1125
Norway	0	188	0	0	25433	0	4300	0
Poland	6333	36025	0	277	767	0	13400	2252
Sweden	551	3051	10167	733	16242	78	8100	0
Baltic Sea	0	0	0	0	0	0	27473	0
Total	36198	90456	14519	6672	57069	40078	118173	6175

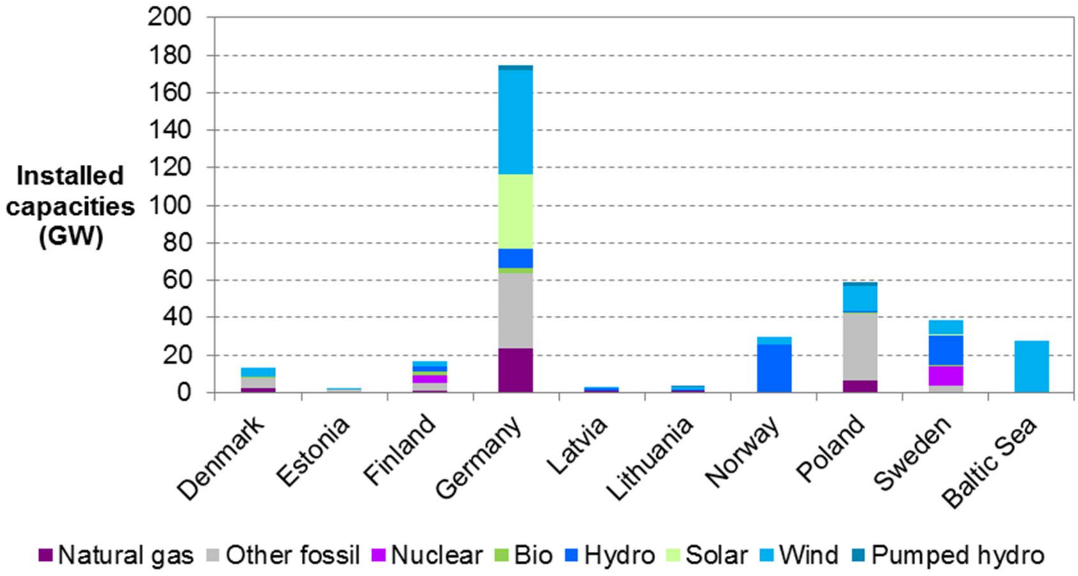

Figure 8 The scenario for installed generation capacities (GW) per country and fuel. Offshore wind power summed to an imaginary country 'Baltic Sea'.

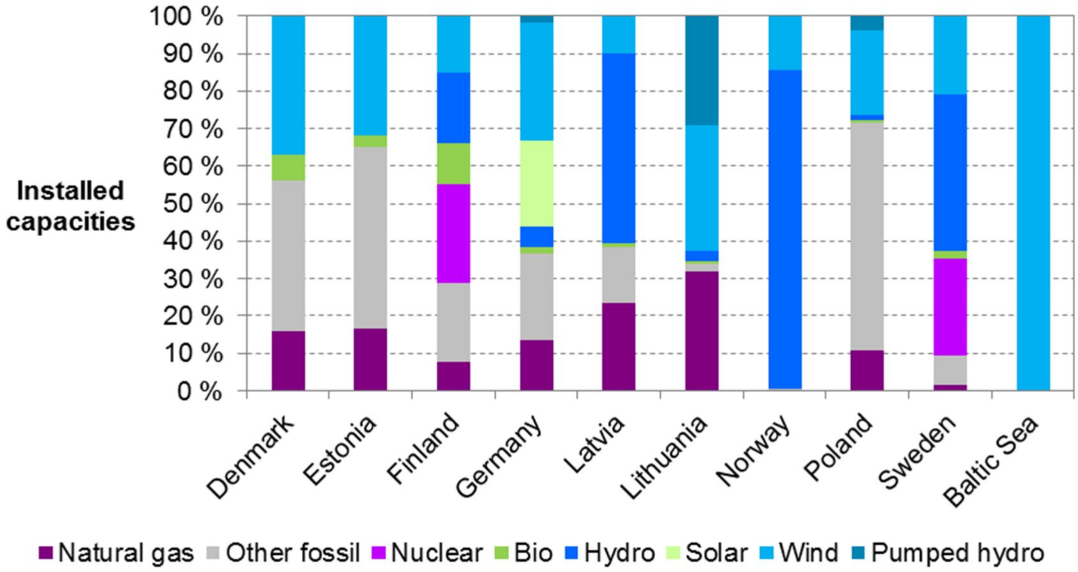

Figure 9 The scenario for installed generation capacities in each country per fuel (%). Offshore wind power summed to an imaginary country 'Baltic Sea'.

Table 3 and Figure 10 present the assumption for prices and CO_2 contents of fuels. CO_2 price was assumed to be 25 €/(t CO_2).

Table 3 Assumption for fuel prices and CO_2 contents

	Fuel price (€/GJ)	CO_2 content (kg/GJ)
Coal	4.5	95
Fuel oil	12	78
Light oil	15	74
Lignite	3.5	101
Municipal waste	0	19
Natural gas	8.5	56.9
Nuclear	1.5	0
Orimulsion	1.5	80
Peat	3.5	107
Shale	1.5	106
Straw	4.5	0
Sun	0	0
Water	0	0
Wind	0	0
Wood	5	0
Wood waste	2.5	0

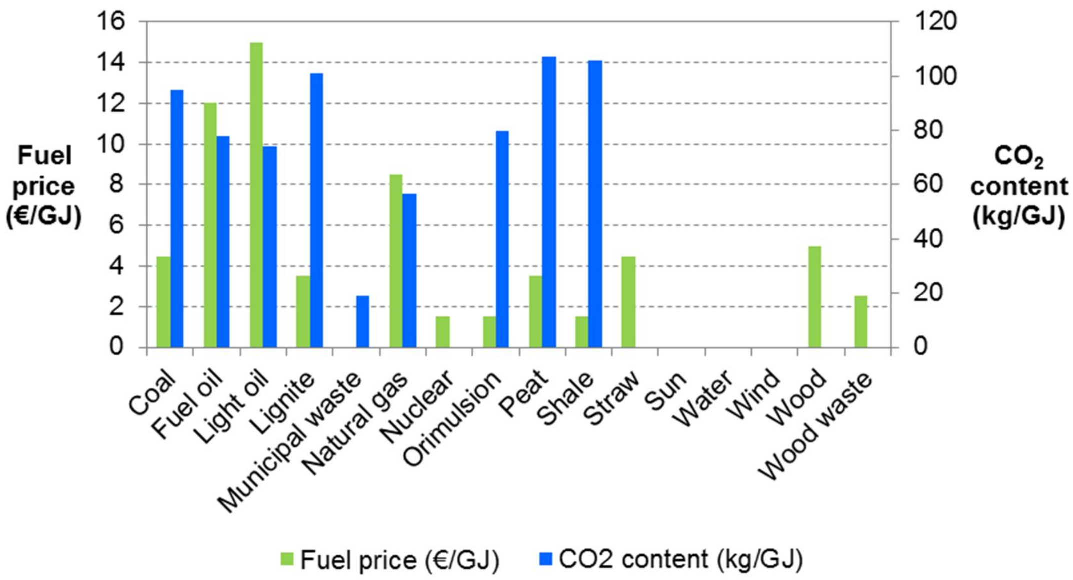

Figure 10 Assumption for fuel prices and CO_2 contents.

3.3 Load

Table 4 and Figure 11 present the assumption for annual demand in each country. The values are based on [27]. The values were further divided into annual demands in each price region. Hourly load variation for each price region was obtained from Nord Pool Spot and ENTSO-E [28],[29]. The hourly profiles were scaled to meet the annual demand in the future scenario.

Table 4 Assumption for annual electricity demands

	Annual demand (TWh)
Denmark	39.1
Estonia	9.2
Finland	90.9
Germany	581.1
Latvia	8.7
Lithuania	10.9
Norway	148.0
Poland	165.3
Sweden	143.1
Total	1173.9

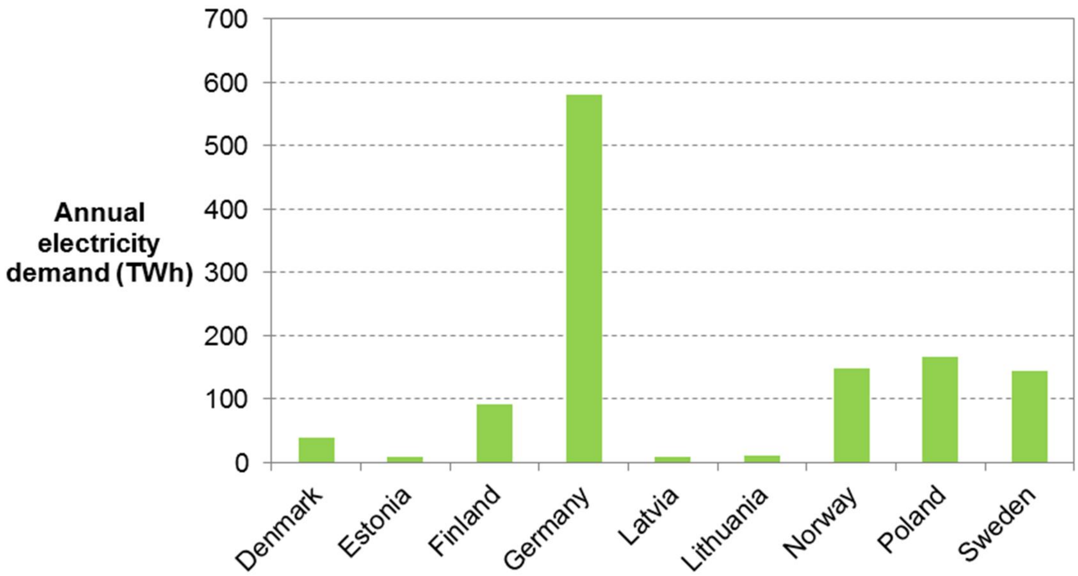

Figure 11 Assumption for annual electricity demands.

3.4 Onshore grid

Grid reinforcement plans taken into account in the study were obtained from ENTSO-E's Ten Year Network Development Plan (TYNDP) [30]. The most recent TYNDP, published in 2014, covers time horizon up to 2030. TYNDP includes several projects with status 'under consideration', and not all of the projects have been modelled in the future onshore grid scenario in this study.

Figure 3 on page 16 shows the whole grid model while Figure 1 on page 10 shows the locations of onshore connection points for the offshore grid. Figure 12 presents the net transfer capacities in Balmorel and WILMAR JMM.

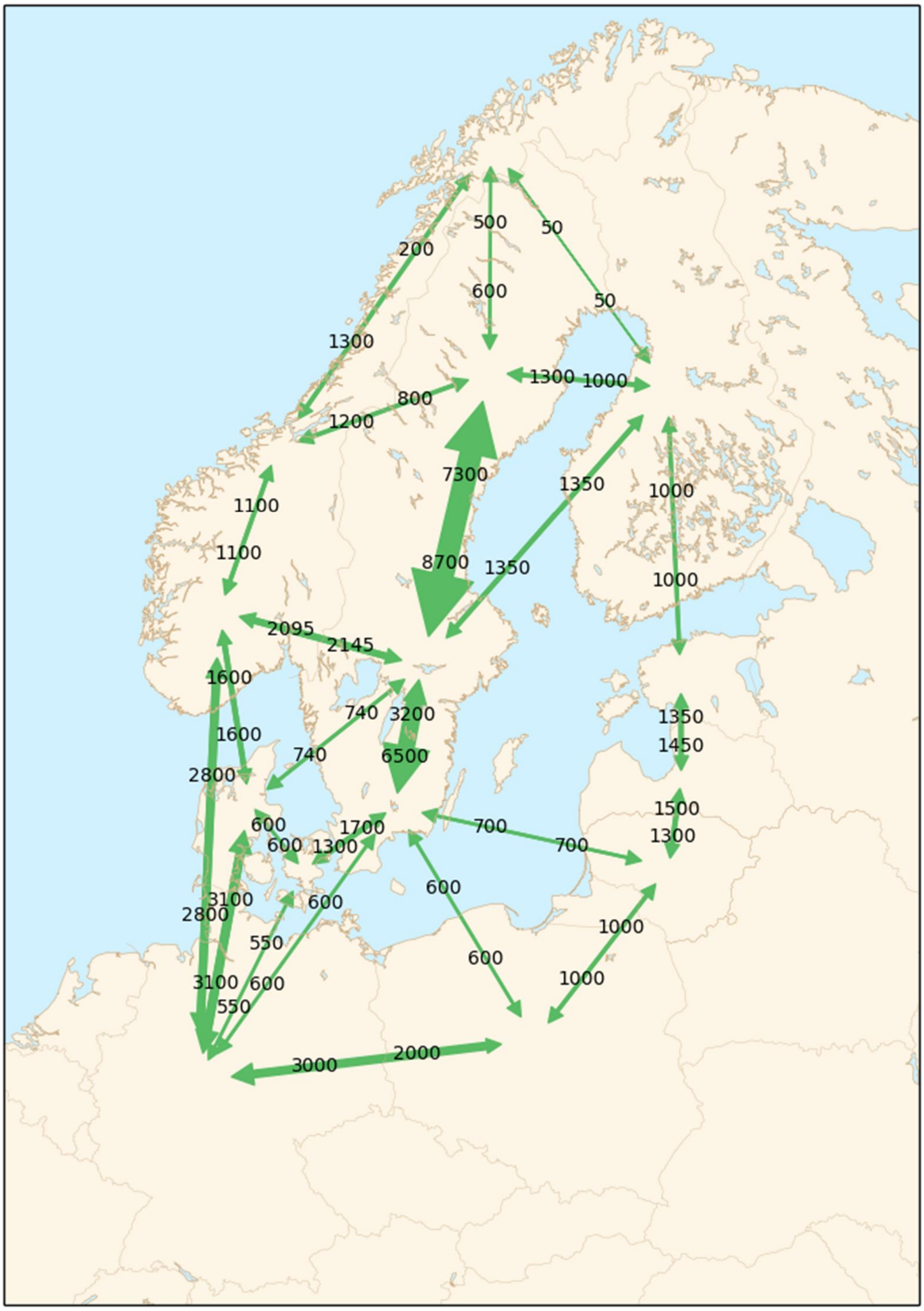

Figure 12 Net transfer capacity limits in the study.

3.5 HVDC components

Table 5 depicts the assumed losses in HVDC components. For example, a 500-km long HVDC connection would have losses of 3 % of transmitted power, consisting of converter station losses of 1 % and cable losses of 2 %.

Table 5 HVDC component losses of transmitted power

Component	Losses
Cable/Line	4 % per 1000 km
Converter station	0.5 % per station

Table 6 describes the linearized HVDC component costs in the optimization with Balmorel. The cost estimates in the *High* cost scenario were determined by linear estimation based on data of existing and planned HVDC connections that had capacities 400–1400 MW. The *Medium* cost scenario assumed 13–23 % and *Low* cost scenario 26–46 % reduction in cable and converter station costs. Two assumptions for offshore converter stations were made: they would be either 50 % or 100 % more expensive than onshore converter stations. The offshore converter station cost was assumed to include, e.g., platform costs. A 500-km long offshore-to-shore connection would cost 900,000 €/MW using the *Medium* cost estimates and 50 % increase in offshore station costs. It was assumed that Gotland, Åland and Hiiumaa islands will accommodate onshore converter stations and all the other offshore wind clusters will have offshore converter stations.

Table 6 Linearized HVDC component costs

Component	Low cost	Medium cost	High cost
Cable/Line	1,100 €/MW/km	1,300 €/MW/km	1,500 €/MW/km
Onshore station	70,000 €/MW	100,000 €/MW	130,000 €/MW
Offshore station (50 % [1])	105,000 €/MW	150,000 €/MW	195,000 €/MW
Offshore station (100 % [1])	140,000 €/MW	200,000 €/MW	260,000 €/MW

[1] More expensive than onshore station

Figure 13 explains different offshore grid implementation options and how they were modelled in this study. In Balmorel, offshore DC grid investments were linearized, and truly multi-terminal links were not modelled. The optimization was performed for two-terminal links and the investment cost was first calculated for such links. However, a comparison was made after the grid optimization by calculating the costs of possible multi-terminal grid solutions consisting of two-terminal links as if they were truly multi-terminal grid solutions. Excess converter stations were removed from the end of the cables, new converter stations were added for wind clusters and HVDC circuit breakers were added to protect the components (compare bottom left and top left schemes in Figure 13). The capacity of the wind cluster converter was assumed to be the minimum of the numbers x_1 and x_2, where x_1 is the sum of the HVDC cable capacity connected to the node and x_2 is the wind cluster capacity. Two cost assumptions were made; the cost of an HVDC circuit breaker was assumed to be one fourth or one eighth of the converter station cost in Table 6; e.g., an HVDC circuit breaker located on an offshore platform was assumed to cost either 37,500 €/MW or 18,750 €/MW in the *Medium* cost scenario.

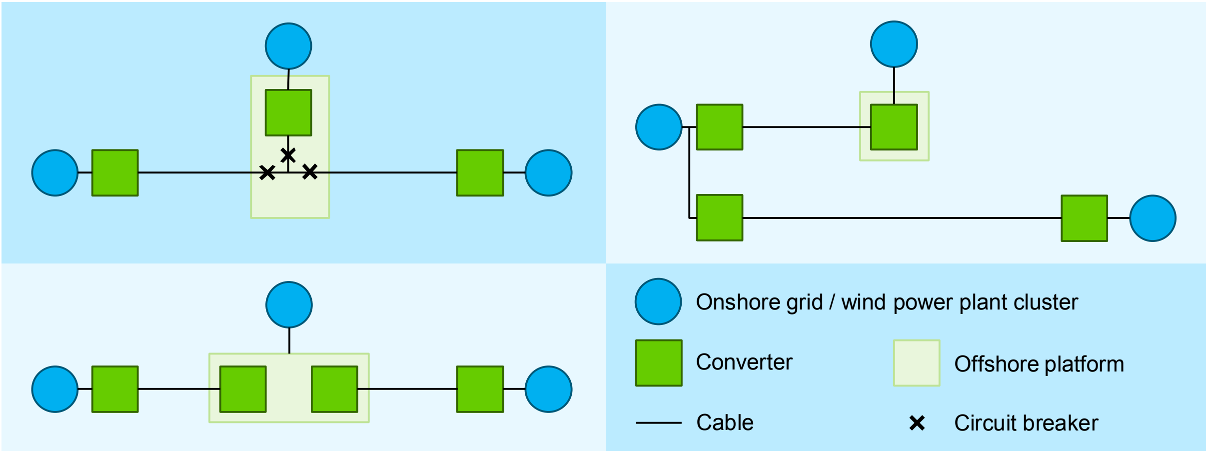

Figure 13 Offshore grid implementation options. Top left: multi-terminal grid solution. Top right: grid solution with two-terminal links. Bottom left: "multi-terminal" grid solution with two-terminal links.

3.6 Offshore grid topology cases

To downscale the grid optimization problem due to computing reasons and to see the effect of different topology types, four different topology cases based on Figure 2 were studied. The first case is called *Limited* (abbreviated to *Lim*) and in that case only one connection from each offshore wind cluster to the shore was allowed. No connections between wind clusters or between onshore connection points were allowed. Figure 14 shows the allowable connections in *Limited* case as well as in the three other cases. Balmorel was let to optimize the capacity of the connections.

The second case is called *Onshore* (*On*). It included the same set of allowable connections as in *Limited*. The connections were possible on each iteration round in Balmorel even if their capacity had been very small. Few additional offshore-to-shore connections were also allowed, mainly in the region between Denmark, Germany and Sweden. In this case, it was also possible to connect wind clusters to the onshore connection point in southern Germany. Interconnections between onshore connection points were also allowed (hence the name *Onshore*). These connections were possible in Balmorel only if their capacity had been large enough on the previous iteration round in Balmorel.

The third case *Offshore* (*Off*) included almost the same set of allowable connections as in *Limited*. Two offshore-to-shore connections in the southern part of the Baltic Sea were changed to offshore-to-offshore connections because in this way it was possible to get shorter connections while still eventually connecting the wind clusters to the same countries as in *Limited* and *Onshore* cases. Balmorel was let to invest in these connections on every iteration round. As in *Onshore* case, few additional offshore-to-shore connections and connections to southern Germany were also allowed. Interconnections between onshore connection points were not allowed. Instead, wind clusters were allowed to be connected to each other (hence the name *Offshore*). These connections were possible in Balmorel only if their capacity had been large enough on the previous iteration round.

The fourth case includes manually defined set of mixed shore-to-shore, offshore-to-shore and offshore-to-offshore connections, and hence this case is called *Mix*. The same set of connections that was always possible in Balmorel in *Offshore* case was always possible in *Mix* as well, and the rest were possible only if their capacity had been large enough on the previous iteration round.

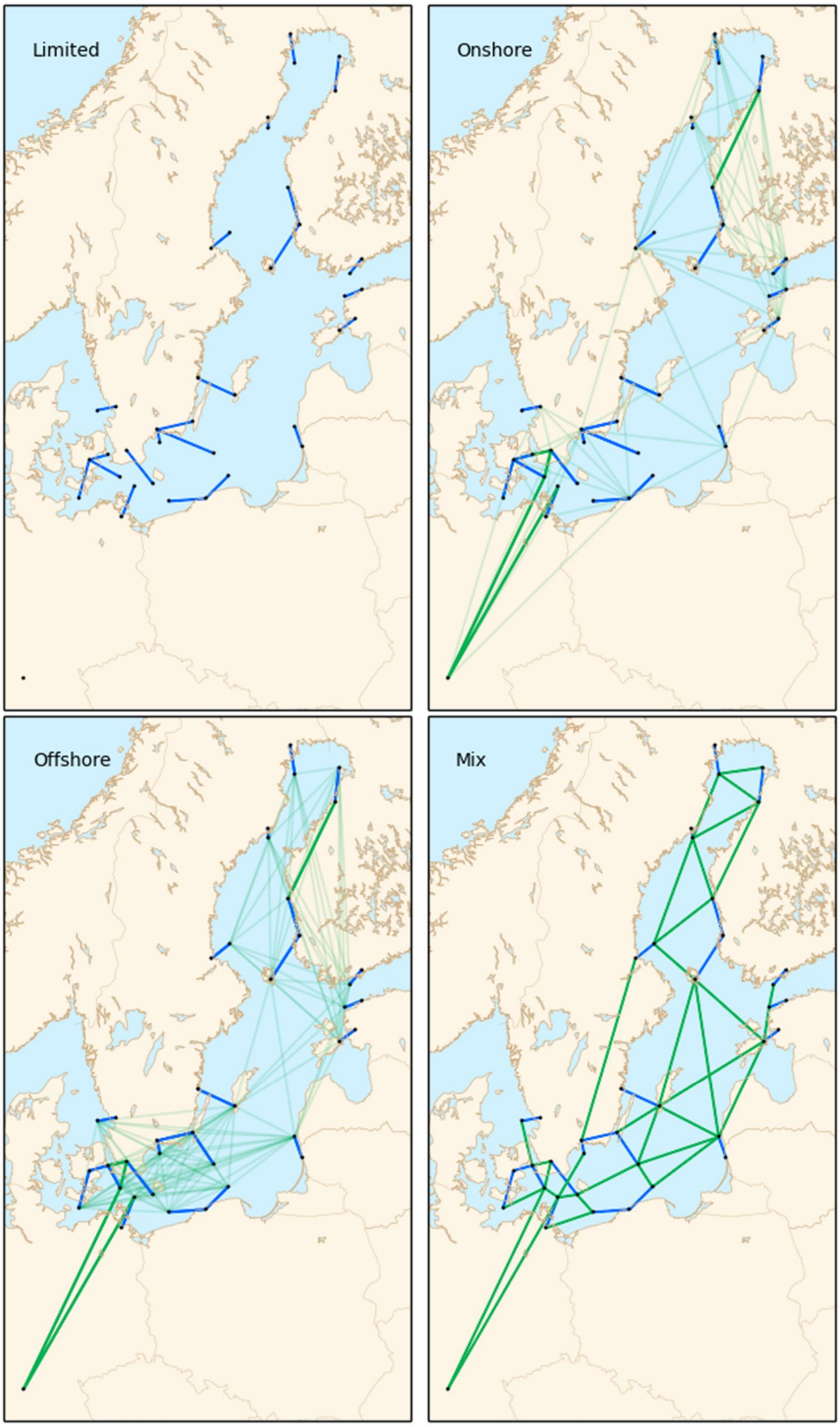

Figure 14 Allowable connections in topology cases 'Limited', 'Onshore', 'Offshore' and 'Mix'. Blue: connections always possible. Green: connections possible if their capacity exceeds the desired limit. Some of the possible connections in cases 'Onshore' and 'Offshore' are shown with transparent green lines due to the large amount of them, but in the grid investment optimization they are treated the same way as the connections shown with non-transparent green lines.

4. Results

4.1 Introduction to the results

This chapter presents the results from Balmorel, WILMAR JMM and PSS®E calculations. Section 4.2 presents first the case naming used in the following sections. Section 4.3 presents the results from Balmorel and WILMAR JMM including total system costs, electricity production per fuel, CO_2 emissions and annual transmissions between price regions. More detailed description of snapshot results for some of the cases, including also linear power flow results, is presented in Section 0.

Because the differences between the cases were often relatively small, results are presented mainly from the simulations with the lower offshore converter station cost assumption (50 % more expensive than onshore converter stations), although cost results are also presented for the higher offshore converter station cost assumption (100 % more expensive than onshore converter stations). To focus on the differences between the impacts of the different topology types, some results are only presented for *Medium* HVDC cost scenario and not for *Low* and *High*.

4.2 Case description

Altogether 16 cases were studied using Balmorel and WILMAR JMM. Table 7 lists the cases and explains the case names.

Table 7 Explanations to case names

Case name	Offshore station cost increase compared to onshore station cost	General HVDC component cost assumption	Offshore grid topology type assumption
On_Low	50 %	Low	On(shore)
Off_Low	50 %	Low	Off(shore)
Lim_Medium	50 %	Medium	Lim(ited)
On_Medium	50 %	Medium	On(shore)
Off_Medium	50 %	Medium	Off(shore)
Mix_Medium	50 %	Medium	Mix
On_High	50 %	High	On(shore)
Off_High	50 %	High	Off(shore)
On_Low+	100 %	Low	On(shore)
Off_Low+	100 %	Low	Off(shore)
Lim_Medium+	100 %	Medium	Lim(ited)
On_Medium+	100 %	Medium	On(shore)
Off_Medium+	100 %	Medium	Off(shore)
Mix_Medium+	100 %	Medium	Mix
On_High+	100 %	High	On(shore)
Off_High+	100 %	High	Off(shore)

Price regions in the case studies were such that Denmark was divided into eastern and western part. Sweden and Norway were both divided into southern, central and northern part. Each of the other countries had one price region. Figure 3 on page 16 shows the borders of the regions.

4.3 Grid optimization and electricity market simulation results

4.3.1 Grid optimization results

Figure 15–Figure 16 show the resulting offshore grid topologies based on Balmorel optimization with HVDC cost scenario *Medium* and the assumption that offshore converter stations cost 50 % more than onshore converter stations. Appendix B presents the grid investment results for all the studied cases. The area between Sweden and Germany has relatively dense offshore grid and high transmission capacities in all of the cases (except *Limited* topology). Poland and Sweden are also very likely to be connected through the offshore grid in Balmorel optimizations. Balmorel also sees additional links from central Sweden or Åland to south beneficial in all of the cases where they are allowed. However, Balmorel did not invest in additional links between northern Sweden and other price regions except in *Onshore* topology case and *Low* cost scenario where Balmorel invested in a link between northern Sweden and Finland. Additional links from Baltic countries to other price regions vary relatively much between the cases.

Some peculiarities in the results may be explained by three reasons:

1. HVDC link costs where linearized which ignores the economies of scale.

2. To avoid investments into HVDC links with unrealistically small capacities, an iteration mechanism was added into Balmorel (described in Section 2.2.3). Small differences in the optimized capacities may have an impact on whether the HVDC links are being removed or not on the next iteration round.

3. HVDC investments were only allowed between offshore wind cluster nodes and onshore connection points. This means that additional connections to, e.g., Norway were not allowed although Norway was included in the simulation.

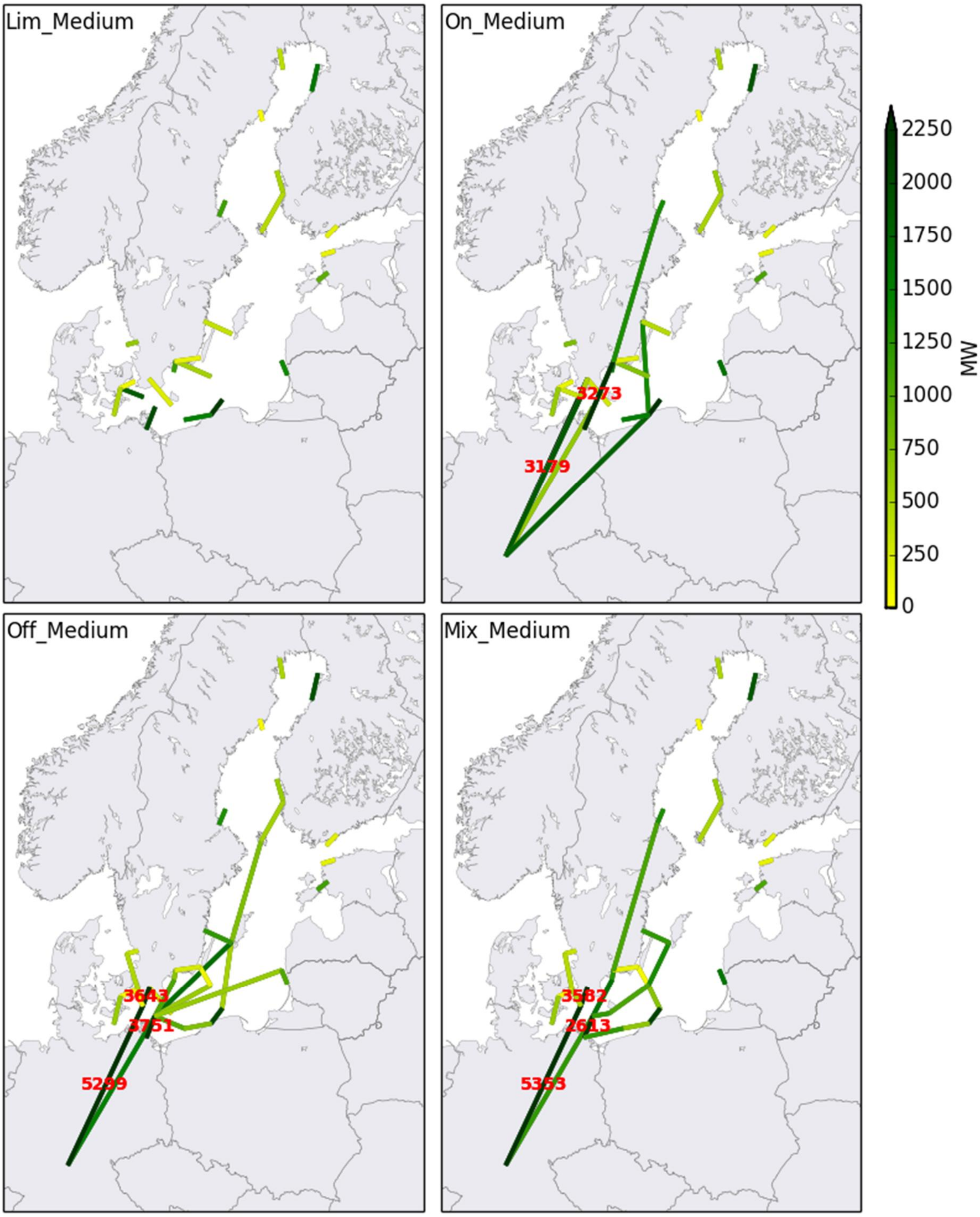

Figure 15 Offshore grids based on Balmorel optimization for all topology cases with HVDC cost scenario 'Medium' and the assumption that offshore converter stations cost 50 % more than onshore converter stations. Values that are higher than the scale maximum are written in the plot.

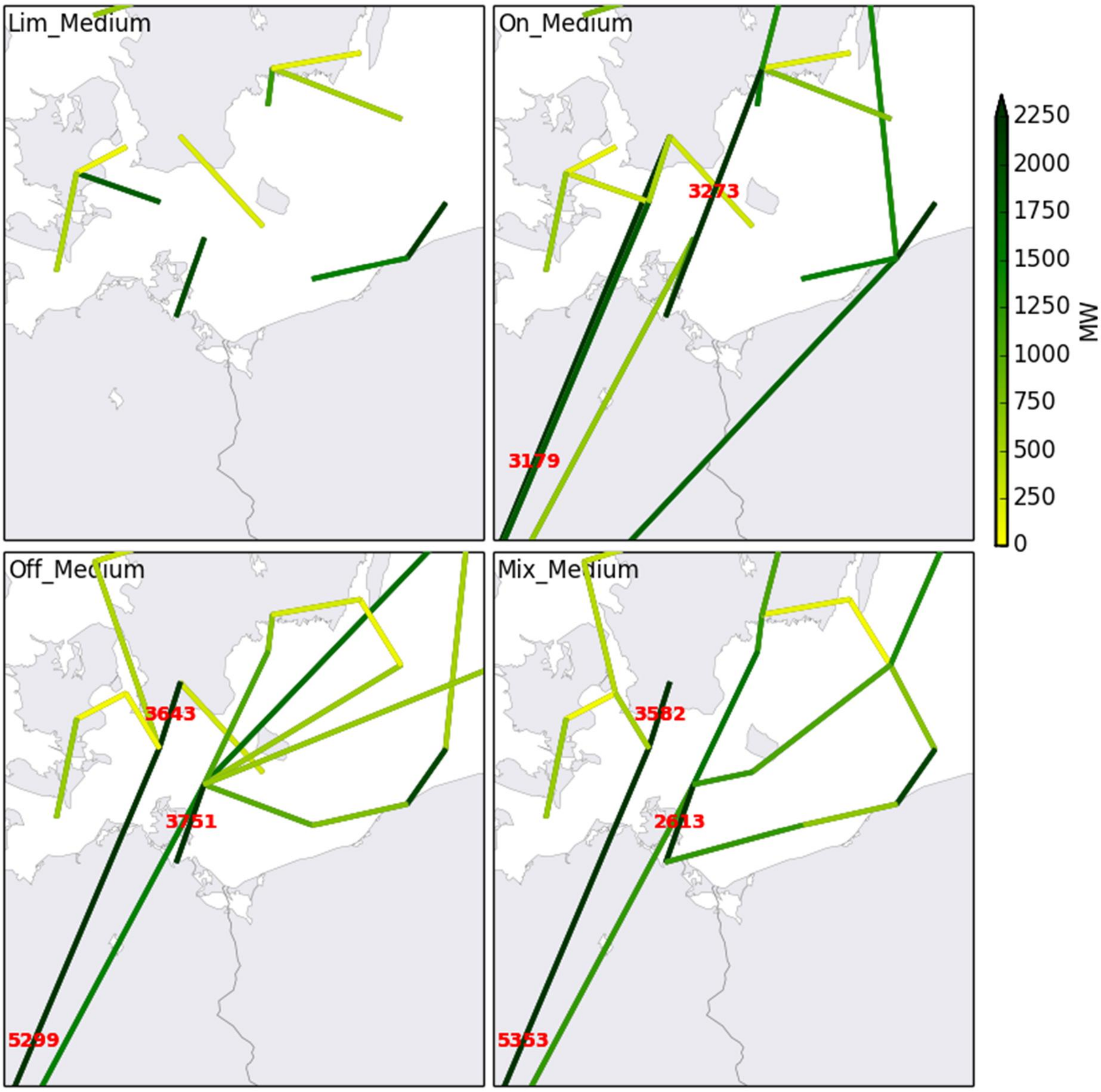

Figure 16 Same results as presented in Figure 15 but with the region between Denmark, Sweden, Germany and Poland shown with more detail. Values that are higher than the scale maximum are written in the plot.

4.3.2 System cost results

Figure 17 shows that with the *Medium* cost assumption, investment costs were lowest in offshore grid topology case *Limited* and second lowest in *Onshore*. Annual investment costs were calculated with an annuity factor of 9.5 (rate per period 8.5 % and number of periods 20). Figure 18 shows the annual operation costs, which were clearly highest in *Limited* and lowest in *Onshore* with the *Medium* cost assumption.

Figure 19, which adds up the annual investment costs and operation costs, shows that in the case of *Medium* cost assumption, *Onshore* topology case yields the best total cost reductions.

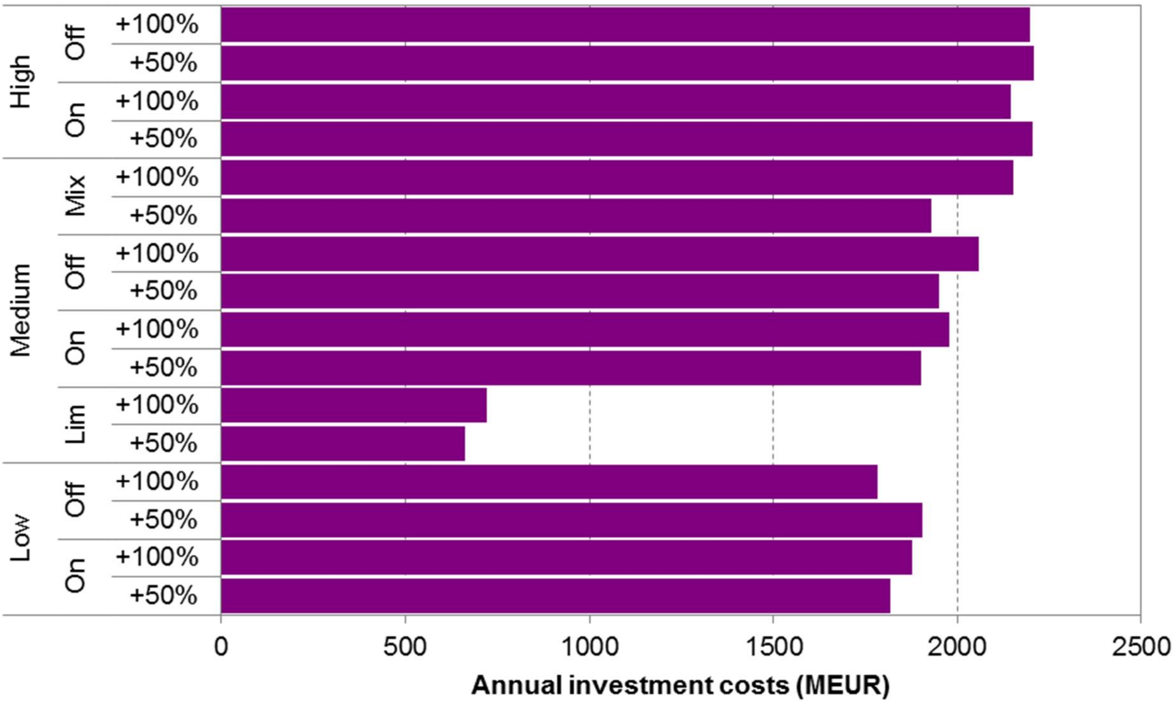

Figure 17 Annual investment costs with different HVDC cost scenarios, topology options and offshore station cost assumptions (50 % or 100 % more expensive than onshore stations).

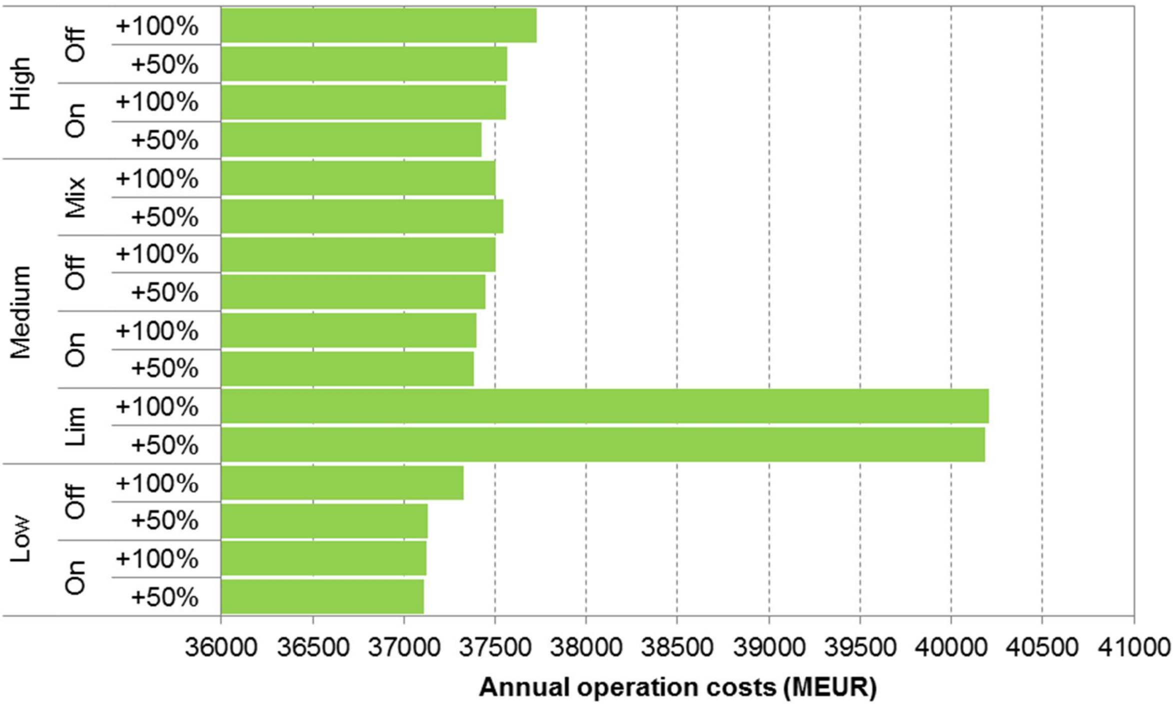

Figure 18 Annual operation costs with different HVDC cost scenarios, topology options and offshore station cost assumptions (50 % or 100 % more expensive than onshore stations). Note the starting value of the scale.

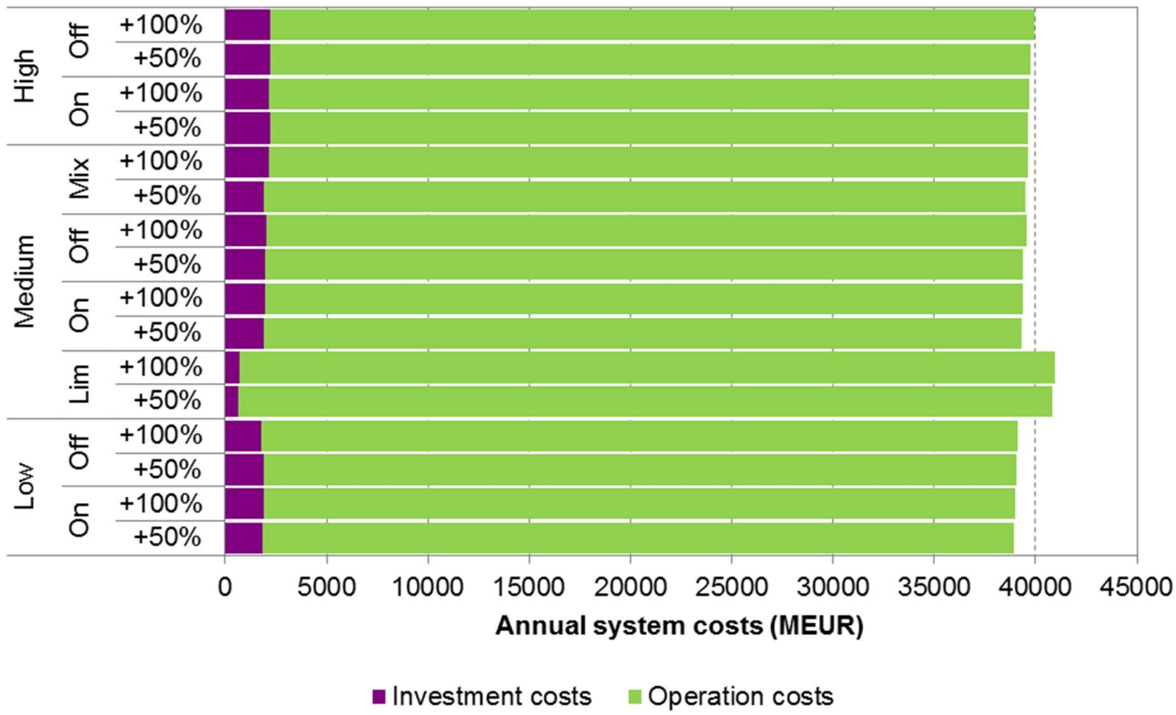

Figure 19 Total annual system costs with different HVDC cost scenarios, topology options and offshore station cost assumptions (50 % or 100 % more expensive than onshore stations).

The investment costs were also calculated assuming multi-terminal solutions with HVDC circuit breakers (see Figure 13). Figure 20 and Figure 21 present the total system cost and benefit results, respectively. Typically, while with the original assumptions (i.e., no multi-terminal solutions with circuit breakers) the total costs were lower with *Onshore* topology compared to *Offshore* topology, with multi-terminal solutions and circuit breakers costing 1/4 of converter station cost the total costs were roughly the same with *Onshore* and *Offshore* topologies. When the circuit breaker cost was reduced to 1/8 of converter station cost, *Offshore* resulted in lower total costs than *Onshore*.

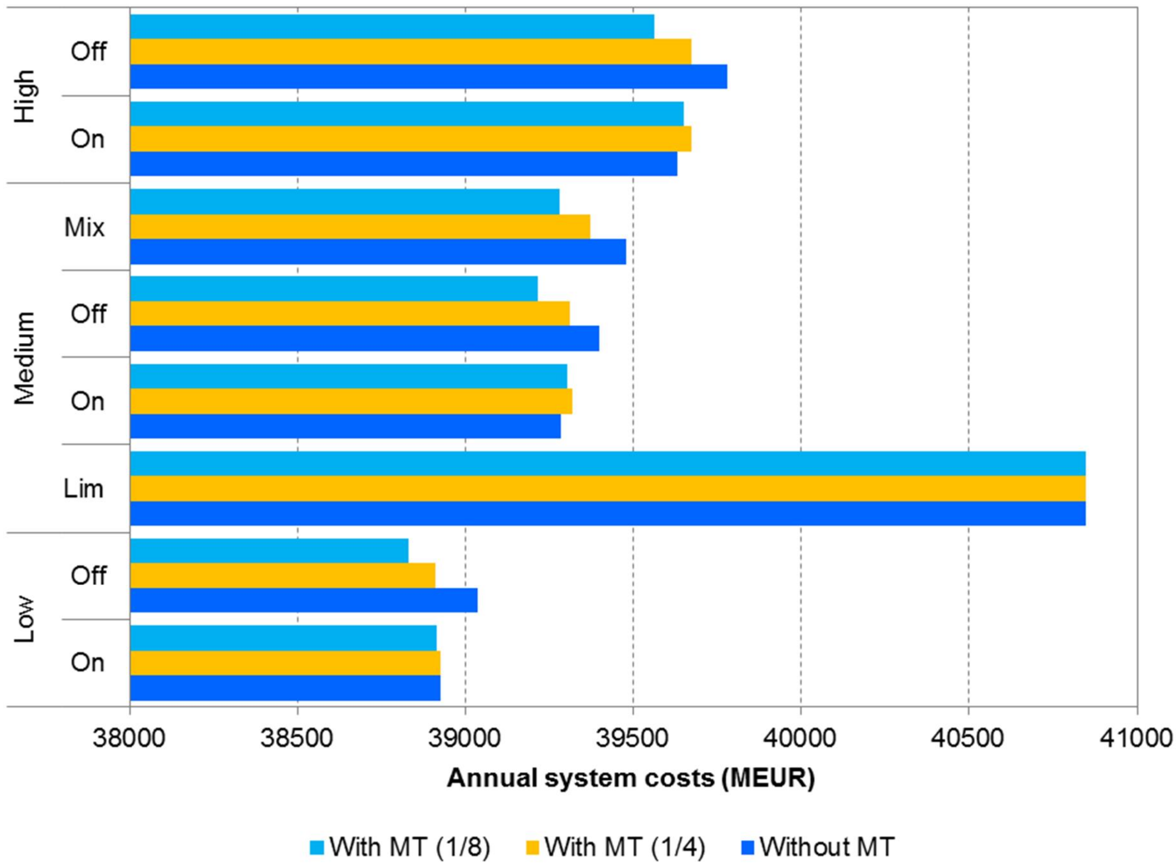

Figure 20 Total annual system costs depending on the multi-terminal (MT) option selected. ‘Without MT option’ signifies the same total costs that were shown in Figure 19. In MT options ‘1/4’ and ‘1/8’, HVDC circuit breaker cost were assumed to be 1/4 and 1/8 of converter station cost, respectively. Note the starting value of the scale. Offshore stations are assumed to be 50 % more expensive than onshore stations.

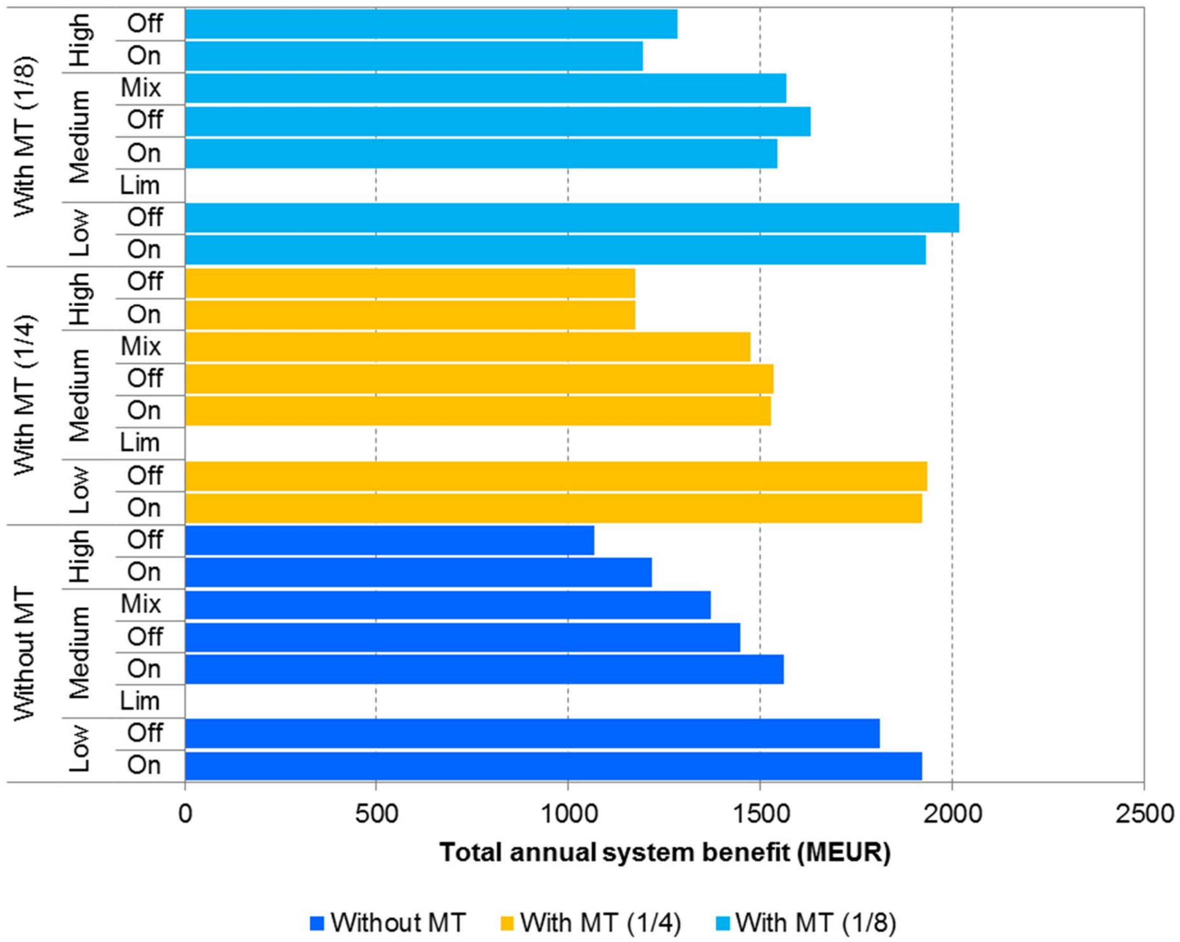

Figure 21 Total system benefits with different multi-terminal (MT) modelling options, HVDC cost scenarios and topology options compared to 'Lim_Medium' case where the total annual system costs were 40850 MEUR. 'Without MT' signifies the same cost savings that were detectable in Figure 19. In MT options '1/4' and '1/8', HVDC circuit breaker cost were assumed to be 1/4 and 1/8 of converter station cost, respectively. Offshore stations are assumed to be 50 % more expensive than onshore stations.

4.3.3 Annual production results

Figure 22 presents the annual electricity production per fuel. In *Limited* cases, natural gas and other fossil fuels were used more than in all other cases, in which nuclear was utilized more. The reason for this is that the model replaces fossil fuel usage in Germany with Swedish and Finnish nuclear when there are stronger interconnections, which can been seen by comparing Figure 23 and Figure 24. The differences between *Mix*, *Onshore* and *Offshore* cases in annual production are very small compared to their differences with *Limited* cases. The share of wind power was approximately 22 % of the annual electricity demand in the modelled area and wind power curtailment varied 1–3 % between the cases. Figure 25 shows expectedly that wind power curtailment occurred the most in *Limited* cases. *Offshore* cases had smaller wind power curtailment than *Onshore* cases. Figure 26 shows that CO_2 emissions were the highest in *Limited* scenario, which is explained by the differences in fossil fuel usage depicted in Figure 22.

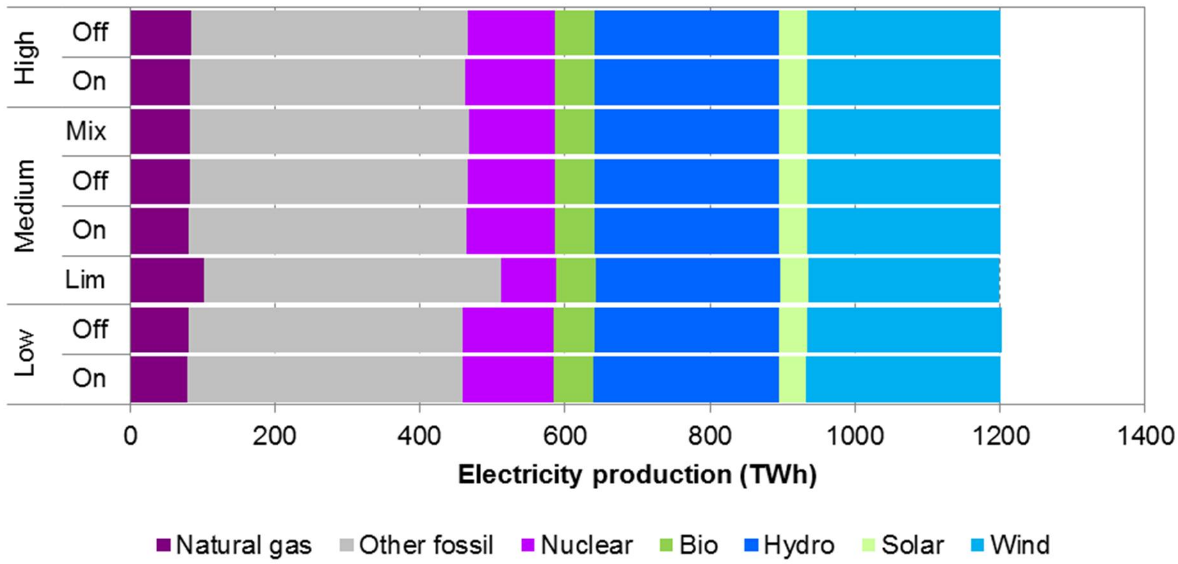

Figure 22 Annual electricity production per fuel with different HVDC cost scenarios and topology options. Offshore stations are assumed to be 50 % more expensive than onshore stations.

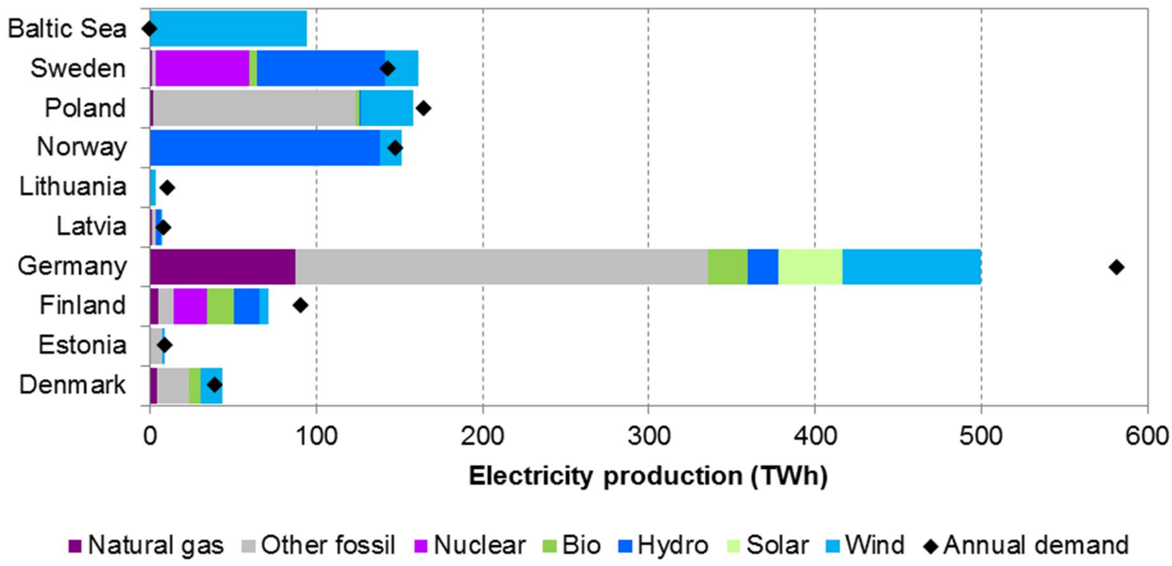

Figure 23 Annual electricity production per fuel per country in 'Lim_Medium' case.

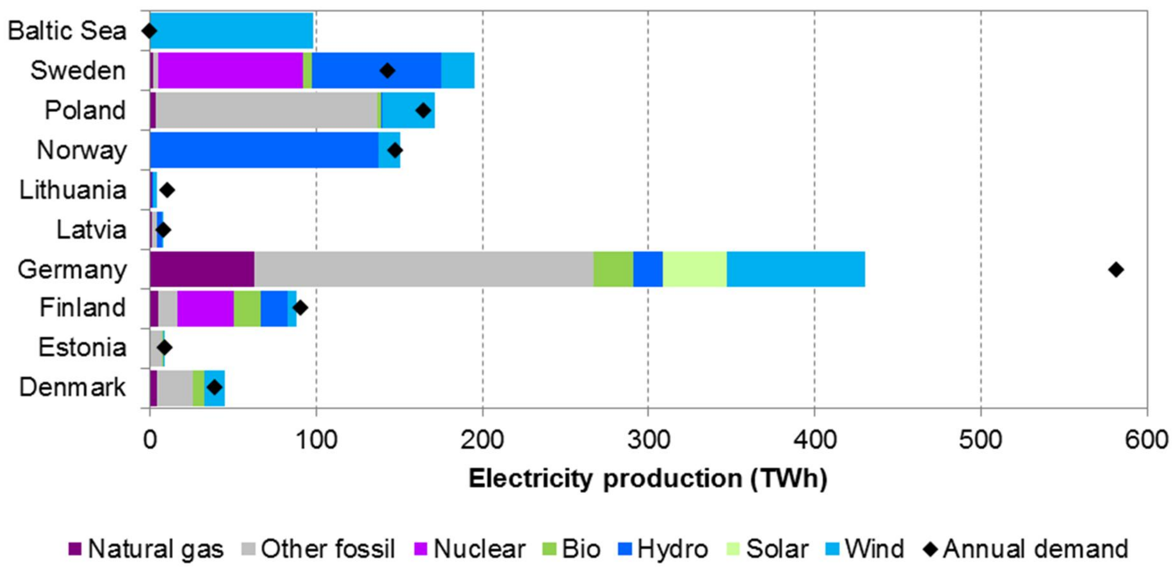

Figure 24 Annual electricity production per fuel per country in 'On_Medium' case.

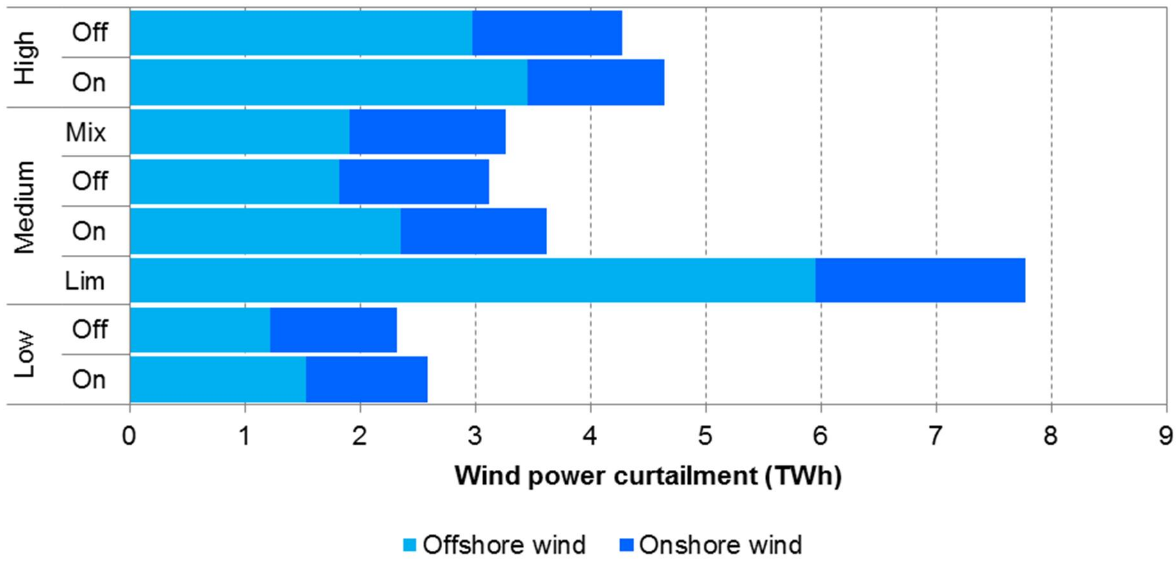

Figure 25 Annual wind power curtailment with different HVDC cost scenarios and topology options. Offshore stations are assumed to be 50 % more expensive than onshore stations. Total annual wind power production was approximately 270 TWh in the cases.

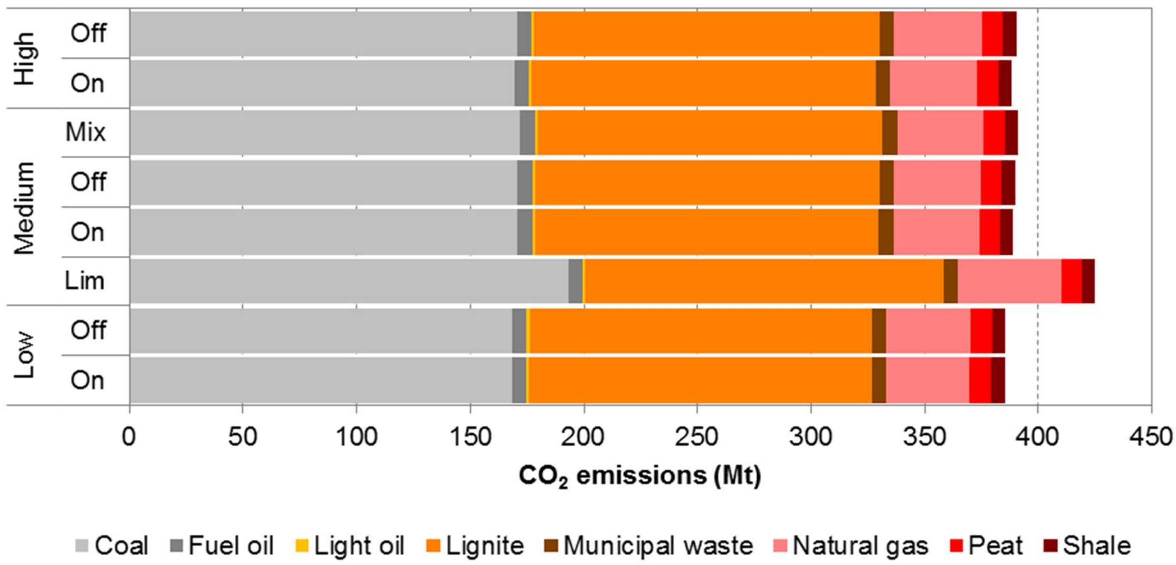

Figure 26 Annual CO_2 emissions with different HVDC cost scenarios and topology options. Offshore stations are assumed to be 50 % more expensive than onshore stations.

4.3.4 Annual transmission results

Figure 27 and Figure 28 show the annual net transmissions between regions and annual net transfer capacity utilizations, respectively. The figures include results only from *Medium* cost scenario with offshore converter stations costing 50 % more than onshore converter stations. Other cost scenarios showed similar behaviour. The transmissions are generally from northeast to southwest in the modelled area. Transmission through Sweden is remarkably large, although the transmission from central Sweden to southern Sweden is much smaller in *Limited* topology, where there is not as much further transmission capacity from southern Sweden to Germany as in other offshore grid topologies.

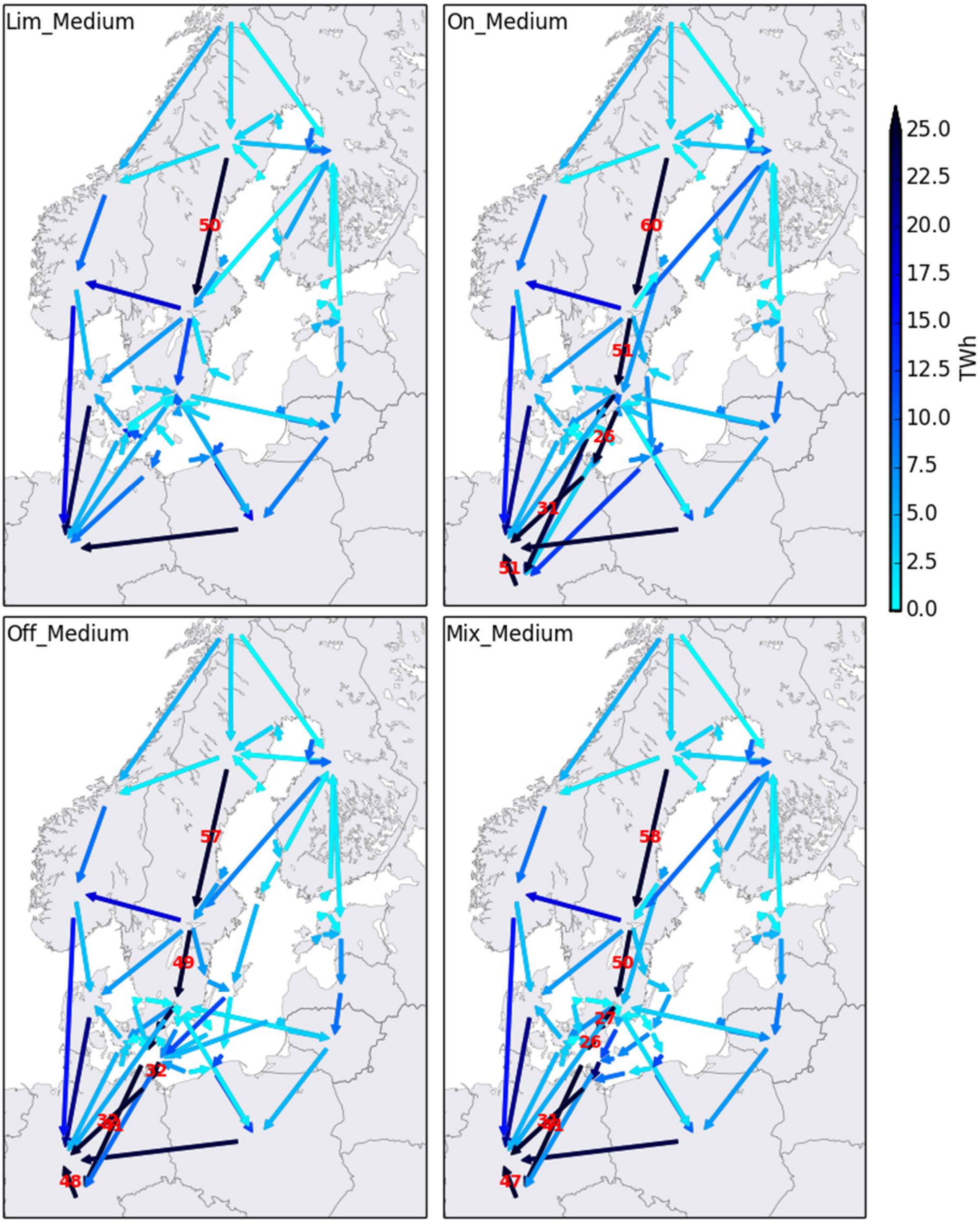

Figure 27 Annual net transmissions between regions. Values that are higher than the scale maximum are written in the plot.

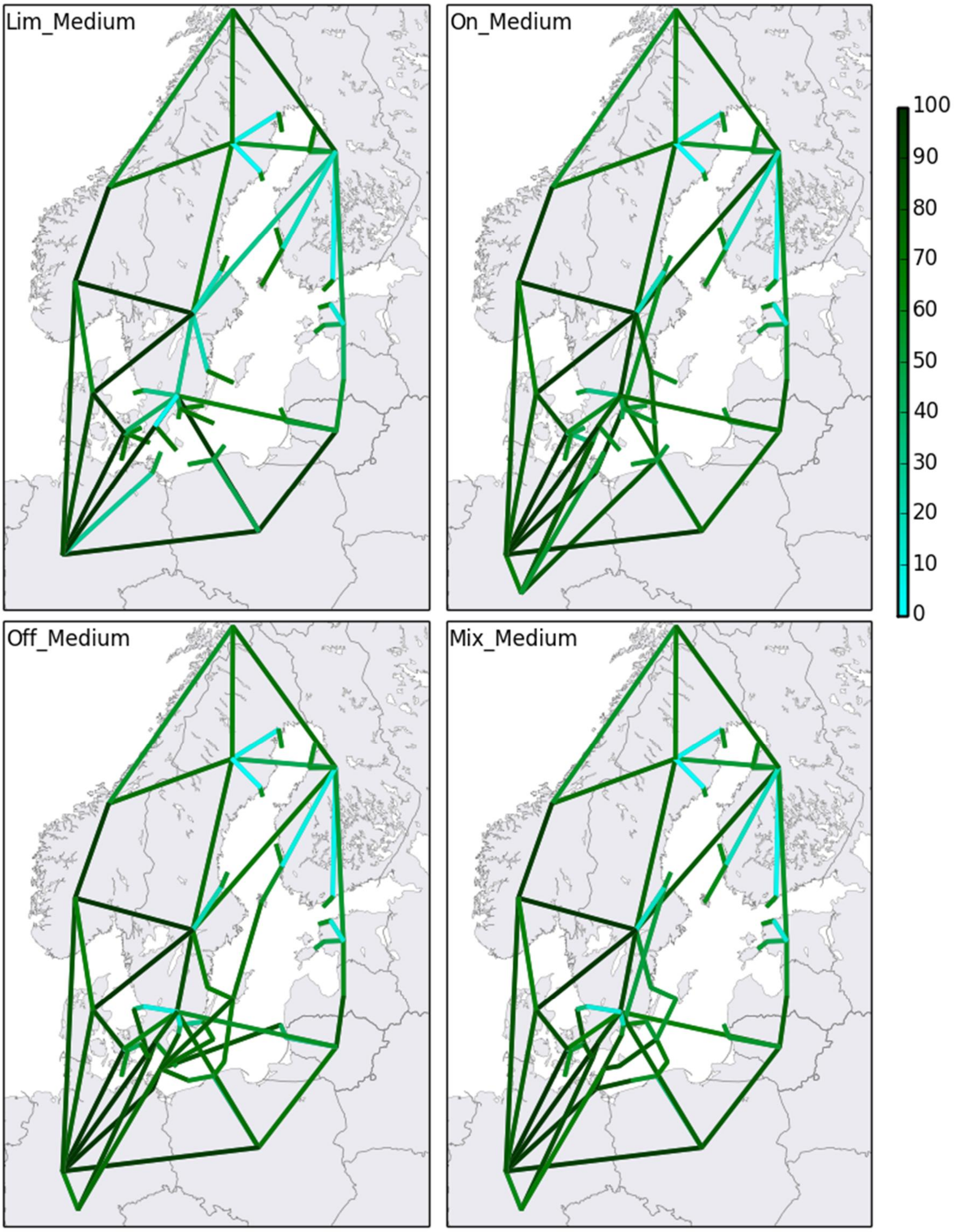

Figure 28 Annual net transfer capacity utilizations.

Figure 29 shows the net transfer capacity utilizations in more detail in the region between Denmark, Sweden, Germany and Poland. The figure also shows node identification numbers which are useful for the interpretation of Figure 30 and Figure 31, which show transmission duration curves for four HVDC links. Both the annual net transfer capacity utilization and the transmission duration curves tell about the necessity of the transmission investments. The extreme limits of the transmission duration curves in Figure 30 and Figure 31 relate to the capacities of the HVDC links.

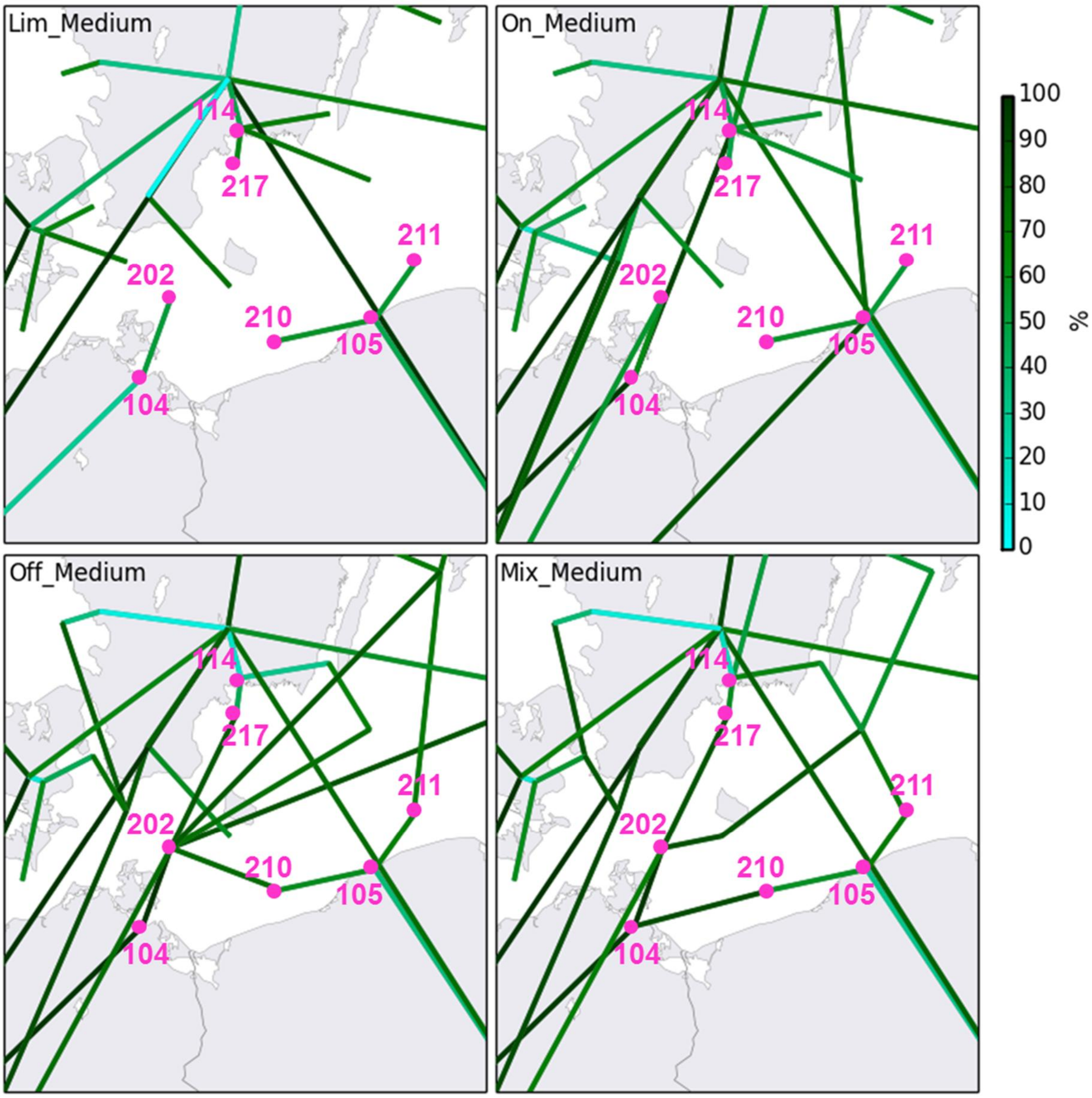

Figure 29 Annual net transfer capacity utilizations in the region between Denmark, Sweden, Germany and Poland. The numbers in the figure signify offshore wind cluster and onshore connection point identification numbers.

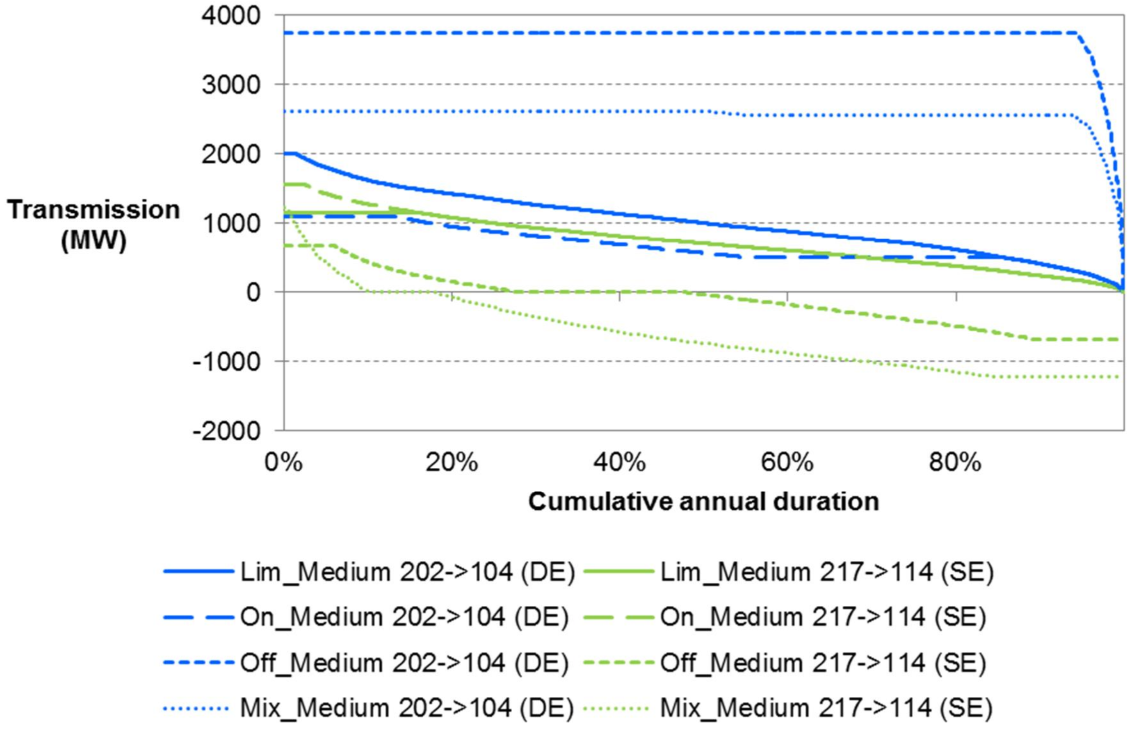

Figure 30 Transmission duration curves for two offshore DC links connected to shore. Node 104 is an onshore connection point in Germany and 114 in Sweden. Nodes 202 and 217 are two offshore wind clusters.

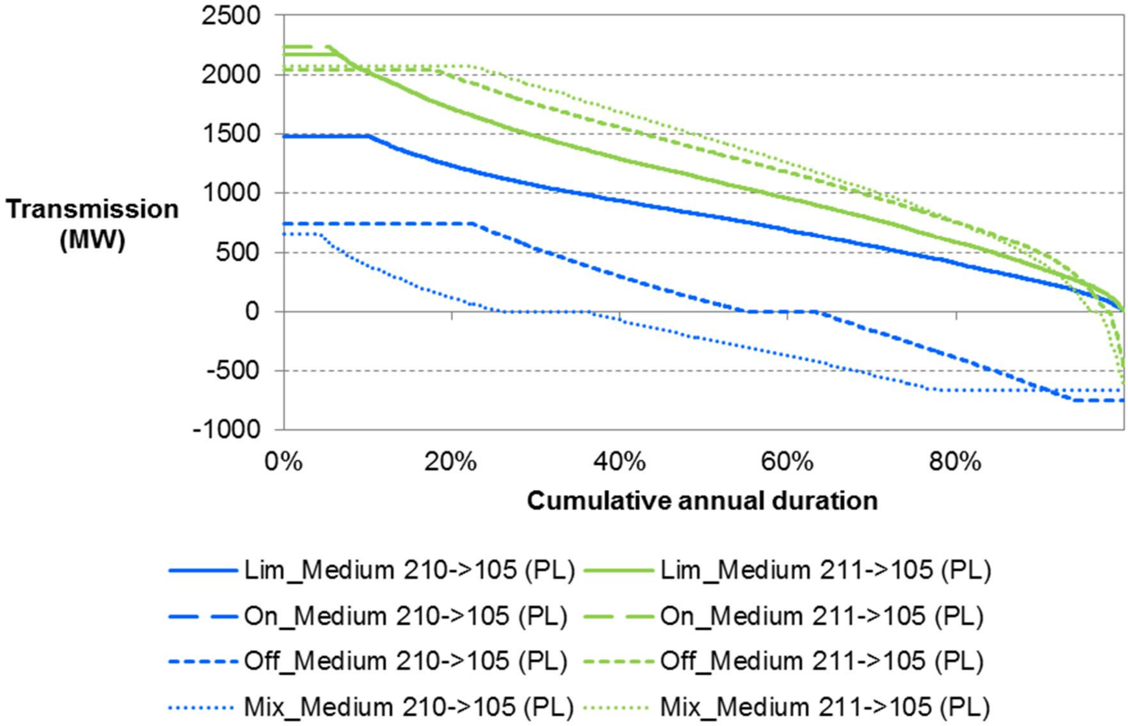

Figure 31 Transmission duration curves for two offshore DC links connected to Poland. Node 105 is an onshore connection point in Poland and nodes 210 and 211 are two Polish offshore wind clusters.

In *Offshore* and *Mix* cases, wind clusters were connected to multiple price regions through other wind clusters. The transmission duration curves show that in these cases, HVDC links are also used for transmission from shore towards a wind cluster (negative transmission values). On the other hand, in the same cases, the links can also be used for full power transmission from a wind cluster to shore almost throughout the year, as is the case for transmission from wind cluster '202' to Germany. Through that wind cluster, Germany has further connections to other regions where electricity is less expensive. To summarize, in *Offshore* and *Mix* cases the offshore grid investments between wind clusters and onshore connection points can be used for transmission in both directions and also efficiently for almost constant full power transmission; essentially, for transmission between price regions.

In *Limited* and *Onshore* case, the HVDC links between wind clusters and onshore connection points cannot be used for transmission between price regions. Thus, they are not used for transmission in both directions nor for constant full power transmission. Instead, in *Onshore* case, transmission between price regions is accomplished using direct HVDC links between onshore connection points. The tasks of offshore wind power production export and transmission between onshore price regions are thus divided among the links.

Figure 30 and Figure 31 show that in general, the time when an offshore-to-shore HVDC link is used for full power transmission in either direction is longer in *Offshore* and *Mix* cases than in *Limited* and *Onshore* cases. However, the time when the link is not used at all is also longer in *Offshore* and *Mix* cases.

4.4 Hourly operation results

4.4.1 Snapshot situations

Table 8 describes the snapshot situations that were selected from the WILMAR JMM market simulations to further linearized power flow analysis in PSS®E. Power flow analysis was carried out for two offshore grid cases: *On_Medium* and *Off_Medium* with *Onshore* and *Offshore* topology types, respectively. The cases shared the same HVDC component cost scenario. Both *Onshore* and *Offshore* topologies had lower costs compared to *Limited* and *Mix* topologies, and offshore grid structures in *Onshore* and *Offshore* were also quite distinct from each other, which makes them relevant to compare. The results are described in the following subsections.

Table 8 Snapshot descriptions

	MM-DD-HH	System load (GWh/h)	Offshore wind power available (GWh/h)
Peak load	02-03-10	195.162	20.323
Minimum load	07-22-04	82.277	9.018
Peak offshore wind power	10-04-10	154.961	25.749
Minimum offshore wind power	08-05-08	103.879	2.537

4.4.2 Case: On_Medium

This subsection presents snapshot results for case *On_Medium*. First, Figure 32 describes the electricity production per fuel in the whole simulated area during the 7-day periods from which the snapshots are selected.

Figure 33 shows the power flow on each AC line in the grid model as calculated with the linearized power flow equations. Power flows on lines and cables that cross price regions are added up to get the transmissions between price regions. Figure 34 and Figure 35 present the results in megawatts and as a percentage of net transfer capacity, respectively. From Figure 35 it is evident that some of the net transfer capacity limits are exceeded. The limits are exceeded only inside and between Sweden and Norway, with some very small overloadings between other regions as well. Figure 36 shows the difference between the transmissions calculated using the power flow equations and the ones given by the unit commitment and economic dispatch model WILMAR JMM. The largest differences are observed inside and between Norway and Sweden, which explains why the power flow analysis shows net transfer capacity overloadings there and not between other regions.

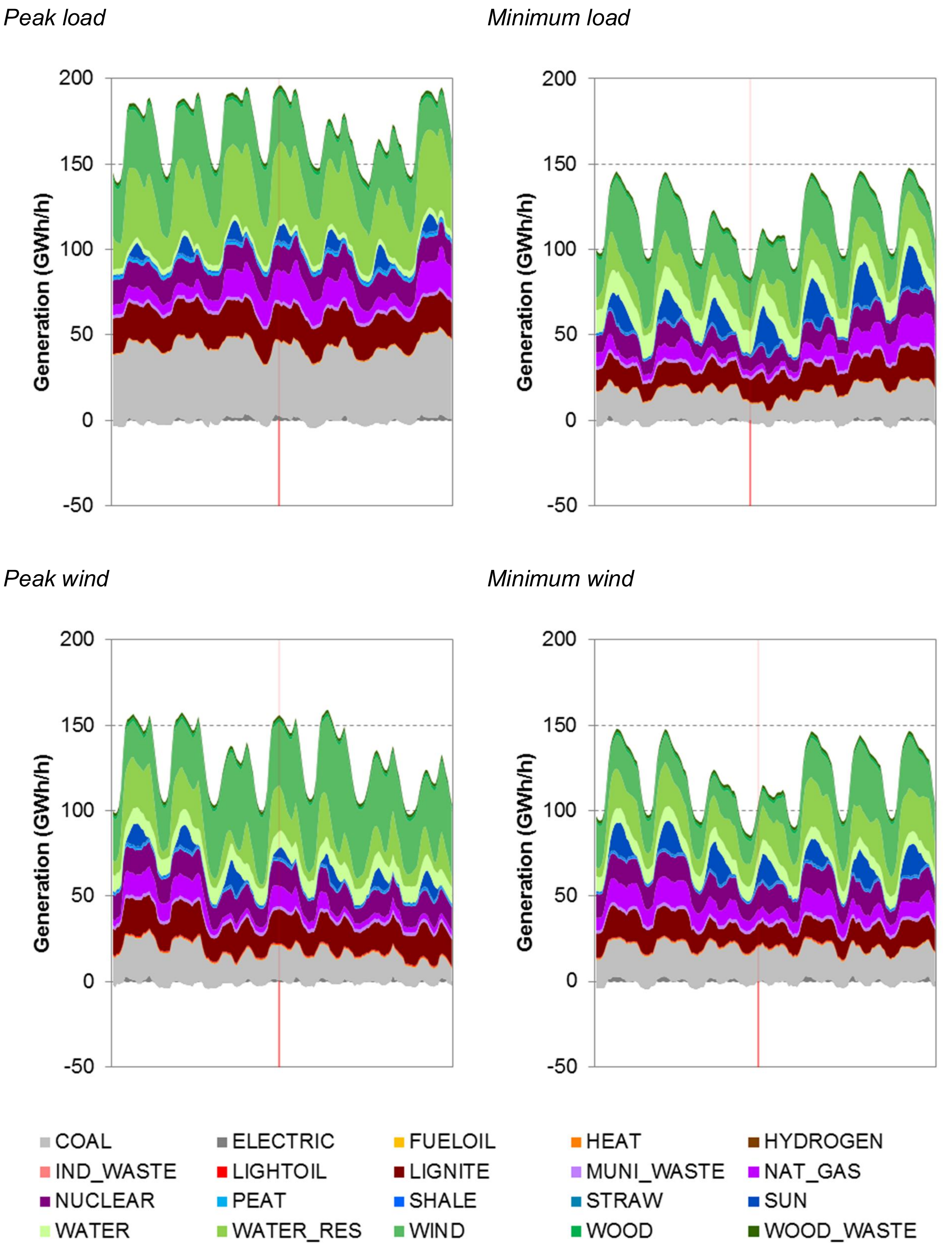

Figure 32 Generation per fuel during the 7-day periods from which the snapshots are selected. The red vertical line marks the snapshot hour. When the bottom of the plot extends below zero, electrical storages are charging.

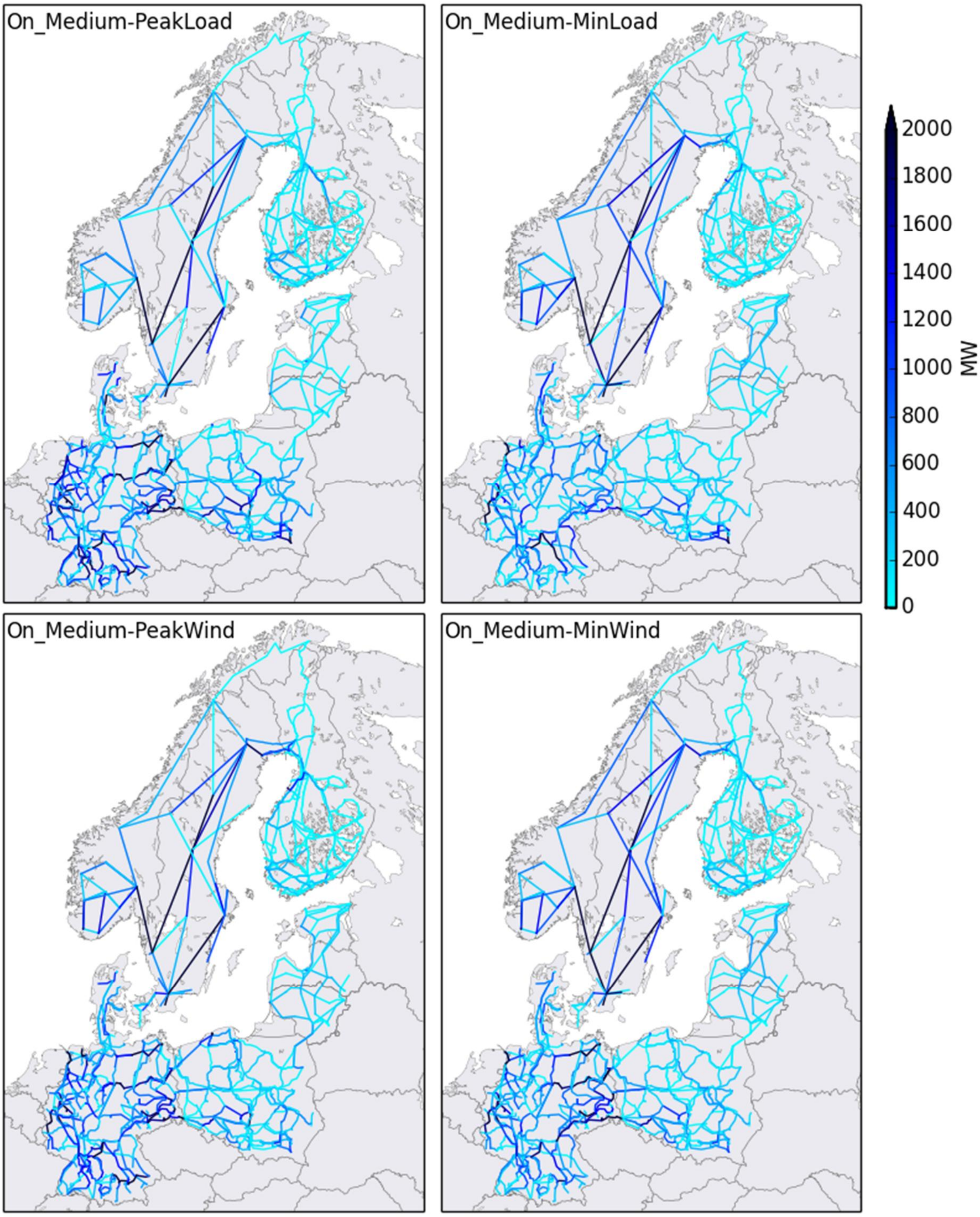

Figure 33 Line loadings in the snapshot situations. Lines where the power flow is more than the scale maximum are not highlighted separately.

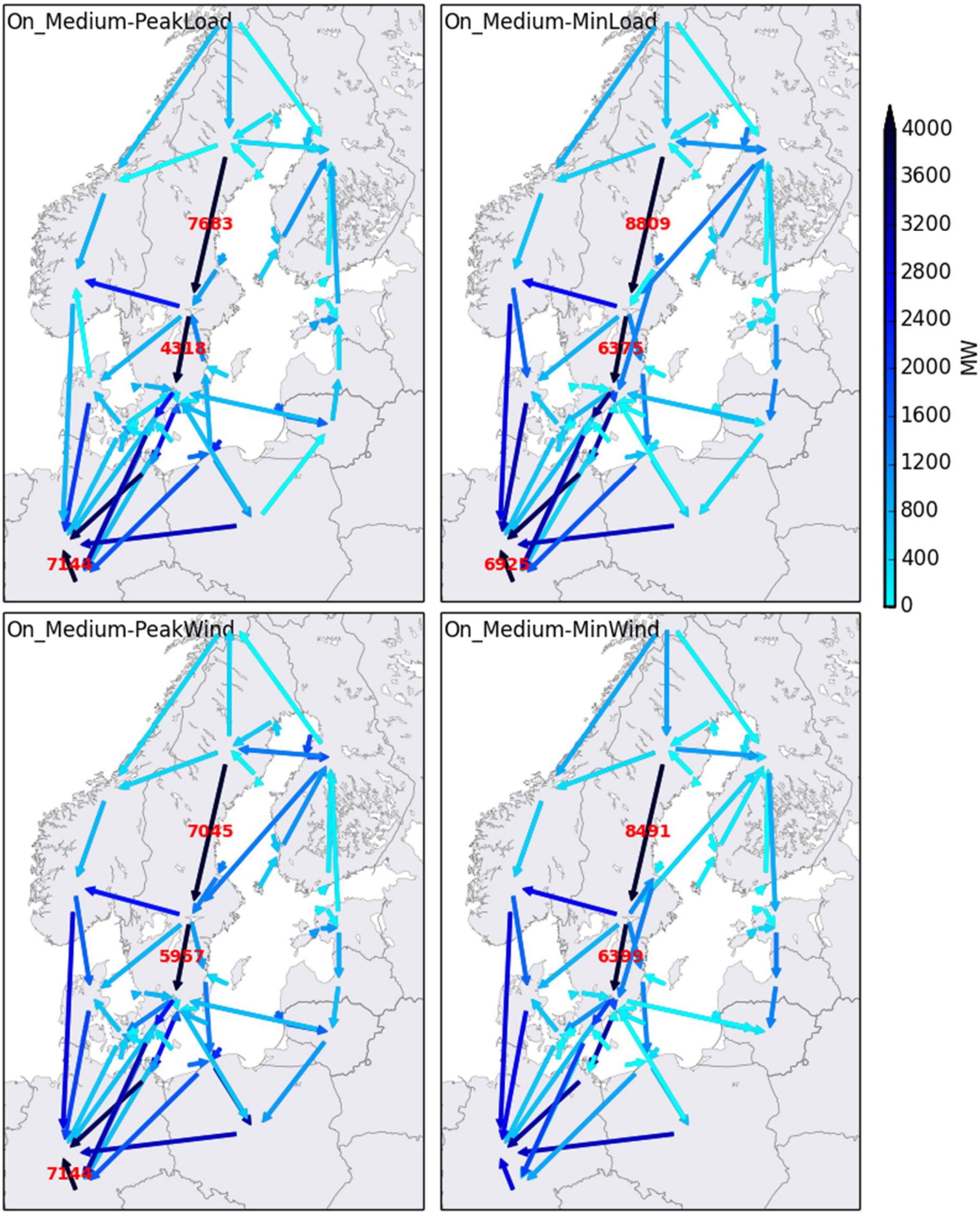

Figure 34 Transmissions in the snapshot situations calculated using linearized power flow equations. Values that are higher than the scale maximum are written in the plot.

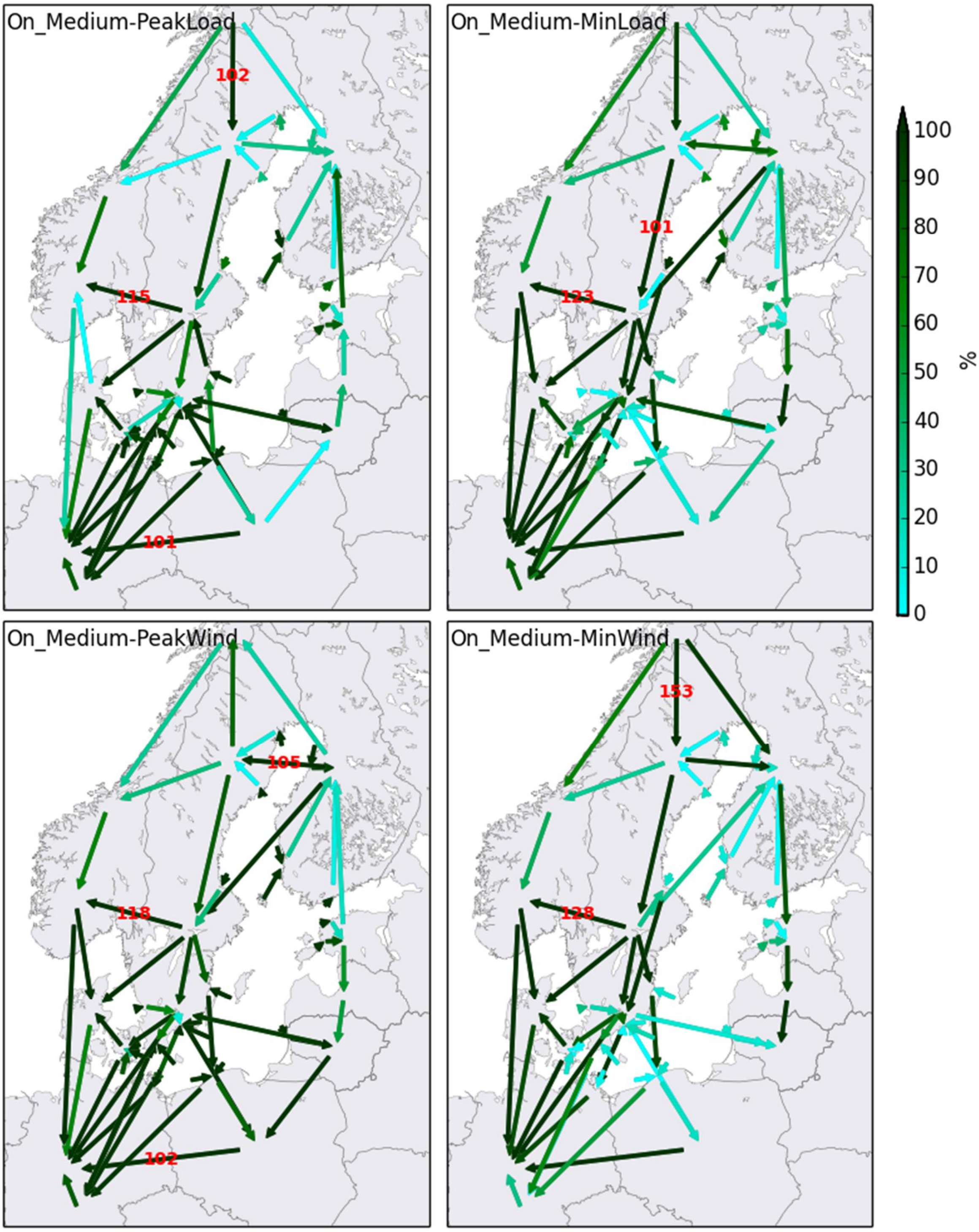

Figure 35 Transmissions in the snapshot situations calculated using linearized power flow equations (% of net transfer capacity). Values that are higher than the scale maximum are written in the plot.

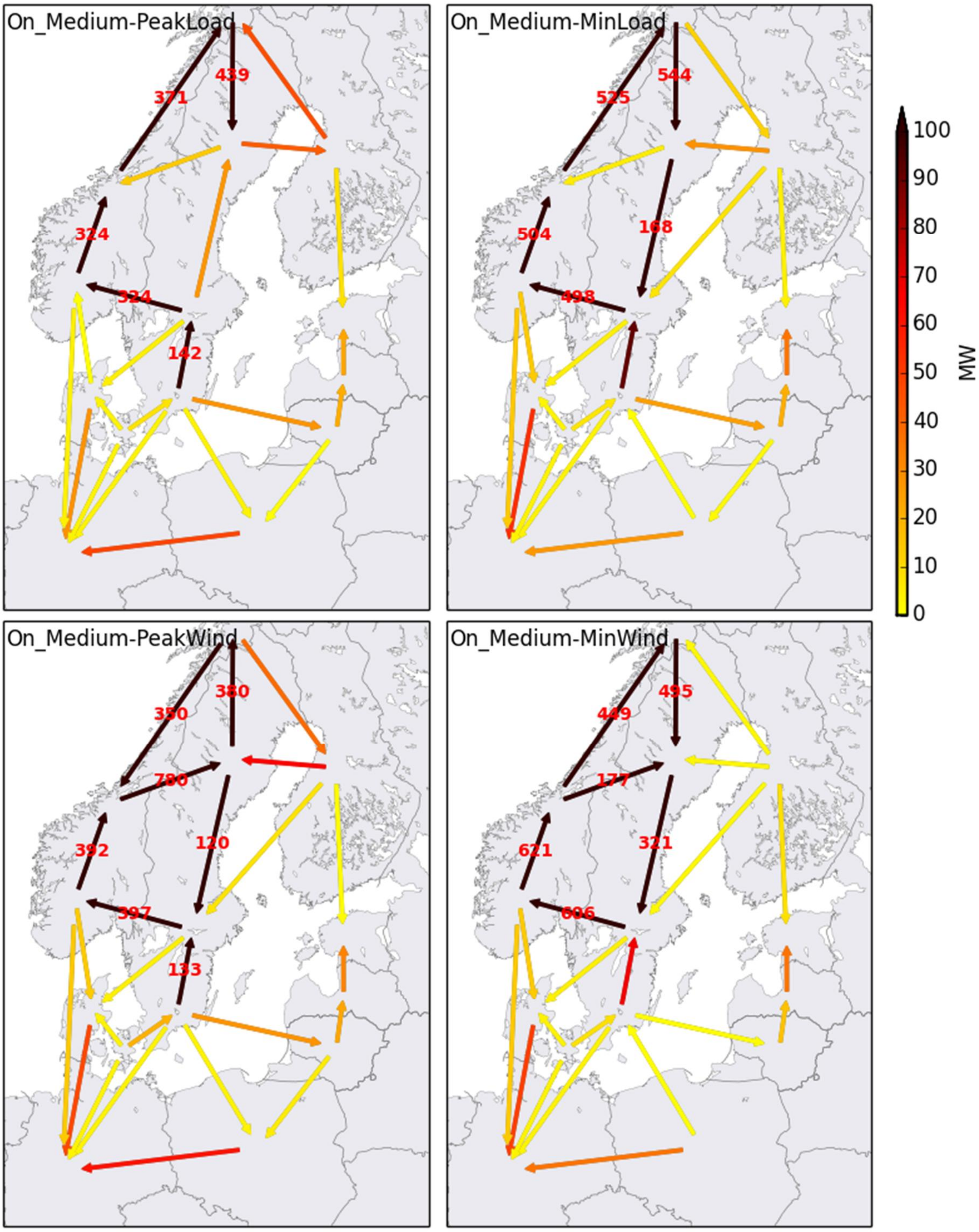

Figure 36 Differences in the market model transmissions and power flow model transmissions in the snapshot situations. Values that are higher than the scale maximum are written in the plot.

The loop flow issue that is evident in Figure 36 can be explained by the fact that other price regions than the ones in Sweden and Norway are actually connected in string in the grid model: Finland has a weak AC connection to the power system in northern Norway, but otherwise it is AC-connected only to the power system in Sweden; eastern Denmark is AC-connected to southern Sweden; Baltic countries are AC-connected in string; and Poland, Germany and western Denmark are also AC-connected in string. The only area in the grid model where the price regions are AC-connected together through a meshed grid is in Norway and Sweden. On the other hand, Norway and Sweden are also the only countries that are represented using a considerably aggregated grid model, which may also not be as up-to-date as other parts of the combined grid model.

Interestingly, southern Sweden is AC-connected only to central Sweden but there are still rather large differences (~100 MW) in the transmissions between those regions in the power flow results and WILMAR JMM results. In addition, if more price regions from Central Europe had been included in the modelling, more loop flows would very likely have been seen there as well.

Table 9 lists the losses in the grid model for each snapshot and price region. Losses in some parts of Sweden and Norway in the model are extremely high when expressed as a percentage of region load. E.g., in northern Sweden the electricity demand is relatively low but there is plenty of hydro power production which is transmitted to south creating large losses, especially when expressed as a percentage of region load. When expressed as a percentage of region generation, the losses in northern Sweden were approximately 3 % in all of the four snapshots.

Losses were treated in the modelling so that the load time series in WILMAR JMM were assumed to include the losses, and when the power flow was calculated in PSS®E, the amount of grid losses calculated by PSS®E was subtracted from the grid loads and the power flow was calculated again. The steps were repeated a few times.

In general, in peak load snapshot the grid losses as a percentage of the region load are smaller than in the other snapshots. The regions that are typically exporting their low-cost energy now need it themselves, which decreases the transmissions between price regions (see Figure 34 on page 48), and therefore possibly also the losses in the regions. In addition, the region load is now higher and even the same amount of losses in megawatts or megawatt-hours would result in smaller percentage of losses. Largely aggregated grid models may also underestimate the losses from internal transmissions and emphasize the losses from transmissions between price regions.

Table 9 Losses in each region of the grid model in different snapshots as % of load (losses as MWh/h in parenthesis)

	Peak load		Minimum load		Peak offshore wind power		Minimum offshore wind power	
Eastern Denmark	2	(53)	1	(7)	1	(29)	1	(14)
Western Denmark	6	(250)	9	(122)	3	(104)	4	(86)
Finland	2	(266)	2	(142)	2	(236)	2	(141)
Central Norway	1	(72)	2	(46)	2	(62)	1	(31)
Northern Norway	4	(55)	10	(70)	4	(37)	12	(95)
Southern Norway	1	(248)	5	(351)	3	(368)	4	(359)
Poland	5	(1241)	5	(615)	4	(877)	4	(645)
Central Sweden	2	(389)	7	(384)	3	(318)	5	(371)
Northern Sweden	8	(348)	20	(439)	13	(357)	16	(396)
Southern Sweden	6	(292)	13	(219)	9	(293)	7	(131)
Estonia	1	(25)	5	(28)	3	(29)	5	(42)
Germany	4	(3790)	4	(1633)	5	(3613)	5	(2544)
Latvia	1	(13)	8	(46)	3	(31)	7	(60)
Lithuania	1	(21)	3	(25)	3	(50)	3	(34)

4.4.3 Case: Off_Medium

This subsection presents snapshot results for case *Off_Medium*. Figure 37 describes the electricity production per fuel in the whole simulated area during the 7-day periods from which the snapshots are selected. The production distribution is very similar to *On_Medium* case presented in Section 4.4.2.

Similarly to the figures and the table in Section 4.4.2, Figure 38 shows the power flow on each AC line in the grid model as calculated with the linearized power flow equations, Figure 39 and Figure 40 present the transmissions between price regions in megawatts and as a percentage of net transfer capacity, respectively, Figure 41 shows the difference between the transmissions calculated using the power flow equations and the ones given by the unit commitment and economic dispatch model WILMAR JMM, and Table 10 lists the losses in the grid model for each snapshot and price region. The results and conclusions are similar to the ones presented for case *On_Medium* in Section 4.4.2.

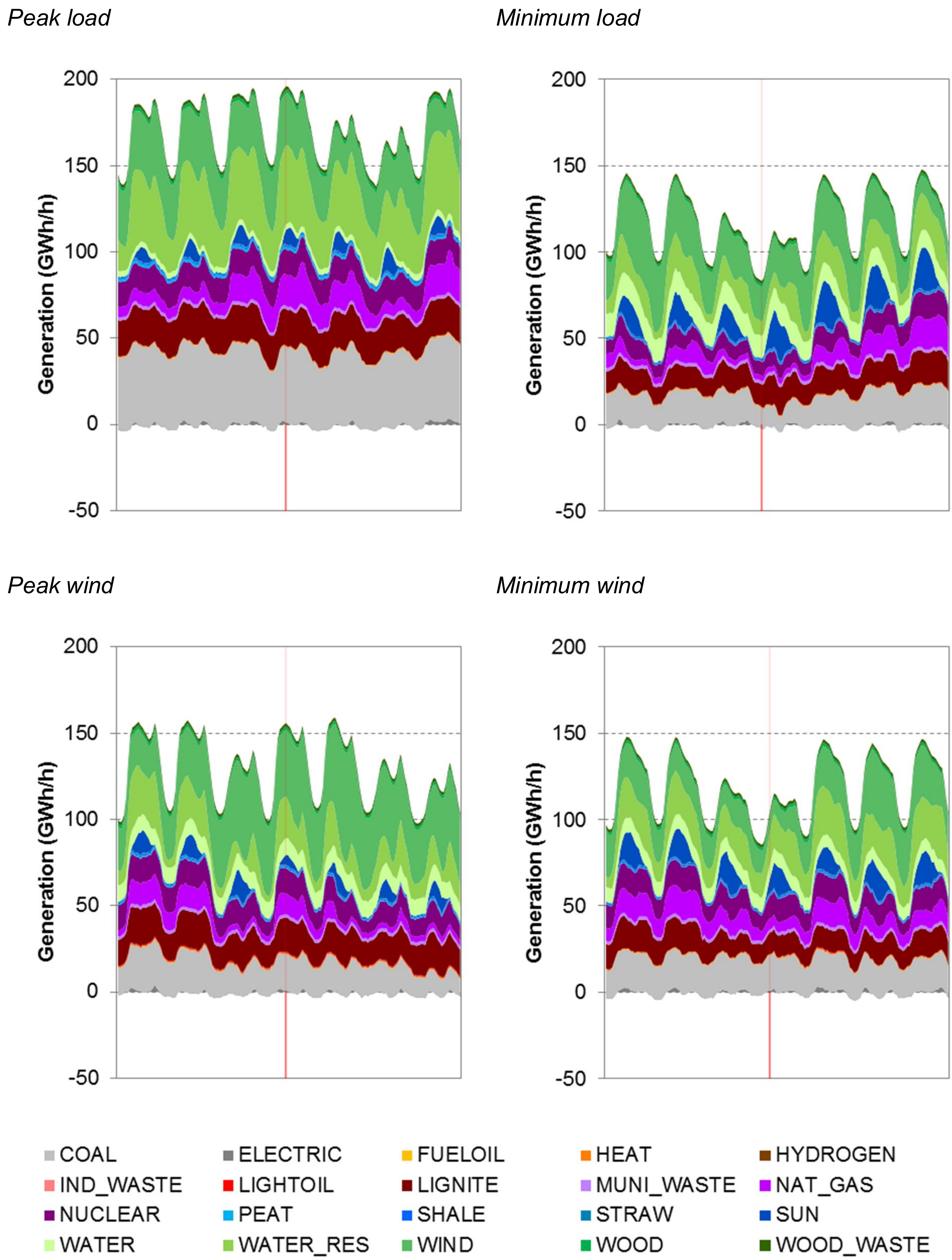

Figure 37 Generation per fuel during the 7-day periods from which the snapshots are selected. The red vertical line marks the snapshot hour. When the bottom of the plot extends below zero, electrical storages are charging.

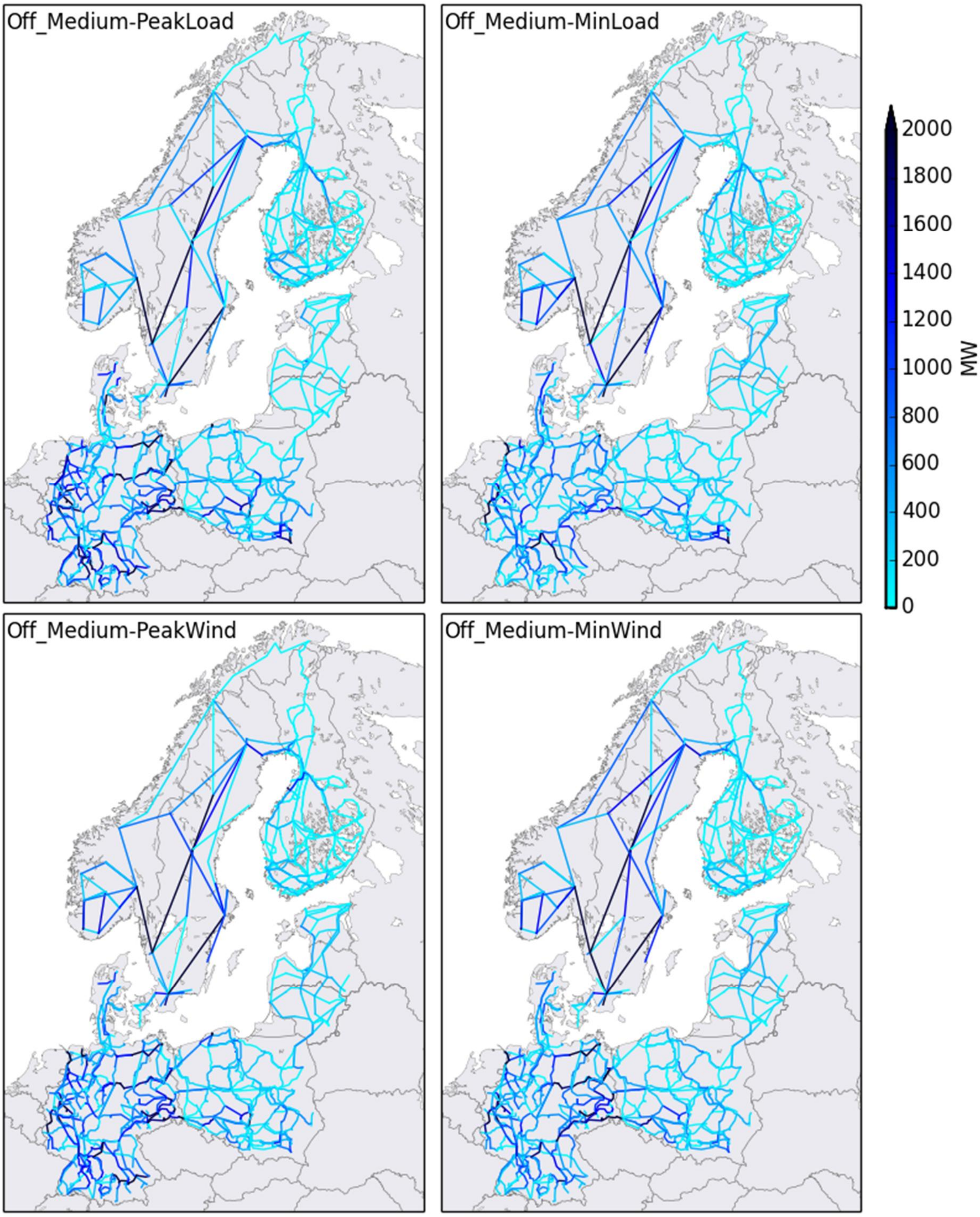

Figure 38 Line loadings in the snapshot situations. Lines where the power flow is more than the scale maximum are not highlighted separately.

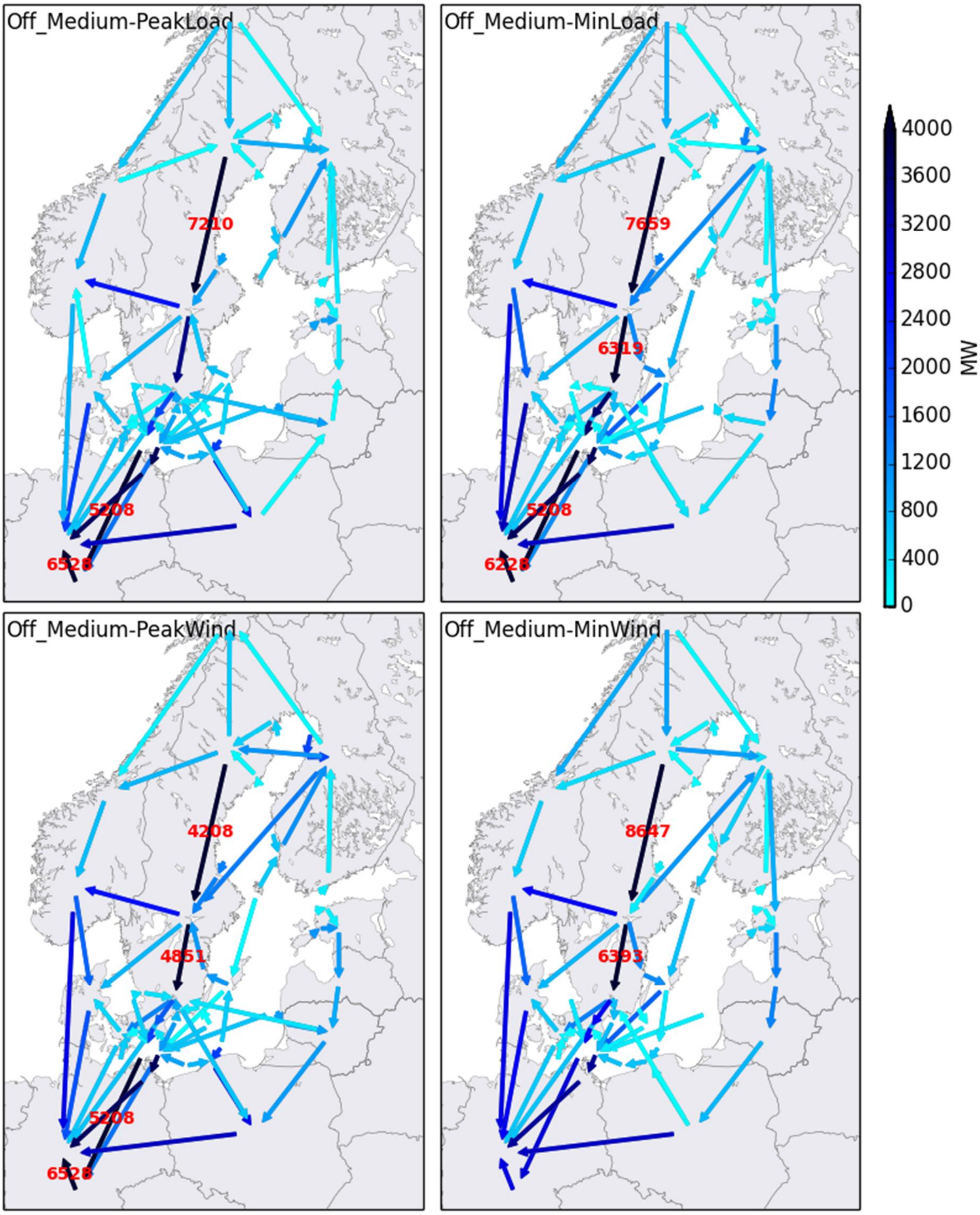

Figure 39 Transmissions in the snapshot situations calculated using linearized power flow equations (MW). Values that are higher than the scale maximum are written in the plot.

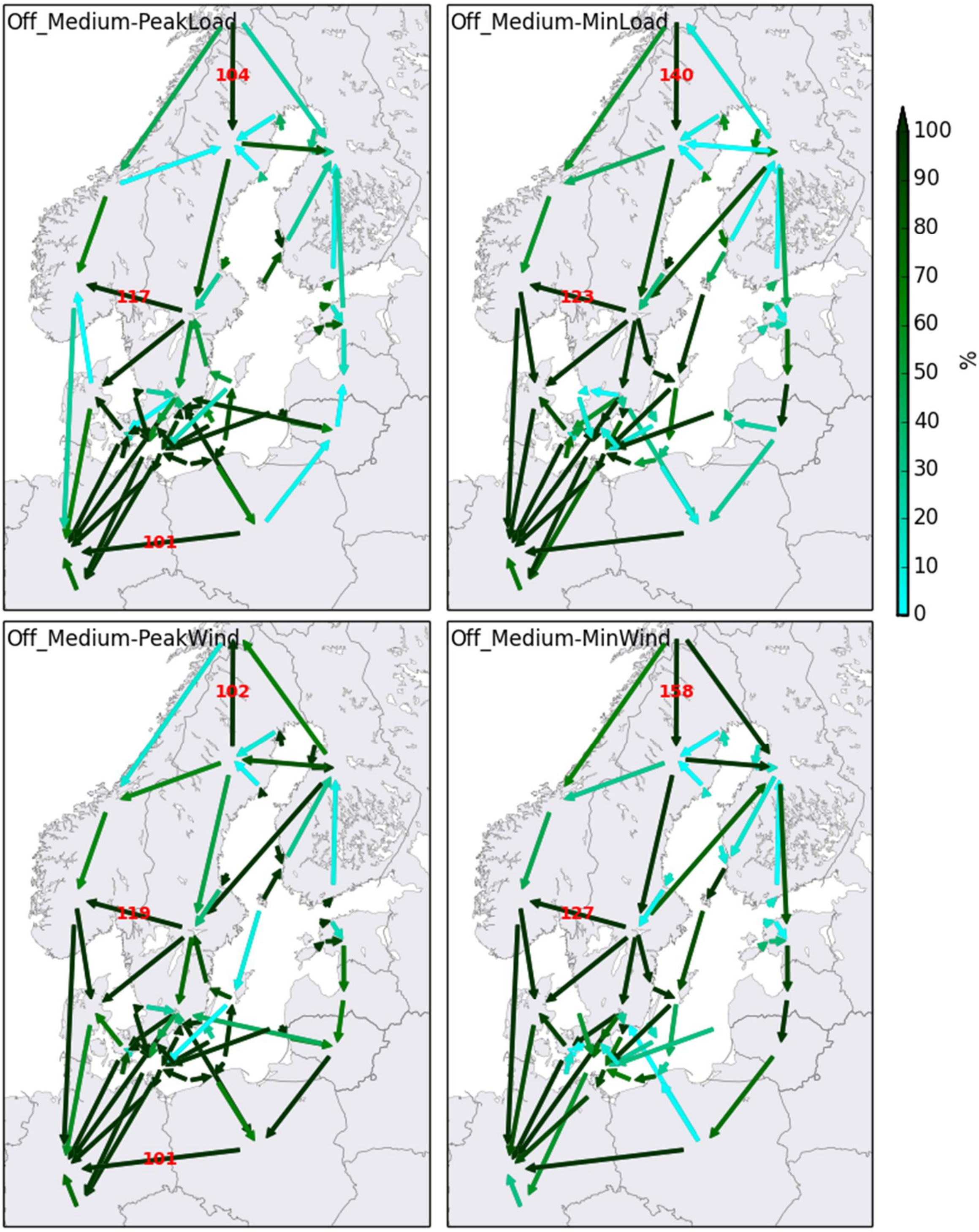

Figure 40 Transmissions in the snapshot situations calculated using linearized power flow equations (% of net transfer capacity). Values that are higher than the scale maximum are written in the plot.

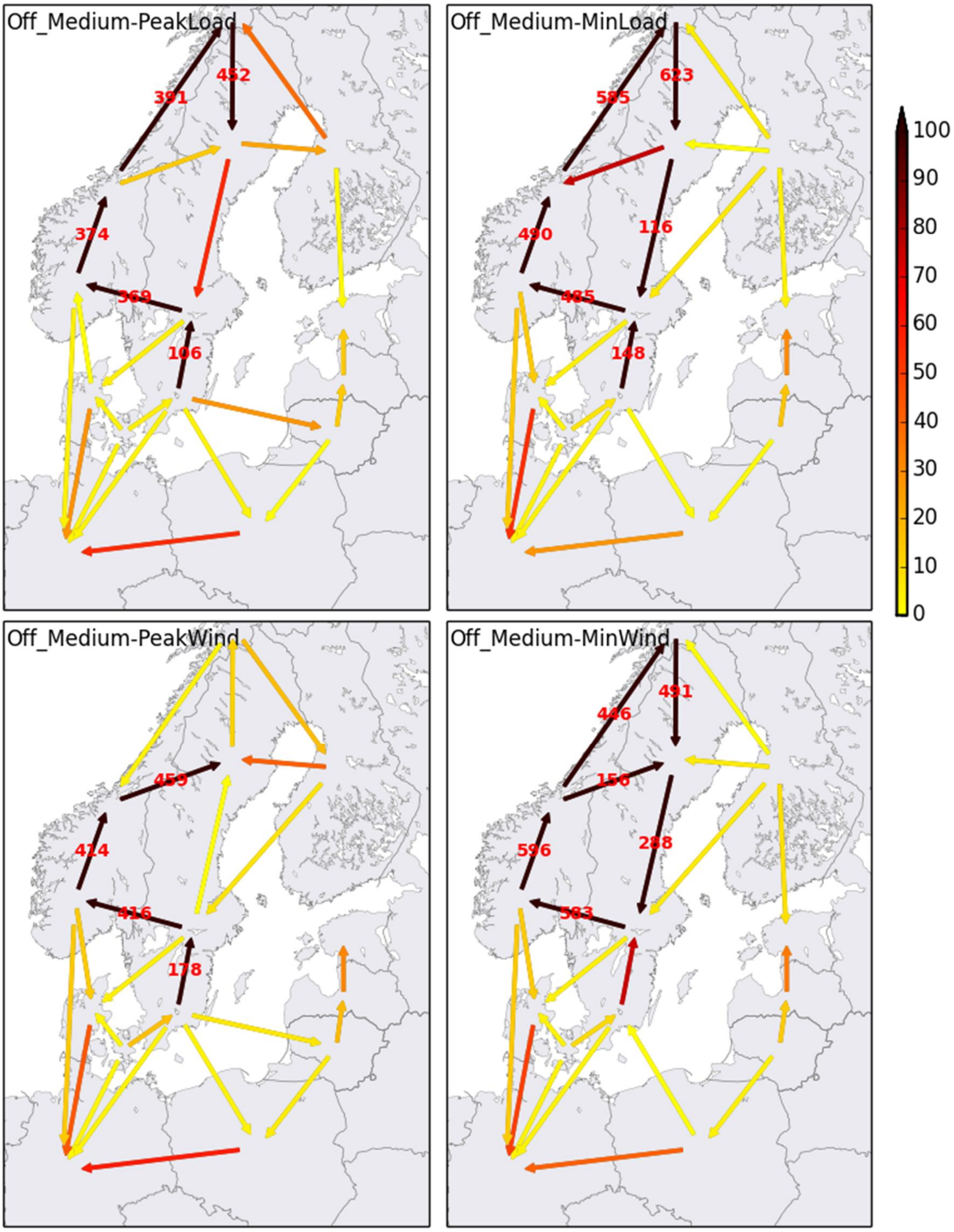

Figure 41 Differences in the market model transmissions and power flow model transmissions in the snapshot situations. Values that are higher than the scale maximum are written in the plot.

Table 10 Losses in each region of the grid model in different snapshots as % of load (losses as MWh/h in parenthesis)

	Peak load		**Minimum load**		**Peak offshore wind power**		**Minimum offshore wind power**	
Eastern Denmark	2	(51)	1	(7)	1	(25)	1	(13)
Western Denmark	6	(250)	9	(122)	3	(93)	4	(86)
Finland	2	(282)	2	(163)	2	(223)	2	(141)
Central Norway	1	(64)	2	(48)	2	(61)	1	(34)
Northern Norway	4	(55)	10	(73)	4	(32)	12	(97)
Southern Norway	1	(249)	5	(351)	3	(369)	4	(358)
Poland	4	(1151)	5	(620)	4	(866)	4	(682)
Central Sweden	2	(355)	6	(329)	2	(205)	6	(385)
Northern Sweden	7	(324)	15	(318)	8	(221)	16	(405)
Southern Sweden	5	(231)	15	(251)	9	(308)	8	(156)
Estonia	1	(19)	5	(28)	3	(36)	5	(42)
Germany	4	(3818)	4	(1591)	5	(3635)	5	(2541)
Latvia	1	(14)	8	(46)	4	(43)	7	(61)
Lithuania	0	(8)	3	(25)	3	(46)	3	(30)

5. Discussion

The profitability of the offshore grid investments depends highly on the assumptions about the underlying power systems as well as on the HVDC component costs. The knowledge of future power plants is typically limited: the initial assumption in this study was that Germany has a deficit of inexpensive generation infrastructure, which had a strong influence on the results. HVDC circuit breaker costs and the cost difference in building converter stations offshore versus onshore also affect the results. In this study, the HVDC component costs were linearized. A more accurate representation of the costs would take into account the decrease of unit costs with increasing capacity. In all of the cases, approximately 27 GW of offshore wind power was assumed to be built in the Baltic Sea. No investment cost was given for this offshore wind power and its profitability was not compared with other generation forms, such as onshore wind power, PV or thermal power.

This study focused on economic assessment of offshore grids while also giving insight into electricity production per fuel type, CO_2 emissions, annual electricity transmissions between regions and power flows in one-hour snapshots. The snapshot transmissions were calculated using linearized power flow equations. The additional value of power flow calculation for the market studies depends on the system. With limited transmission capacity and the possibility of loop flows it is important. If there are no possibilities for loop flows in the grid model and thermal limits are not the limiting factors for transmission, power flow calculation may not change the results. However, it ought to be remembered in the analysis and conclusions that there may be possibilities for loop flows in the real system although they are not included in the grid model.

The power flow results presented in this report may contain inaccuracies and errors due to the following possible sources of error:

- Using DC power flow method instead of the more accurate AC power flow method due to lack of grid models that are accurate enough and due to lack of good starting values that are important for the AC power flow to converge.
- When the production of WILMAR JMM generation units is divided among grid model generators, part of the production inside each price region may be located in a way which is not economic or which does not take into account the patterns of PV and especially wind power production inside each region.
- Seasonal, daily or hourly profiles of grid loads were not modelled; instead, the ratio of each grid load to the total hourly region load stayed the same throughout a year; the ratio is naturally different for different grid loads. Thus, the division of WILMAR JMM region load among grid loads does take into account the geographical and timely variation of the load inside a price region precisely.

It is important to assess the technical risks of the different offshore grid topologies, including the following questions:

- What is the redundancy in the different grid topologies?
- Is it better to build a two-terminal link using several cables and converters instead of the minimum needed?
- Is it important to have several routes (a meshed grid) for power transmission?
- What are the consequences of a sudden disconnection of a wind power plant cluster?
- What are the impacts of offshore-to-shore link failures, shore-to-shore link failures and offshore-to-offshore link failures including their downtime?

The comparison of the cases applies mainly to southern parts of the Baltic Sea, as in northern parts there were not as many differences between the cases. In *Onshore* topologies there are some multi-terminal radial connections to which the comparison does not apply either. Some of the HVDC links in the optimized grids are so large (e.g., > 2000 MW) that it is unlikely that they would be built as only one link due to both technical and reliability reasons. Instead of building several links side by side, a different route for the power flow, both electrically and geographically, could be created by building a meshed grid to prepare for possible failures. Both in *Mix* and *Offshore* topologies, the grid optimization resulted in meshed structures in areas between Sweden and Poland. In *Limited* and *Onshore* cases, meshed structures were disabled by definition. In general, a meshed structure is more secure than radial structure. If a link between two nodes has a failure, there is another route for the power flow assuming that there is enough capacity in the links that remain in operation. If it is not probable to have simultaneous failures in links that have been laid in the same route between two stations, a similar effect can be achieved by building one large link as two or more smaller links roughly in the same route. However, it may not be economically feasible to build all links as several smaller links because of the economy of scale.

If a whole wind power plant cluster is disconnected, more than 2000 MW of wind power can be lost. E.g., in the Nordic power system the reserves are sized for the biggest generation unit 1600 MW. Therefore, also the wind power plant cluster would probably not be connected to the offshore station with only one connection.

In *Limited* and *Onshore* topologies, if a connection from offshore wind power plant cluster to shore has a failure and if there is no redundancy in the connection, the total production of the wind power cluster will be lost. However, interconnection capacity would not be lost, as the wind power plant clusters were not allowed to be operating as mid points in the interconnections.

In *Mix* and *Offshore* topologies, a similar situation would not necessarily mean a loss of the total wind power production. The wind power production could flow into some other price region if there is enough transmission capacity available to that direction. However, interconnection capacity between the price regions would decrease or be lost if there is no alternative path for the region-to-region power flow. Failures in connections between two offshore wind clusters would have similar impacts: decrease of interconnection capacity but not total loss of offshore wind power plant cluster production.

In *Onshore* topologies, a failure in a connection between two onshore connection points would result in loss of interconnection capacity. Offshore wind power production would not be lost. However, the offshore wind power production would possibly need to be curtailed if there is significant surplus of power in one of the regions where the faulted interconnection was connected, the interconnection was used for exporting offshore wind power and the offshore wind power cannot be transmitted to other load centres during the failure downtime.

6. Conclusions

Costs: The results show that interconnections will decrease the total costs significantly in the Baltic Sea region compared to only two-terminal connections from offshore wind power plant clusters to shore. Building separate offshore interconnectors and wind power plant connections instead of a multi-terminal-like offshore grid based on two-terminal links may result in lower investment and operation costs. According to the results, multi-terminal and meshed offshore grid structures will have lower costs than structures based on separate offshore wind cluster connections and interconnectors provided that HVDC circuit breakers are available and their price is low enough. The threshold that was found out in the study for the circuit breaker cost is approximately one fourth of converter station cost.

Electricity production: With the generation infrastructure that was used in the simulations, there are clear differences in electricity production per fuel type depending on whether there are new interconnections built across the Baltic Sea or not. If there are no interconnections, fossil fuels are used more, and if interconnections are built, especially nuclear but also wind power is used more. The topology of the offshore grid did not have a significant impact on the annual production results.

Annual transmissions: In all the studied cases, the annual transmissions were generally from north to south and from east to west. This is a result from the assumed deficit of inexpensive generation infrastructure in Germany. The annual transmissions were also very large from northern Sweden to southern Sweden. However, the initial transmission capacities from northern to central Sweden appear to be large enough since the optimization model did not invest in new connections from the Gulf of Bothnia to central parts of the Baltic Sea in any of the cases. With the exception of a link between Finland and northern Sweden in the low HVDC cost scenario, interconnections were not created north from Åland.

Hourly transmissions: Hourly power flow analysis results showed similar patterns as the annual transmissions. Loop flows and overloadings were detected inside and between Sweden and Norway. If the model had included more regions from Central Europe, very likely more loop flows would have been seen there as well.

Technical risks: The availability of the infrastructure was concluded to be generally lower with radial structures compared to meshed structures in N−1 situations. The lack of alternative routes in radial structures can be bypassed to some extent by building large links between two nodes as several smaller links.

7. Summary

The focus in this study was in the possible offshore grid development paths in the Baltic Sea region. Assuming large amount of offshore wind power in the Baltic Sea, the objective was to find answers to the following questions: Are additional interconnection important? Are multi-terminal offshore grids more beneficial than separate wind power plant cluster connections and interconnectors? What are general power transfers like? Are there significant loop flows in the Nordic countries?

There are vast wind resources in the Baltic Sea. This study assumed that 27 GW of offshore wind power will be built there. The wind power plant plans taken into account in this study were clustered into 22 wind clusters, which were assumed to operate as nodes in the offshore grid. To connect the offshore grid to the onshore power systems, 17 onshore connection points were selected, mostly from the coastal area. One connection point was selected deeper from the continent because the connection capacity in the coastal area may be insufficient.

The modelled and simulated system was comprised of the power systems of Denmark, Finland, Norway, Sweden, Estonia, Latvia, Lithuania, Germany and Poland. Some countries were divided into several price regions, whereas other countries were modelled with one price region in each. The electricity demand in Germany covered almost half of the total annual electricity demand in the modelled area. Nuclear capacity was assumed to exist in Finland and Sweden but not in other countries. The amount of onshore and offshore wind power in the study was approximately 22 % of the annual electricity demand.

The costs of HVDC cables and converter stations were linearized in the study based on data about existing and planned HVDC connections in Europe with capacities between 400 MW and 1400 MW. This means that the economy of scale was not taken into account properly. Three cost scenarios were created for the costs: *Low*, *Medium* and *High*. In the *Medium* cost scenario, cables were assumed to cost 1,300 €/MW/km and onshore converter stations were assumed to cost 100,000 €/MW. For offshore converter stations, two assumptions were used: they would be either 50 % or 100 % more expensive than onshore converter stations.

To downscale the problem of optimizing all possible connections between the 22 wind clusters and 17 onshore connection points and to create differences between the offshore grid scenarios, four topology groups were created: *Limited*, *Onshore*, *Offshore* and *Mix*. In *Limited* scenario, only one connection from each wind cluster to shore was allowed. *Onshore* scenario included the same set of possible connection as *Limited*. In addition, it included a few additional offshore-to-shore connections (mainly between Denmark, Sweden and Germany) and interconnections between onshore connection points. *Offshore* scenario included almost the same set of possible connections as *Limited*. As in *Onshore* scenario, it also included a few additional offshore-to-shore connections. However, instead of interconnections between onshore connection points, it was possible to connect wind clusters to each other. *Mix* scenario included a manually defined set of mixed shore-to-shore, offshore-to-shore and offshore-to-offshore connections. *Limited* and *Onshore* scenarios were based on separate wind cluster connections and interconnectors, whereas *Offshore* and *Mix* scenarios utilized also multi-terminal structures.

The methodology included transmission investment planning, unit commitment and economic dispatch simulation and power flow calculation. First, offshore HVDC grid investments were optimized using an investment optimization model Balmorel. Balmorel optimized the capacities of the possible transmission links in each topology scenario. Those results were then fed to a unit commitment and economic dispatch model WILMAR JMM, which was used to simulate the market operation in more detail. Both in Balmorel and in WILMAR JMM the transmissions between price regions were modelled using net transfer capacity constraints without modelling the power grid. A few one-hour snapshots from WILMAR JMM were selected for further linearized power flow analysis in PSS®E transmission system analysis tool and a grid model with almost 1000 nodes. Linearized power flow analysis was used instead of the full nonlinear one due to lack of data in some parts of the grid model and also due to lack of knowledge about voltage controlling strategies and good starting values for the iterative solution methods needed for the nonlinear problem.

Balmorel showed only few transmission investments in *Limited* scenario, because only few investments were allowed. All other topology scenarios resulted in strong links from the Baltic Sea and southern Sweden to Germany. Links between Sweden, Poland and Germany were also very likely to get invested in. HVDC cost scenario *Low* resulted in more and larger investments than HVDC cost scenario *High*, as expected. The assumption about offshore station costs in comparison to onshore station costs did not seem to have as high impact.

The annual investment costs in *Limited* scenario were relatively low but the annual operation costs determined by WILMAR JMM were very high compared to other topology scenarios. Thus, *Limited* was clearly the most expensive in total costs. *Onshore* seemed to be less expensive than *Offshore* topology, which was still cheaper than the manually defined *Mix* topology. However, these results were with the assumption that no HVDC circuit breakers are available and the multi-terminal structures need actually to be built using two-terminal links. When HVDC circuit breakers and truly multi-terminal structures were taken into account and the cost of HVDC circuit breaker was assumed to be low enough, *Offshore* topology resulted in lower total costs than *Onshore* topology. When the HVDC circuit breaker cost was assumed to be one fourth of converter station costs, the two topologies had about the same total system costs, but when the HVDC circuit breaker cost assumption was decreased to one eighth of converter station costs, *Offshore* topology had already lower costs than *Onshore* topology.

The annual electricity transmissions were generally from north to south and from east to west. Germany was importing relatively high amounts of electricity due to the assumed lack of inexpensive generation capacity in Germany. Transmissions from northern Sweden to southern Sweden were higher when further additional connections existed from southern Sweden to Germany. Because of this, the transmissions through Sweden were not as large in *Limited* scenario as in the other scenarios.

A few WILMAR JMM snapshots were also selected for linearized power flow analysis to check whether the transmissions between price regions change significantly because of loop flows. Otherwise no significant loop flows were detected, but inside and between Sweden and Norway the differences between the market transfers and power flow results were quite large. One reason for this is that all other price regions were AC-connected in string in the grid model and only the price regions in Sweden and Norway were connected through a meshed-like AC-grid. If more countries from Central Europe had been included in the modelling in addition to Germany and Poland, very likely more loop flows would have been detected there as well. The power systems in Sweden and Norway were also modelled with a very aggregated model compared to other power systems, which may have an influence on the results. It was also noticed that according to the linearized power flow analysis with the grid model, some net transfer capacities inside and between Sweden and Norway will be exceeded in the generation and load snapshots determined by WILMAR JMM due to the loop flows which were not possible to capture with WILMAR JMM.

N−1 situations or other security-related issues with offshore HVDC grids were not simulated in this study. However, it was concluded that radial structures in general have lower availability compared to meshed structures in N−1 situations. The lack of alternative routes in radial structures can be bypassed to some extent by building large links between two nodes as several smaller links.

References

[1] D. Van Hertem and M. Ghandhari, “Multi-terminal VSC HVDC for the European supergrid: Obstacles,” *Renew. Sustain. Energy Rev.*, vol. 14, no. 9, pp. 3156–3163, Dec. 2010.

[2] T. K. Vrana, J. Beerten, R. Belmans, and O. B. Fosso, “A classification of DC node voltage control methods for HVDC grids,” *Electr. Power Syst. Res.*, vol. 103, pp. 137–144, Oct. 2013.

[3] A. Egea-Alvarez, J. Beerten, D. Van Hertem, and O. Gomis-Bellmunt, “Hierarchical power control of multiterminal HVDC grids,” *Electr. Power Syst. Res.*, vol. 121, pp. 207–215, Apr. 2015.

[4] O. Gomis-Bellmunt, J. Liang, J. Ekanayake, R. King, and N. Jenkins, “Topologies of multiterminal HVDC-VSC transmission for large offshore wind farms,” *Electr. Power Syst. Res.*, vol. 81, no. 2, pp. 271–281, Feb. 2011.

[5] M. K. Bucher, S. Member, R. Wiget, S. Member, G. Andersson, C. M. Franck, and S. Member, “Multiterminal HVDC Networks — What is the Preferred Topology ?,” *IEEE Trans. Power Deliv.*, vol. 29, no. 1, pp. 406–413, 2014.

[6] J. De Decker, P. Kreutzkamp, J. Pieter, A. Woyte, S. Cowdroy, P. MacGarley, L. Warland, H. Svendsen, J. Völker, C. Funk, H. Peinl, J. Tambke, L. von Bremen, K. Michalowska, and G. Caralis, “OffshoreGrid: Offshore Electricity Grid Infrastructure in Europe: Final Report,” 2011.

[7] A. Flament, P. Joseph, G. Gerdes, L. Rehfeldt, A. Behrens, A. Dimitrova, F. Genoese, I. Gajic, M. Jafar, N. Tidemand, Y. Yang, J. Jansen, F. Nieuwenhout, K. Veum, I. Konstantelos, D. Pudjianto, and G. Strbac, “NorthSeaGrid: Offshore Electricity Grid Implementation in the North Sea: Final Report,” 2015.

[8] L. Meeus, F. Lévêque, I. Azevedo, M. Saguan, and J.-M. Glachant, “THINK: Topic 5: Offshore Grids: Towards a Least Regret EU Policy: Final Report,” 2012.

[9] N. Helistö and S. Uski-Joutsenvuo, “Initializing Network Simulations for Case Studies of Offshore Wind Power and Offshore DC Grid Integration in the Power System of Northern Europe,” in *12th International Workshop on Large-Scale Integration of Wind Power into Power Systems as well as on Transmission Networks for Offshore Wind Power Plants, WIW2013*, 2013.

[10] N. Helistö and S. Uski, “Electricity Market and Power Flow Impact of Offshore Grids in the Baltic Sea Region,” in *14th International Workshop on Large-Scale Integration of Wind Power into Power Systems as well as on Transmission Networks for Offshore Wind Power Plants, WIW2015*, 2015.

[11] T. Trötscher and M. Korpås, “A framework to determine optimal offshore grid structures for wind power integration and power exchange,” *Wind Energy*, vol. 14, Issue 8, pp. 977 – 992, 2011.

[12] H. G. Svendsen, “Planning Tool for Clustering and Optimised Grid Connection of Offshore Wind Farms,” *Energy Procedia*, vol. 35, pp. 297–306, 2013.

[13] www.balmorel.com

[14] H. Ravn et al., Balmorel: A Model for Analyses of the Electricity and CHP Markets in the Baltic Sea Region, 2001.

[15] P. Meibom, R. Barth, B. Hasche, H. Brand, and M. O'Malley, "Stochastic optimization model to study the operational impacts of high wind penetrations in Ireland," *IEEE Trans. Power Syst.*, vol. 26, no. 3, pp. 1367 - 1379, Aug. 2011.

[16] J. J. Grainger and W. D. Stevenson, Jr., "Power system analysis," McGraw-Hill, 1994.

[17] I. Norheim, E. Lindgren, S. Uski, P. Sørensen, and C. Jauch, "WILMAR WP5 - Deliverable D5.1 System stability analysis," 2005.

[18] V. Akhmatov, T. Lund, A. D. Hansen, P. Sørensen, and A. H. Nielsen, "A Reduced Wind Power Grid Model for Research and Education," in Sixth International Workshop on Large-Scale Integration of Wind Power and Transmission Networks for Offshore Wind Farms, 2006, pp. 173–180.

[19] N. Hutcheon and J. W. Bialek, "Updated and validated power flow model of the main continental European transmission network," in IEEE PowerTech (POWERTECH), 2013, pp. 1–5.

[20] N. Belonogova, "Development of power flows around Baltic countries with new grid links," Master's thesis, Lappeenranta University of Technology, 2009.

[21] N. Helistö, "Modelling the Finnish Transmission Grid for Power Flow Studies," Master's thesis (in Finnish), Aalto University, 2012.

[22] Siemens Industry, Inc., Siemens Power Technologies International, "PSS®E 33.5 Program Operation Manual," October 2013.

[23] J. Kiviluoma, E. Rinne, N. Helistö, and M. Azevedo, "Modelling framework for power systems," Espoo, Finland, VTT Technology 196, 2014.

[24] N. A. Cutululis, "TWENTIES Deliverable 16.1: Offshore Wind Power Data."

[25] P. Sørensen, P. Pinson, N. A. Cutululis, H. Madsen, L. E. Jensen, J. Hjerrild, M. H. Donovan, J. R. Kristoffersen, and A. Vigueras-Rodríguez, "Power fluctuations from large wind farms - Final report," 2009.

[26] N. A. Cutululis, "UpWind Deliverable D 9.5: Reliability of offshore wind power production under extreme wind conditions," 2010.

[27] P. Capros, L. Mantzos, N. Tasios, A. De Vita, and N. Kouvaritakis, "EU energy trends to 2030 - Update 2009," European Comission, Directorate-General for Energy in collaboration with Climate Action DG and Mobility and Transport DG, Luxembourg, 2010. [Online].

[28] http://www.nordpoolspot.com/

[29] https://www.entsoe.eu/

[30] https://www.entsoe.eu/major-projects/ten-year-network-development-plan/Pages/default.aspx

APPENDIX A Finnish transmission grid model

For each of the three voltage levels 400 kV, 220 kV and 110 kV, two types of transmission lines are used in the Finnish transmission grid model developed at VTT. Table 1 lists basic parameters of the line types.

Table 2 lists transformer parameters in the Finnish transmission grid model. In addition to the listed transformer types, the model also includes several three-winding transformers, especially 440/110/21 kV transformers with reactors connected to the third winding.

The total hourly load of Finland is divided into grid loads utilizing municipalities' annual electricity demand in three different sectors (housing and agriculture; industry; service and building).

Table 1 Line parameters in the Finnish transmission grid model [1]

Voltage level (kV)	Line type	Resistance (Ω/km)	Reactance (Ω/km)	Susceptance (μS/km)	Thermal rating (A)
400	3-Finch	0.0171	0.291	4.04	2960
400	2-Finch	0.026	0.33	3.57	2000
220	2-Hawk	0.059	0.31	3.65	1160
220	Condor	0.074	0.41	2.79	760
110	2-Duck	0.048	0.3	3.788	1260
110	Duck	0.096	0.409	2.808	630

Table 2 Transformer parameters in the Finnish transmission grid model

Transformer type	Resistance (%)	Reactance (%)	Power base (MVA)
400/220 kV	5	15	400
400/110 kV	5	20	380
220/110 kV	5	15	160

[1] L. Haarla and J. Elovaara, "Sähköverkot 1: Järjestelmätekniikka ja sähköverkon laskenta," (in Finnish), Gaudeamus Helsinki University Press, 2011.

APPENDIX B Additional grid maps

Figure 1–Figure 8 show the resulting grid investments in Balmorel optimization in different cost and topology scenarios. Table 1 lists the cases and explains the case names.

Table 1 Explanations to case names

Case name	Offshore station cost increase compared to onshore station cost	General HVDC component cost assumption	Offshore grid topology type assumption
On_Low	50 %	Low	On(shore)
Off_Low	50 %	Low	Off(shore)
Lim_Medium	50 %	Medium	Lim(ited)
On_Medium	50 %	Medium	On(shore)
Off_Medium	50 %	Medium	Off(shore)
Mix_Medium	50 %	Medium	Mix
On_High	50 %	High	On(shore)
Off_High	50 %	High	Off(shore)
On_Low+	100 %	Low	On(shore)
Off_Low+	100 %	Low	Off(shore)
Lim_Medium+	100 %	Medium	Lim(ited)
On_Medium+	100 %	Medium	On(shore)
Off_Medium+	100 %	Medium	Off(shore)
Mix_Medium+	100 %	Medium	Mix
On_High+	100 %	High	On(shore)
Off_High+	100 %	High	Off(shore)

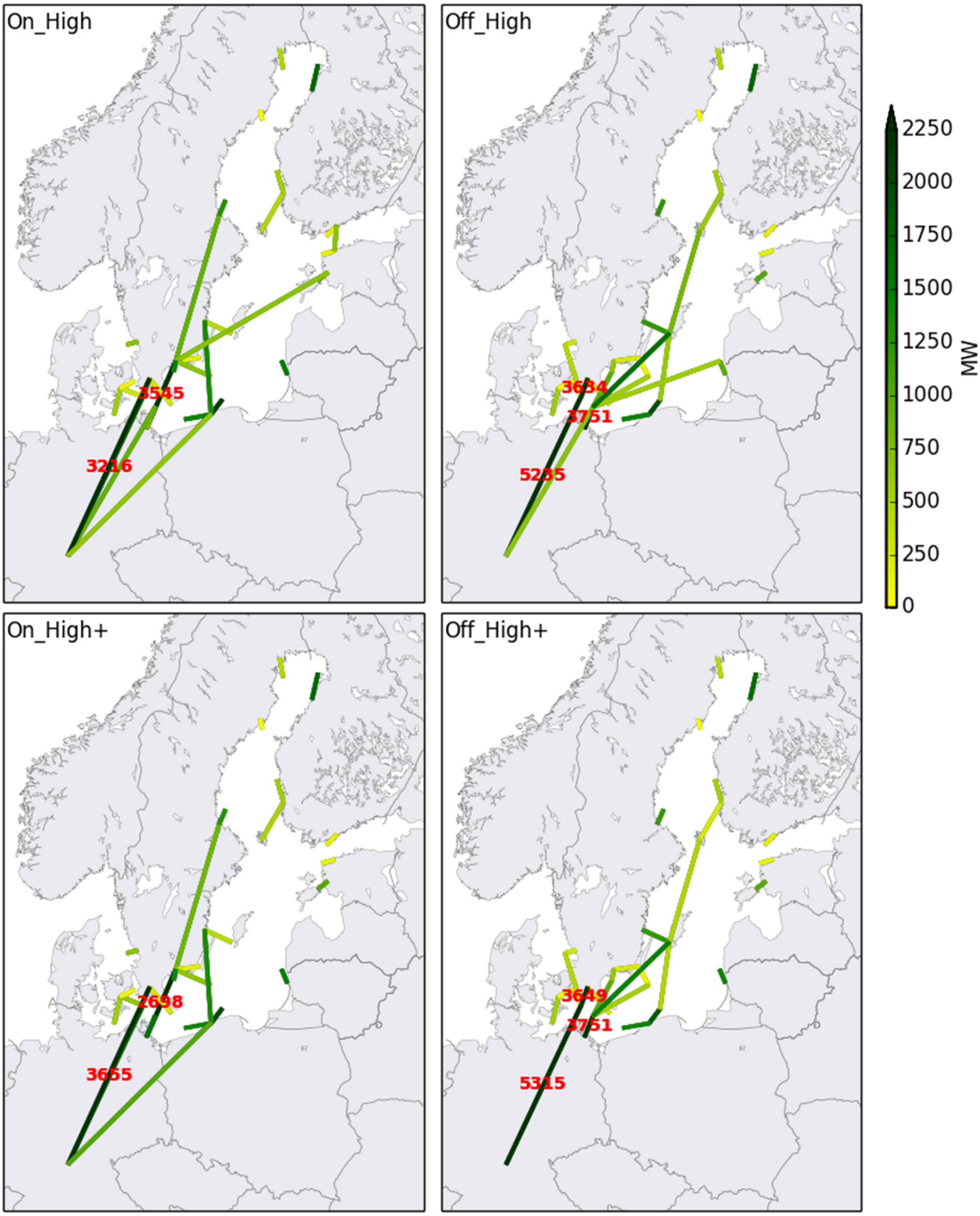

Figure 1 'High' cost scenario grids. Values that are higher than the scale maximum are written in the plot.

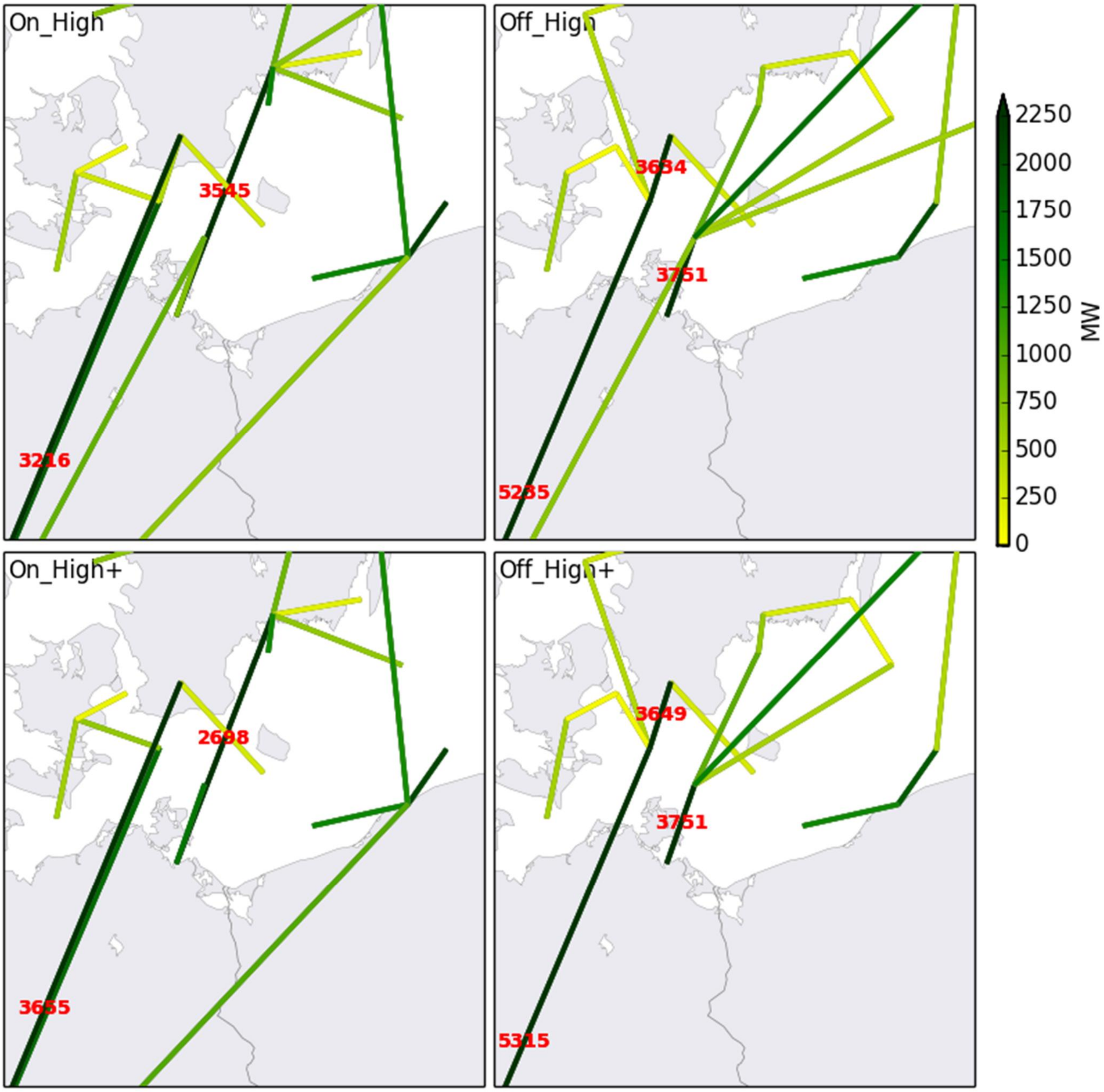

Figure 2 'High' cost scenario grids (zoomed into the region between Denmark, Sweden, Poland and Germany). Values that are higher than the scale maximum are written in the plot.

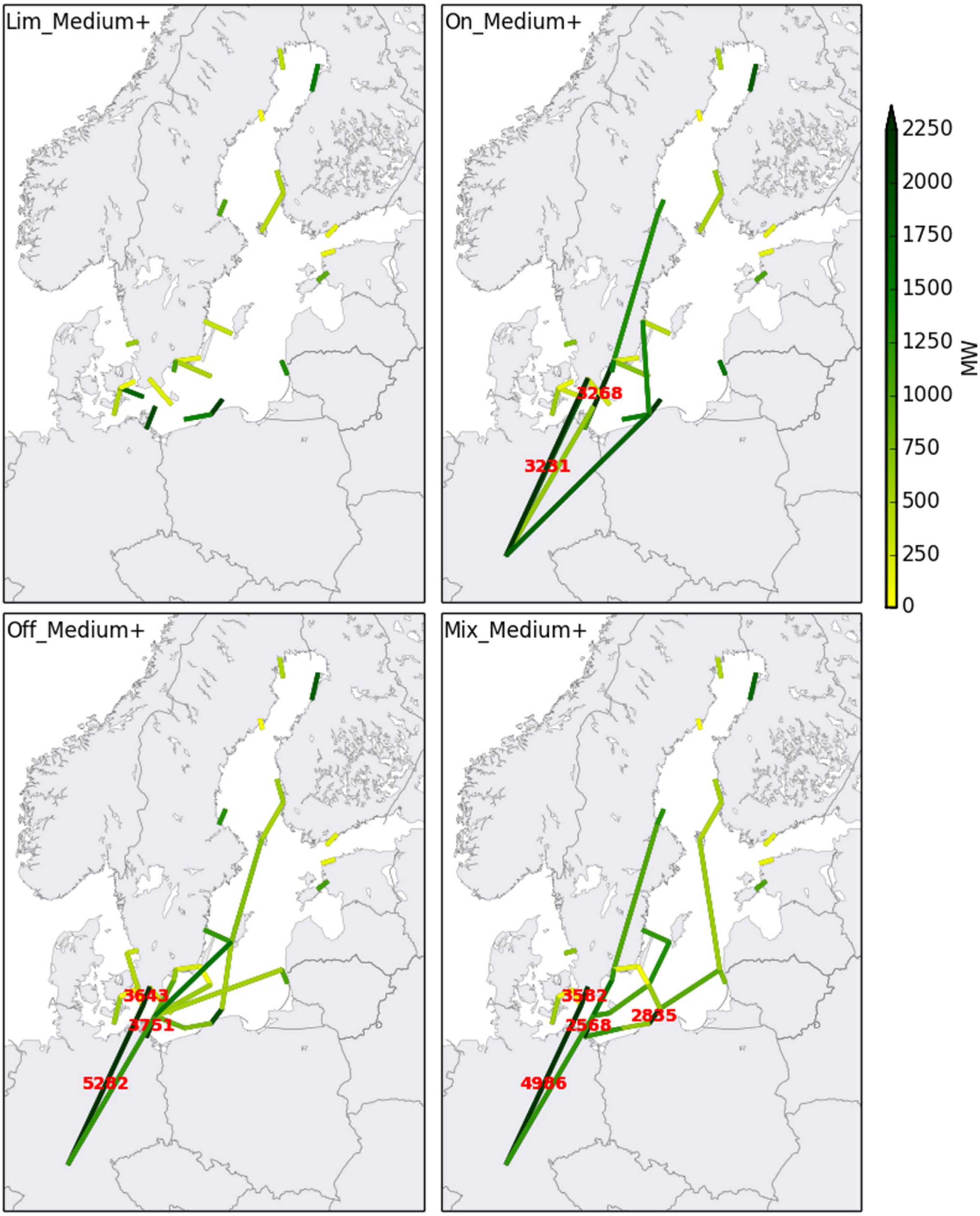

Figure 3 'Medium' cost scenario grids, with offshore converter stations costing 100 % more than onshore converter stations. Values that are higher than the scale maximum are written in the plot.

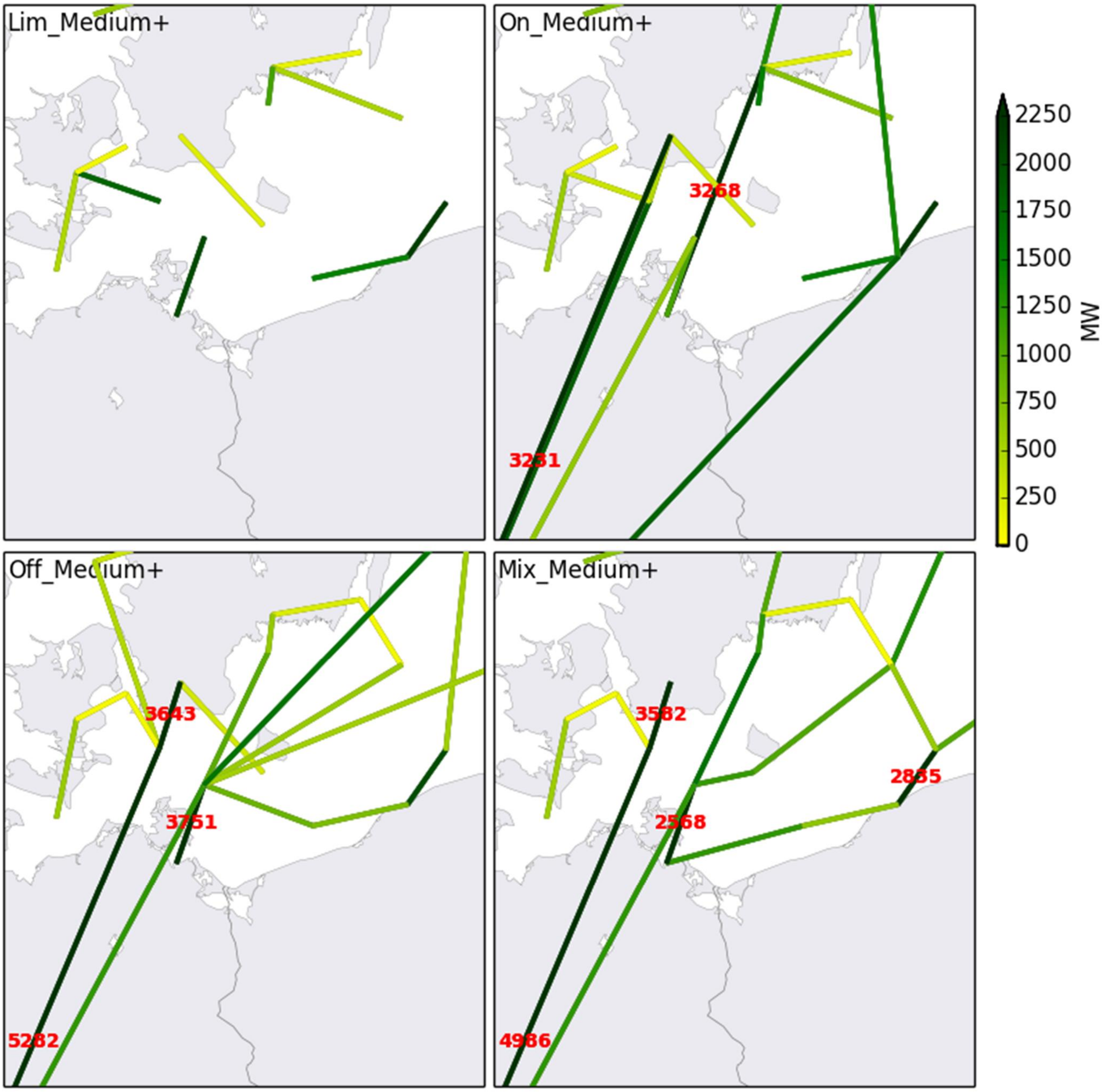

Figure 4 'Medium' cost scenario grids, with offshore converter stations costing 100 % more than onshore converter stations (zoomed into the region between Denmark, Sweden, Poland and Germany). Values that are higher than the scale maximum are written in the plot.

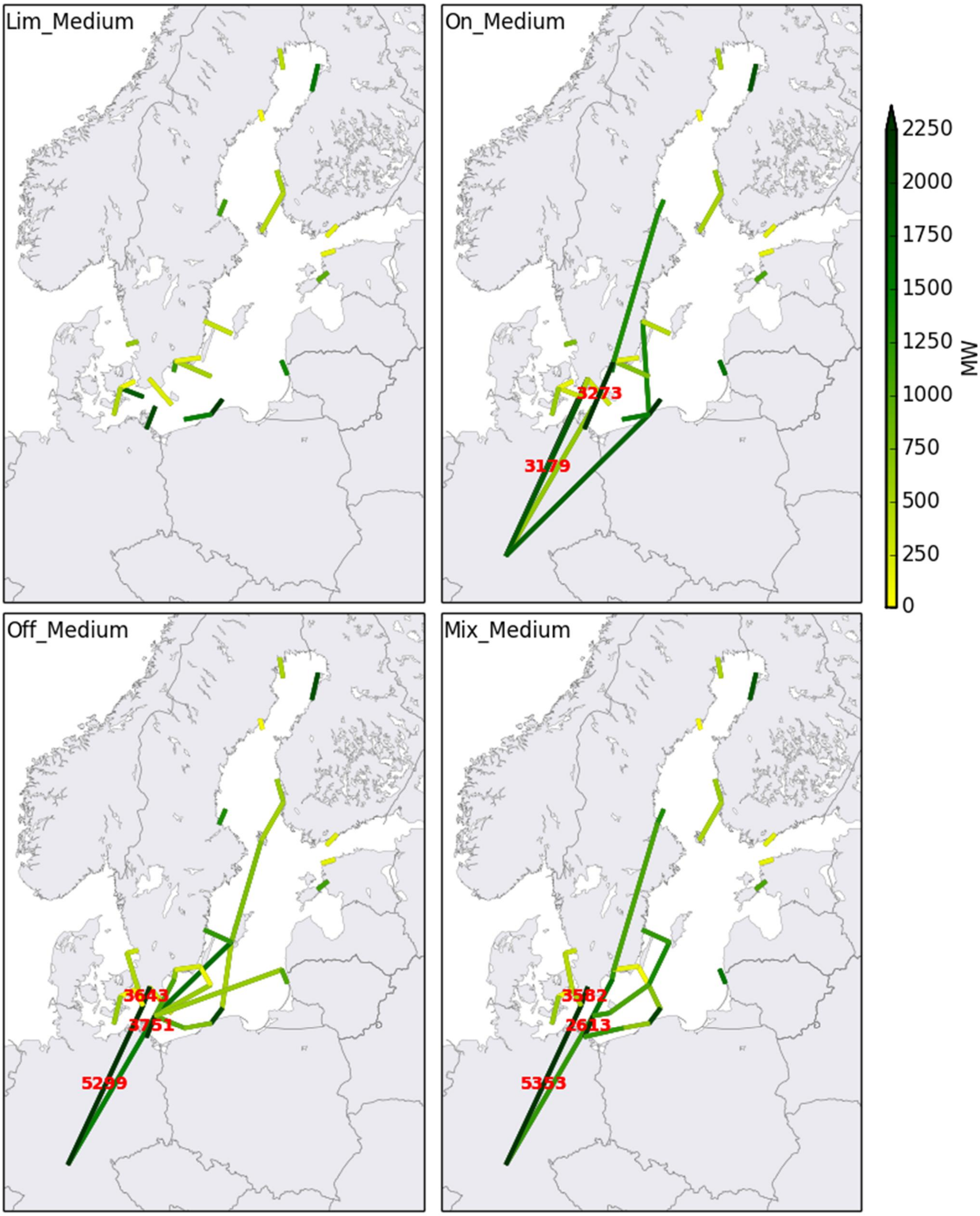

Figure 5 'Medium' cost scenario grids, with offshore converter stations costing 50 % more than onshore converter stations. Values that are higher than the scale maximum are written in the plot.

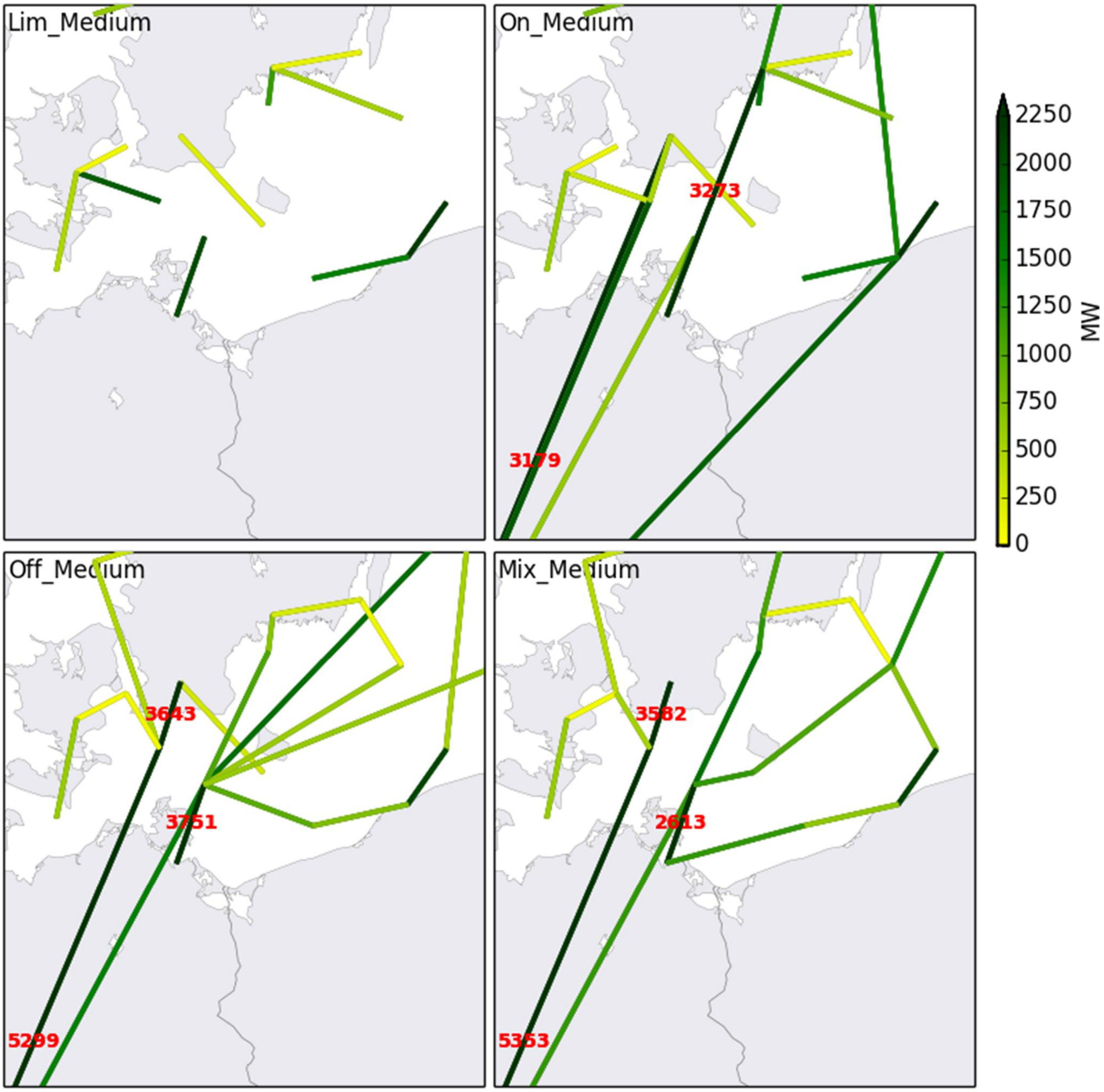

Figure 6 'Medium' cost scenario grids, with offshore converter stations costing 50 % more than onshore converter stations (zoomed into the region between Denmark, Sweden, Poland and Germany). Values that are higher than the scale maximum are written in the plot.

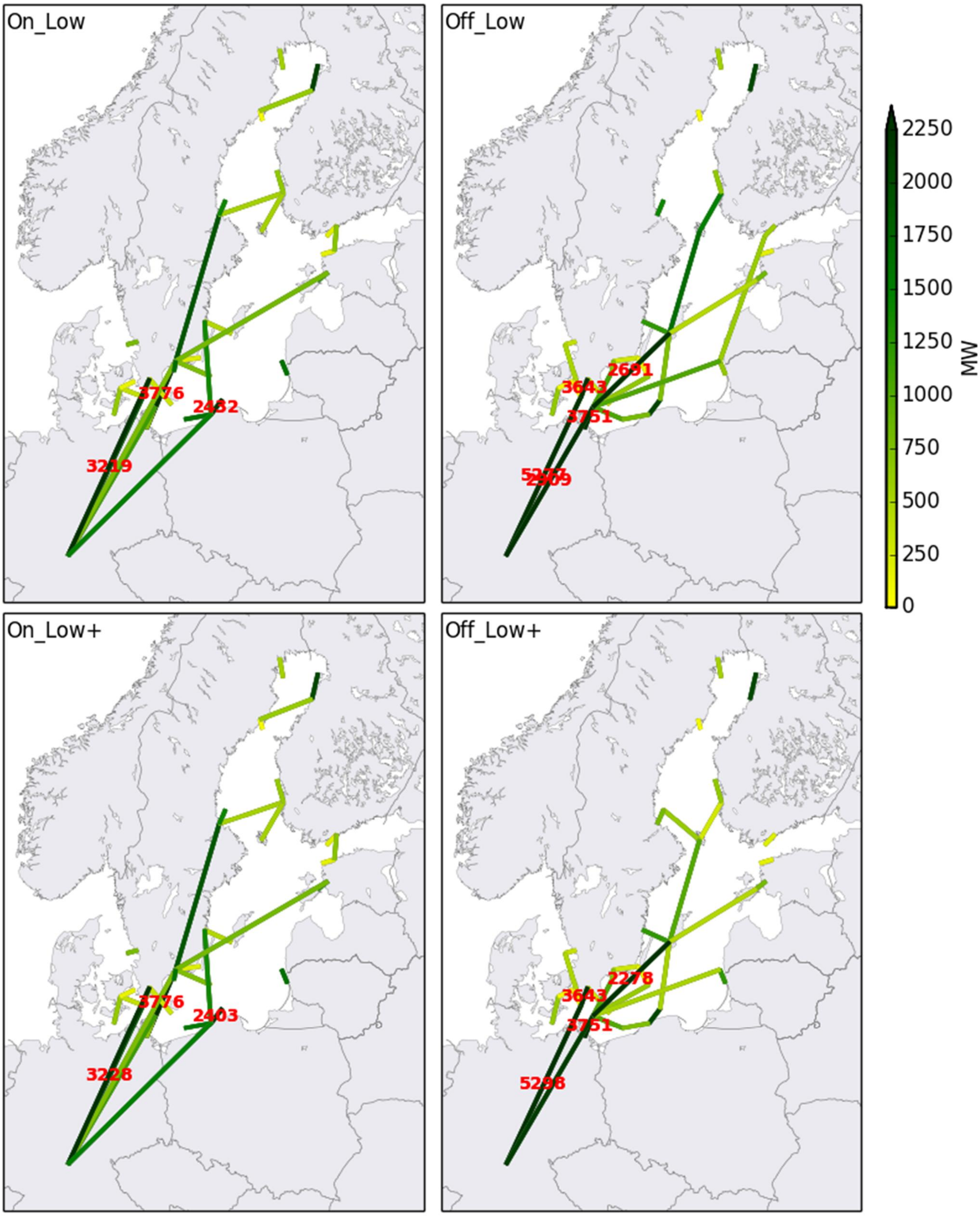

Figure 7 'Low' cost scenario grids. Values that are higher than the scale maximum are written in the plot.

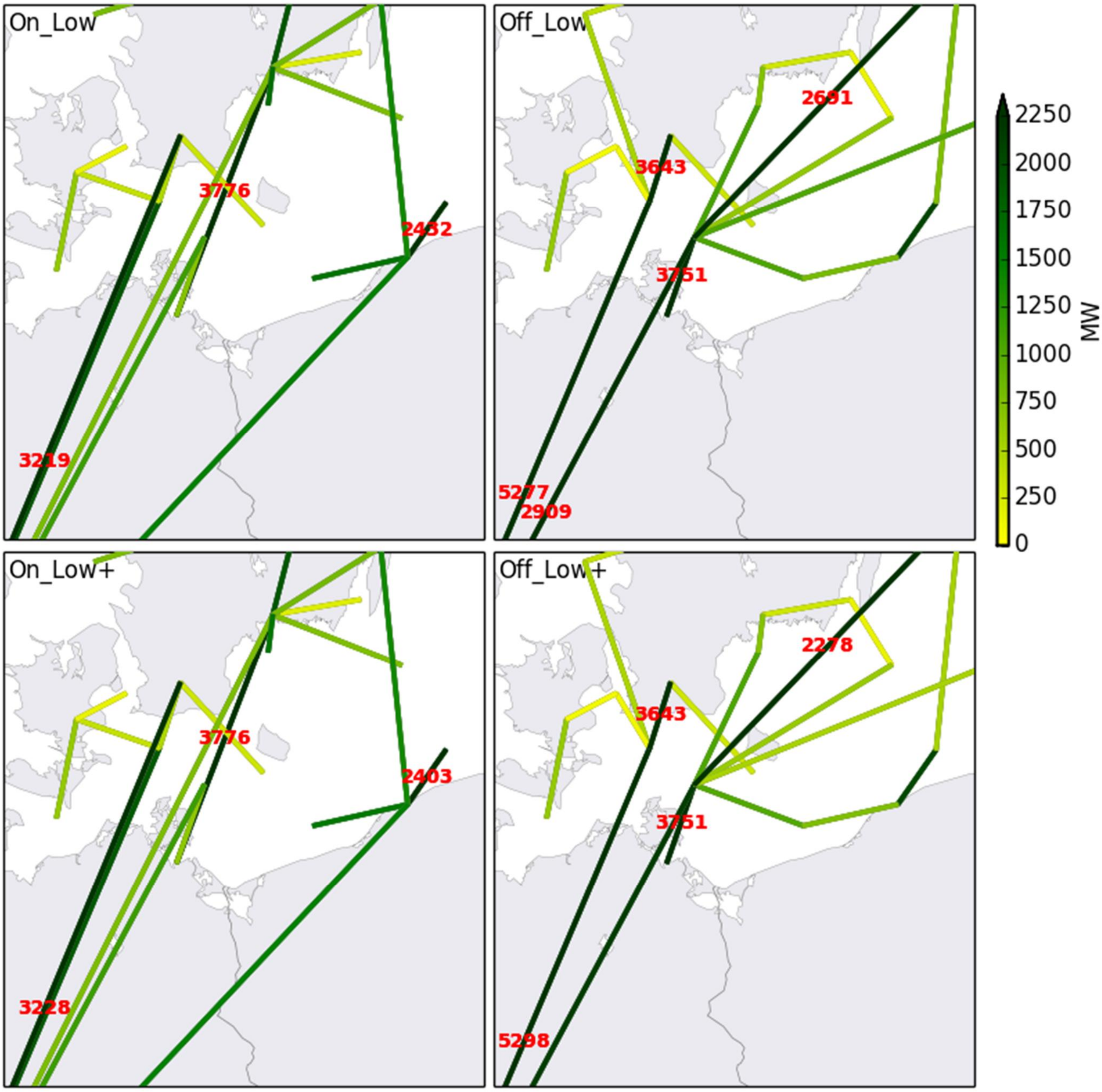

Figure 8 ‘Low’ cost scenario grids (zoomed into the region between Denmark, Sweden, Poland and Germany). Values that are higher than the scale maximum are written in the plot.